ASSESSMENT OF HEMODYNAMIC PARAMETERS IN THE FETAL AND UTERO-PLACENTAL CIRCULATION USING DOPPLER ULTRASOUND

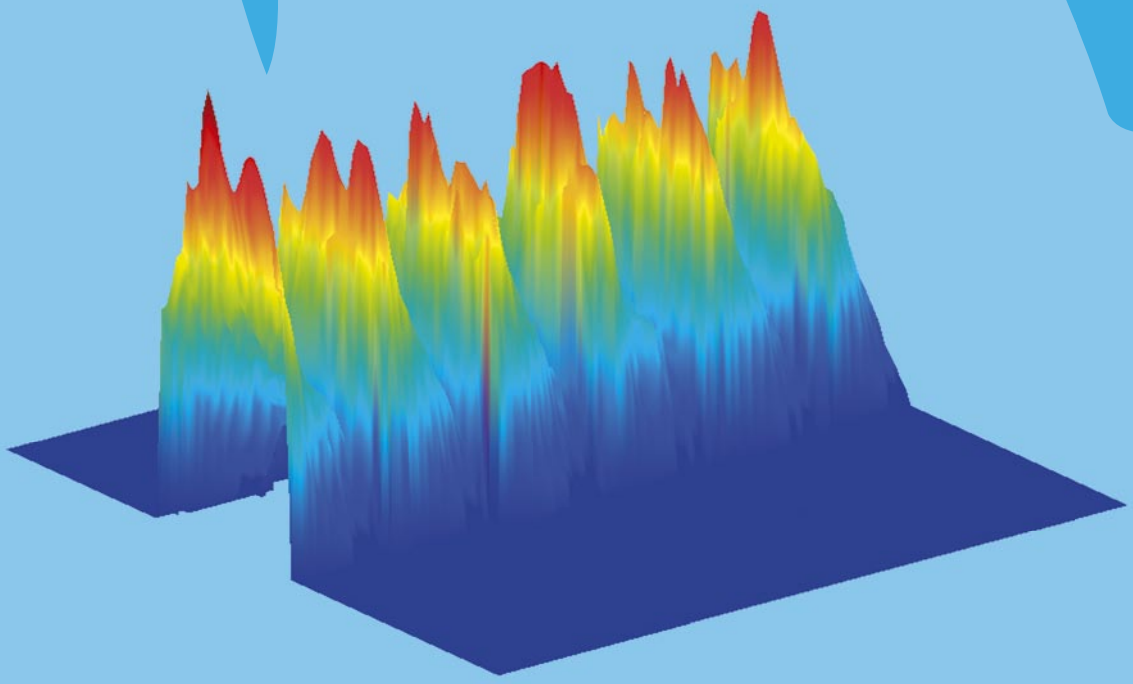

PIETER C. STRUIJK

Assessment of Hemodynamic Parameters in the Fetal and Utero-placental Circulation using Doppler Ultrasound

Bepaling van hemodynamische parameters van de foetale en utero-placentaire circulatie gebruik makend van Doppler ultrageluid

Proefschrift

ter verkrijging van de graad van doctor aan de
Erasmus Universiteit Rotterdam
op gezag van de
rector magnificus

Prof.dr. S.W.J. Lamberts

en volgens besluit van het college voor Promoties.

De openbare verdediging zal plaatsvinden op

woensdag 13 december 2006 om 9.45 uur

door

Pieter Cornelis Struijk

geboren te Sliedrecht

Promotiecommissie

Promotoren:	Prof.jhr.dr. J.W. Wladimiroff
	Prof.dr. E.A.P. Steegers
Overige leden:	Prof.dr.ir. A.F.W. van der Steen
	Prof. V. J. Mathews PhD
	Prof.dr. J.B. van Goudoever

Assessment of Hemodynamic Parameters in the Fetal and Utero-placental Circulation using Doppler Ultrasound

© Pieter Cornelis Struijk
Thesis Erasmus University Rotterdam, The Netherlands

ISBN 90-8559-239-9

Voor Sjanie

CONTENTS

CHAPTER 1 **5**

Introduction

CHAPTER 2 **15**

Power spectrum analysis of heart rate and blood flow velocity variability measured in the umbilical artery and uterine artery in early pregnancy

CHAPTER 3 **31**

Fetal heart rate and umbilical artery flow velocity variability in intrauterine growth restriction

CHAPTER 4 **47**

The magnitude-squared coherence function between the uterine and umbilical flow velocity waveforms as an additional predictor of placental dysfunction

CHAPTER 5 **65**

Wall shear stress and related hemodynamic parameters in the fetal descending aorta derived from color Doppler velocity profiles

CHAPTER 6 **91**

Blood pressure estimation in the human fetal descending aorta

CHAPTER 7 **111**

General Discussion

CHAPTER 8 **125**

Summary 126
Samenvatting 130
Curriculum vitae 135
Publicatie lijst 136
Dankwoord 141

CHAPTER 1

Introduction

History

The history of ultrasound in obstetrics and gynecology spans nearly half a century. The first publication entitled "Investigation of abdominal masses by pulsed ultrasound" has been written by the gynecologist Ian Donald and published in the Lancet as early as 1958 [1]. In this paper it is reported that ultrasound saved a patient's life by diagnosing a huge, easily removable, ovarian cyst in a woman who had been diagnosed as having inoperable cancer of the stomach. In the same paper the two biological effects of ultrasound, -thermal and mechanical (cavitation)-, are described. Being concerned, Ian Donald investigated ultrasound biological effects on newborn kittens. He stated, *"…… it was vital to establish beyond all shadow of doubt that susceptible tissues would not suffer even from these dosages…".* The kittens exposed for an hour to more than thirty times the dose of diagnostic ultrasound produced no detectable neuropathological change. An extensive review of the history of ultrasound in obstetrics and gynecology is written by Joseph Woo and can be found on the internet (www.ob-ultrasound.net/history1.html).

Cavitation, that is the production of microscopic gas bubbles, may be produced if considerable energies are present. The output intensity of modern ultrasound diagnostic equipment is limited to 720 mW/cm^2 and the mechanical index should not exceed 1.9. It is now accepted that with diagnostic ultrasound cavitation is not initiated in soft tissues and that there are no pre-existing gas bubbles within the uterus so no gas-body activation can occur.

The ability to absorb ultrasound energy varies with different tissues. In water and soft tissues ultrasound energy absorption is minimal. However, adult bone absorbs nearly all of the acoustic energy and therefore, thermal effect is maximal in bony structures. The thermal index, which is an estimate of maximum possible increase in temperature, is nowadays displayed on the monitor of ultrasound scanners. This is helpful information upon which the user may decide to use lower machine output settings or limit examination time to minimize any possible risk from tissue warming. Although diagnostic ultrasound energy can warm tissues by several degrees under some

circumstances, all the evidence points to the conclusion that past and current practice presents no actual risk and may be considered safe.

Ian Donald was the first to obtain well-defined echoes from the fetal head [1]. Stuart Campbell described the use of both the A- and B-mode scan to measure the fetal biparietal diameter [2]. The described method had quickly become standard practice in ultrasound examinations. With the further refinement of the ultrasound technique, crown-rump length, head circumference, femur length, and abdominal circumference became standard measurements for the study of fetal growth known as fetal biometry [3-8]. With the static B-scan, Campbell reported the diagnosis of an anencephalic fetus at 17 weeks [9] and later the diagnosis of a spina bifida [10]. Subsequently, a host of information has appeared on the sonographic detection of fetal anomalies.

The effect that an ultrasound wave reflected by a moving target is shifted in frequency is known as the Doppler effect. Blood consists of a suspension of mainly red cells that move at different velocities and act as point back-scatterers. Therefore, the frequency shift cannot be considered as a single sinusoid waveform but should be considered as a complex waveform consisting of many frequencies. By applying spectral analysis on short time intervals the intensity-weighted frequencies of the Doppler signal plotted against time is called the sonogram or spectrogram. It is the study of these Doppler waveforms that has become known as Doppler velocimetry. To describe the flow velocity waveform, angle independent parameters such as the resistance index [11], the Pulsatile Index [12] and the A/B ratio [13] were utilized. Particularly in umbilical arteries the Pulsatile Index has become the most popular index to indicate disturbed placental resistance. Wladimiroff was the first who described the brain sparing effect by the increase of end diastolic flow in the internal carotid artery of the compromised fetus [14]. Measuring the flow velocity waveform in the middle cerebral artery became standard shortly afterwards. The joint absence or reversal of end-diastolic flow in the umbilical arteries and increase in end-diastolic flow in the middle cerebral artery in the compromised fetus demonstrated that Doppler velocimetry could be applied to identify fetal pathology.

Sturla Eik-nes devised the first hand-held 2D real-time array coupled with a range gated Doppler device to determine human fetal blood flow. A diversity of factors such as operator skill, fetal position, angle of insonation and the pulsatile nature of arteries, do affect accurate measurement of bloodflow. These limitations have been acknowledged right from the beginning [15-18]. Our group adopted the methodology described by Eik-nes and in addition applied the time-distance recorder to obtain the pulsatile diameter of the fetal aorta. It was demonstrated that the accuracy of fetal blood flow measurements could be improved. Good results were derived in an in vitro setting. However, in a sheep experiment Doppler flow in the fetal aorta differed from simultaneously derived magnetic flow up to 17 %. Additional errors up to 19% can occur if the pulsations of the aortic wall are not taken into account in the flow calculation [19]. It was concluded from this study that continuous recording of the pulsatile vessel diameter by a time–distance recorder provides a more correct approach for volume flow calculation.

The time-distance recorder uses the phase-locked echo tracking principle to measure the displacement of moving targets. Initially a window that is slightly smaller than the period time of the ultrasound emitting frequency is positioned such that the zero crossing within an ultrasound reflection of the target appears in the middle of the time window. Each time the echo reflection is received the window is repositioned. The minimal detectable displacement in such systems is very good since it is mainly determined by the clock frequency used in the digital system. This approach is successfully applied for recording arterial diameter changes in the adult as well as the fetal circulation [20-22]. Our group developed such a digital system capable of monitoring the fetal descending aorta and its pulsatile diameter changes along two chosen image lines of a linear array ultrasound scanner. In earlier work using this system, we were able to assess the pulse wave velocity by obtaining pulsatile aortic diameter recordings at two different locations of the fetal descending aorta. Pulse pressure data estimated from aortic diameter recordings and simultaneously derived pulse wave velocities were subsequently published [23].

Two-dimensional flow mapping, nowadays better known as color Doppler, is a fascinating technique first described and successfully applied in the mid 1980's [24]. With

the advancement of computer technology in terms of computational speed and power it has become possible to calculate Doppler shifts in a few thousand sample volumes located in an image plane. For each sample volume the average Doppler shift is encoded as a color and displayed on top of the B-mode image. Color flow mapping has become successful in the assessment of fetal cardiac malformations and has become indispensable in visualizing the fetal circulatory system. New generation broadband beam-forming technology has improved spatial color Doppler resolution. Modern ultrasound equipment is capable of digitally storing the Doppler data gathered at high two-dimensional update rates for off line analysis.

Outline of this thesis

Fetal heart rate gradually decreases from approximately 180 beats per minute at 10 weeks gestation and stabilizes at 150 beats per minute after 15 weeks while beat-to-beat heart rate variability increases from that time. Maturation of vagal function is considered responsible for the gestational age related changes in heart rate and heart rate variability [25]. Autonomic nervous activity causes frequency specific alterations in the heart rate power spectrum. The high frequency band (>0.2 Hz) reflects parasympathetic activity whereas the low frequency band (<0.2 Hz) is influenced by sympathetic control. Their ratio is thus a reflection of sympathovagal balance [26, 27]. Little information is available on sympathetic and parasympathetic control in the early developing fetus or in intrauterine growth restriction. Heart rate variability and arterial flow velocity variability as established by power spectrum analysis could provide further information on fetal sympathetic and parasympathetic development both in uncomplicated early pregnancies (10 – 20 weeks, Chapter 2) and in fetal growth restriction (Chapter 3).

Placental dysfunction may have serious consequences for mother and fetus such as manifestation of pregnancy induced maternal hypertension, preeclampsia and fetal growth restriction. Although Doppler velocimetry can discriminate between fetal physiology and pathophysiology, it has become clear that the predictive values of velocimetry-derived parameters are poor [28]. We hypothesized that quantification of the

interaction between uterine and umbilical Doppler waveforms by means of the magnitude squared coherence function will improve the prediction of placental dysfunction. This hypothesis is tested in a group of 299 pregnant women who had an ultrasound examination at 20 weeks of gestation (Chapter 4).

Epidemiological studies have shown that children born small for gestational age are at higher risk for cardio vascular diseases in later life [29]. In this perspective it is of importance to have tools available to compare cardiovascular development in the normal and growth restricted fetus. Understanding the mechanisms involved in normal growth might lead to strategies to avoid growth restriction. Wall shear stress interacts with endothelial cell function such that ideally blood vessel growth will match with blood flow. In order to better appreciate the complex mechanism by which the physical environment interacts with endothelial cell function detailed information on arterial wall shear stress is needed. Color Doppler cineloops could play a role in this (chapter 5).

Both pressure and flow waveforms are needed to describe a hemodynamic system. Since Doppler information is derived from moving erythrocytes, most studies of the fetal hemodynamic system focus on blood flow velocity or blood flow in the fetal circulation. Without pressure information, important developmental parameters such as peripheral resistance and compliance cannot be measured. Moreover, as in the adults, knowledge of blood pressure might be of vital importance in a life-threatening situation. Indirect pressure estimation could be based on the physical principles that in an elastic tube the wall extension is related to pressure and the elasticity constant of the elastic wall is related to the pulse wave velocity [30]. By modeling the downstream impedance as arterial compliance parallel to the peripheral resistance (Windkessel model), an algorithm could be found to estimate aortic pressure from simultaneously derived aortic blood flow and diameter waveforms (Chapter 6).

Research objectives

We started this research project in order to assess hemodynamic parameters in the fetal and utero-placental circulation, which can be used to study the physiology and pathophysiology of fetal development. Based on the above objectives, this thesis can be summarized as follows:

1. To obtain maternal and fetal variability parameters in heart rate and blood flow velocity to compare mature and developing systems for autonomic regulation of cardiovascular function.
2. To use time domain and frequency domain derived heart rate and umbilical artery flow velocity variability parameters to investigate parasympathetic and sympathetic functional development in the presence of fetal growth restriction.
3. To examine whether the magnitude-squared coherence between uterine and umbilical blood flow velocity waveforms can predict placental dysfunction.
4. To derive from two-dimensional color Doppler cineloops of the fetal descending aorta (i) the fetal aortic blood flow waveform; (ii) the abdominal fetal aortic diameter recording; (iii) the ratio between inertial and viscous forces by means of the so-called Womersley number; (iv) the pressure gradient; and (v) the shear stress in the fetal descending aorta.
5. To estimate fetal blood pressure from two-dimensional color Doppler derived aortic blood flow and diameter waveforms by applying the Womersley model in combination with the two-element Windkessel model.

REFERENCES

1. Donald I, Macvicar J, Brown TG. Investigation of abdominal masses by pulsed ultrasound. Lancet 1958;1:1188-95.
2. Campbell S. An improved method of fetal cephalometry by ultrasound. J Obstet Gynaecol Br Commonw 1968;75:568-76.
3. Thompson HE, Holmes JH, Gottesfeld KR, Taylor ES. Fetal Development as Determined by Ultrasonic Pulse Echo Techniques. Am J Obstet Gynecol 1965;92:44-52.
4. Robinson HP. Sonar measurement of fetal crown-rump length as means of assessing maturity in first trimester of pregnancy. Br Med J 1973;4:28-31.
5. Campbell S, Wilkin D. Ultrasonic measurement of fetal abdomen circumference in the estimation of fetal weight. Br J Obstet Gynaecol 1975;82:689-97.
6. Shepard MJ, Richards VA, Berkowitz RL, Warsof SL, Hobbins JC. An evaluation of two equations for predicting fetal weight by ultrasound. Am J Obstet Gynecol 1982;142:47-54.
7. Hadlock FP, Deter RL, Harrist RB, Park SK. Computer assisted analysis of fetal age in the third trimester using multiple fetal growth parameters. J Clin Ultrasound 1983;11:313-6.
8. Hadlock FP, Deter RL, Harrist RB, Roecker E, Park SK. A date-independent predictor of intrauterine growth retardation: femur length/abdominal circumference ratio. Am J Roentgenol 1983;141:979-84.
9. Campbell S, Johnstone FD, Holt EM, May P. Anencephaly: early ultrasonic diagnosis and active management. Lancet 1972;2:1226-7.
10. Campbell S, Pryse-Davies J, Coltart TM, Seller MJ, Singer JD. Ultrasound in the diagnosis of spina bifida. Lancet 1975;1:1065-8.
11. Planiol T, Pourcelot L. Doppler effect study of the carotid circulation. Proceedings of the 2nd world congress of ultrasound in medicine. New York: American Elsevier Publications Company, 1975.

12. Gosling RG, King DH. Arterial assessment by Doppler-shift ultrasound. Proc R Soc Med 1974; 67:447-9.
13. Stuart B, Drumm J, FitzGerald DE, Duignan NM. Fetal blood velocity waveforms in normal pregnancy. Br J Obstet Gynaecol 1980;87:780-5.
14. Wladimiroff JW, Tonge HM, Stewart PA. Doppler ultrasound assessment of cerebral blood flow in the human fetus. Br J Obstet Gynaecol 1986;93:471-5.
15. Tonge HM, Struijk PC, Wladimiroff JW. Blood flow measurements in the fetal descending aorta: technique and clinics. Clin Cardiol 1984;7:323-9.
16. Tonge HM, Struijk PC, van Kooten C, Wladimiroff JW, Bom N. The first derivative as a means of synchronizing pulsatile flow velocity and vessel diameter waveforms in the fetal descending aorta. J Perinat Med 1988;16:299-304.
17. Eik-Nes SH, Marsal K, Brubakk AO, Kristofferson K, Ulstein M. Ultrasonic measurement of human fetal blood flow. J Biomed Eng 1982;4:28-36.
18. Eik-Nes SH, Marsal K, Kristoffersen K. Methodology and basic problems related to blood flow studies in the human fetus. Ultrasound Med Biol 1984;10:329-37.
19. Struyk PC, Pijpers L, Wladimiroff JW, Lotgering FK, Tonge M, Bom N. The time-distance recorder as a means of improving the accuracy of fetal blood flow measurements. Ultrasound Med Biol 1985;11:71-7.
20. Mori A, Iwabuchi M, Makino T. Fetal haemodynamic changes in fetuses during fetal development evaluated by arterial pressure pulse and blood flow velocity waveforms. Bjog 2000;107:669-77.
21. Sindberg Eriksen P, Gennser G, Lindstrom K, Benthin M, Dahl P. Pulse wave recording -development of a method for investigating foetal circulation in utero. J Med Eng Technol 1985;9:18-27.
22. Hokanson DE, Mozersky DJ, Sumner DS, Strandness DE, Jr. A phase-locked echo tracking system for recording arterial diameter changes in vivo. J Appl Physiol 1972;32:728-33.

23. Struijk PC, Wladimiroff JW, Hop WC, Simonazzi E. Pulse pressure assessment in the human fetal descending aorta. Ultrasound Med Biol 1992;18:39-43.
24. Bonnefous O, Pesque P. Time domain formulation of pulse-Doppler ultrasound and blood velocity estimation by cross correlation. Ultrason Imaging 1986;8:73-85.
25. Wladimiroff J, Seelen JC. Fetal heart action in early pregnancy. Development of fetal vagal function. Europ J Obstet Gynec 1972;2:55-63.
26. Malliani A, Pagani M, Lombardi F, Cerutti S. Cardiovascular neural regulation explored in the frequency domain. Circulation 1991;84:482-92.
27. Akselrod S, Gordon D, Ubel FA, Shannon DC, Berger AC, Cohen RJ. Power spectrum analysis of heart rate fluctuation: a quantitative probe of beat-to-beat cardiovascular control. Science 1981;213:220-2.
28. Hindmarsh PC, Geary MP, Rodeck CH, Kingdom JC, Cole TJ. Intrauterine growth and its relationship to size and shape at birth. Pediatr Res 2002;52:263-8.
29. Barker DJ. Fetal origins of coronary heart disease. Bmj 1995;311:171-4.
30. Womersley JR. Oscillatory flow in arteries: the constrained elastic tube as a model of arterial flow and pulse transmission. Phys Med Biol 1957;2:178-87.

CHAPTER 2

Power spectrum analysis of heart rate and blood flow velocity variability measured in the umbilical artery and uterine artery in early pregnancy

P.C. Struijk, N.T.C. Ursem, J.V. Mathews*, E.B. Clark**, B.B. Keller***

J.W. Wladimiroff

*Department of Obstetrics and Gynaecology, University Hospital Rotterdam-Dijkzigt, The Netherlands, *Department of Electrical Engineering, The University of Utah, Salt Lake City, USA, **Department of Pediatrics, Primary Children's Medical Center, The university of Utah, Salt Lake City, USA, ***Department of Pediatrics, University of Kentucky, USA.*

Ultrasound Obstet Gynecol 2001; 17:316-21.

ABSTRACT

Objective

To compare power spectral derived variability parameters from the fetal side of the placental circulation with the same parameters derived from the maternal side of the placental circulation, during early pregnancy.

Methods

Doppler velocity waveforms were obtained from both the umbilical and uterine artery in a study group of 40 pregnant women between 10–14 (n=25) and 15-20 (n=15) weeks of gestation. The coefficient of variation (CV) of both the beat-to-beat heart rate variability and the blood flow velocity variability was determined. Moreover, the ratio of the integrated low (L) frequency components (<0.2 Hz) and the integrated high (H) frequency components (>0.2 Hz) from normalized power spectrum analysis (LH-ratio) was established, to reflect sympatho-vagal balance.

Results

The CV and LH-ratio of fetal heart rate variability constitute only a fraction of the same maternal heart rate variability parameters. Nevertheless a highly significant increase ($p<0.001$) in LH-ratio could be demonstrated with advancing gestational age.

The CV and LH-ratio of blood flow velocity variability are significantly lower in the fetal umbilical artery only in the 10-14 weeks gestation age group. Due to a decrease of the maternal uterine blood flow velocity variability parameters with advancing gestational age, statistically equal fetal and maternal values for CV and LH-ratio are found in the 15-20 weeks gestation group.

Conclusions

It is concluded that the increase in LH-ratio of fetal heart rate variability indicates functional development of the fetal autonomic nervous system at 15-20 weeks gestation. The umbilical blood flow velocity variability may be secondary to maternal uterine arterial flow variability rather than due to primary changes in fetal cardiovascular function.

INTRODUCTION

Doppler velocimetry of the fetal circulation can accurately characterise cardiac and extra-cardiac arterial and venous blood flow velocities [1,2]. Recently, we published the results of a study concerning the variability of both the fetal heart rate and velocity waveform in the umbilical artery during early human development [3,4,14]. Variability analysis in the frequency domain typically requires long (at least 20 seconds) data records to resolve low (< 0.1 Hz) frequency content. Spectral analysis decomposes variability data in the frequency domain so that a relationship can be established between various frequency components and specific control processes. Typically, the adult heart rate power spectrum demonstrates heart rate variability concentrated in two principal frequency ranges, the high frequency band (above 0.2 Hz) and the low frequency band (below 0.2 Hz) [5-8]. The high frequency band reflects parasympathetic activity, whereas the low frequency band is influenced by combined sympathetic and parasympathetic control [5]. Their ratio is thus a reflection of sympatho-vagal balance [9].

Little information is available on the presence of sympathetic and parasympathetic control in the early developing fetus. Functional parasympathetic regulation of cardiovascular function has been suggested on the basis of a marked reduction in fetal heart rate at 10-15 weeks of gestation [10]. Alternatively, an increase in fetal cardiac stroke volume due to improved cardiac function has been proposed as an explanation for these heart rate changes [4]. Since autonomic nervous activity causes frequency specific alterations in the heart rate power spectrum, the power spectrum analysis of these fluctuations provides a quantitative noninvasive means of assessing the functionality of cardiovascular control.

We measured umbilical and uterine flow velocity waveforms at 10-20 weeks of gestation to determine both maternal and fetal heart rate variability and flow velocity variability as parameters of functional control of the autonomic nervous system [11]. The aim of the study is to establish maternal and fetal variability in heart rate and blood flow velocity to compare developing and mature systems for autonomic regulation of cardiovascular function.

MATERIAL AND METHODS

Subjects

A total of 40 women with a normal singleton pregnancy between 10-20 weeks of gestation participated in the study. Two different gestational age groups were enrolled into the study: 10-14 weeks (group 1; median 12 wks; n=25) and 15-20 weeks (group 2; median 16 wks; n=15). Each woman was included in the study only once. The Hospital Ethics Committee approved the study and women were enrolled following informed consent. Maternal age ranged between 15-41 years (median 30 yrs). Pregnancy duration was estimated from the last menstrual period and confirmed by ultrasound measurement of the fetal crown-rump-length (10-12 wks) or biparietal diameter (12-20 wks) All pregnancies were uncomplicated and resulted in a term delivery of a normal infant with a birth weight between the 10th and 90th centile corrected for maternal parity and fetal sex[15].

Doppler recordings

Ultrasound Doppler studies were performed with a Toshiba SSH 140A (Toshiba corp., Medical Systems Division, Tokyo, Japan). A combined transvaginal real-time and pulsed Doppler system (carrier frequency 6 MHz and 5 MHz, respectively) was used at 10-13 weeks of gestation and a combined transabdominal real-time and pulsed Doppler system (carrier frequency 5.0 MHz and 3.75 MHz, respectively) was applied at 14-20 weeks of gestation. The system operates at power outputs of < 100 mW/cm² spatial peak-temporal average in both imaging and Doppler modes by manufacturer's specification. All Doppler studies were performed with the women in the semirecumbent position and during fetal apnea. The Doppler recordings were performed by one examiner (NTCU). The high pass filter was set at 100 Hz to attenuate low frequency components originating from the vessel wall and the sample volume length was set between 0.2 - 0.3 cm to cover the centre of the umbilical or uterine artery. Flow velocity waveforms from the umbilical artery were obtained from the free-floating loop. For the uterine artery velocity waveforms, the transducer was placed in the lower lateral quadrant of the uterus on the placental side and angled medially until the cross-over of the main uterine artery and

external iliac artery and vein could be identified. This cross-over was used as a reference point to identify the main uterine artery. In two-dimensional color Doppler mode, for both the umbilical and uterine artery the sample volume was placed there where the highest color Doppler velocity was seen, to ensure that the insonation angle was close as possible to zero degrees. A high quality Doppler recording of 20 s duration was selected for each vessel in each patient. Umbilical and uterine artery flow velocity waveforms were obtained in sequence with a time-interval between the Doppler recordings of the two vessels of less than five minutes.

Data processing

Uterine artery and umbilical artery Doppler recordings were stored on sVHS video tape in PAL format using a Panasonic model AG7350 machine (Matsushita Electric Ind Co, Japan). The forward and backward audio signals were digitised at a sampling frequency of 12 kHz using an AD data acquisition board (LabPC+ and BNC-2081 boards, National Instruments, Austin, TX). A digital maximum velocity reconstruction method was used to estimate the maximum velocity envelope. A more detailed description of the maximum velocity reconstruction method has been published previously [3].

The time averaged velocity was calculated from recordings of 20 s duration and used as a threshold to determine the instantaneous heart rate as expressed by the reciprocal of the time interval between successive interpolated threshold crossings. This was followed by calculation of the time-averaged velocity per heartbeat. (Fig 1) For both the umbilical artery and maternal uterine artery, the mean and standard deviation (SD) for all heart beats occurring during the 20s recording were calculated and the coefficient of variation (SD/mean) was taken as a measure of heart rate variability or time averaged flow velocity variability.

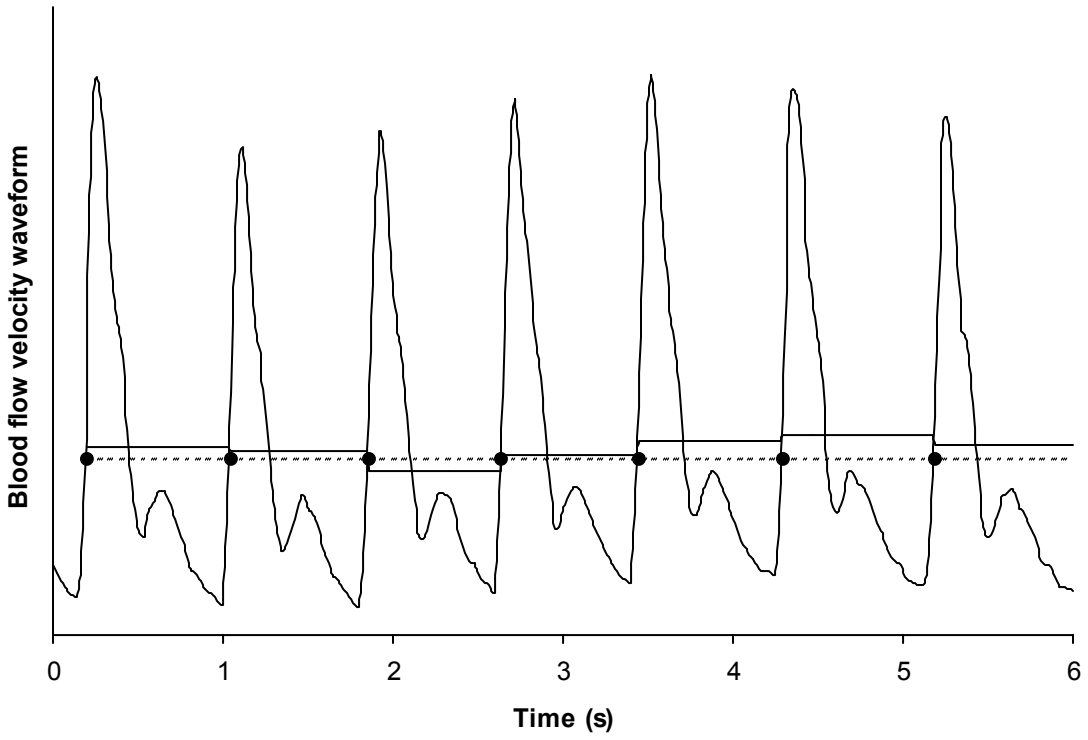

Figure 1. *Sonographic recording of maternal uterine blood flow velocity waveform at 12 weeks of gestation. Dotted line (---) shows threshold level and the threshold crossings* (●)*, bold line shows the time averaged velocity per heartbeat.*

The beat-to-beat data points from all flow velocity waveforms were converted into time series using linear interpolation. After quadratic de-trending, these time series of 20 s were divided into 64 time intervals from which the mean values were taken as data points for spectral analysis resulting in a frequency range from 0.05 to 1.6 Hz. For scaling purposes and to make the velocity tracings angle independent, the data points were expressed as percentages of the mean before Fourier transformation. Two frequency bands were defined: (i) a low-frequency band (LF: 0.05-0.2 Hz) and (ii) a high-frequency band (HF: 0.25-1.6 Hz) [7,12]. The ratio between the integrated power of the LF band and the integrated power of the HF band was used for further analysis (LH-ratio).

The mean data for the two gestational age groups separately (10-14 wks; 15-20 wks) or the entire study period (10-20 wks) as presented in Figure 2 - 5 were calculated by averaging the squared values of the Fourier transform for each frequency bin from 0.05 Hz to 1.6 Hz.

Statistical analysis

The results were expressed as medians and inter quartile ranges (QR). The Wilcoxon signed ranks test was used to compare differences between fetal and maternal derived coefficients of variation and LH-ratios. The Mann-Whitney test was used to compare coefficients of variation and LH- ratios between the two gestational age groups. A p-value of <0.05 was considered statistically significant.

RESULTS

Heart rate variability and time-averaged flow velocity variability derived from umbilical artery and maternal uterine artery flow velocity waveforms are summarised in Tables 1 and 2. Averaged power spectral density (PSD) of heart rate variability and time-averaged flow velocity variability determined from these two vessels are displayed in Figures 2-5.

Fetal circulation (umbilical artery)

The median fetal heart rate decreased significantly ($p<0.001$) from 165 bpm (QR 156-171) at 10-14 weeks to 147 bpm (QR 143-154) at 15-20 weeks of gestation. The median coefficient of variation values demonstrate that fetal heart rate variability did not differ significantly between the two gestational age periods (Table 1). However, the median LH-ratio for fetal heart rate variability increased significantly ($p<0.001$) from 0.05 at 10-14 weeks to 0.17 at 15-20 weeks of gestation (Table 2).

Figure 2 shows that this result is derived from low intensities in the low frequency range of the mean power spectral density distribution at 10-14 weeks, whilst the 15-20 weeks period is characterized by markedly increased low frequency components.

The median coefficient of variation for the umbilical artery time-averaged flow velocity variability is similar between the two gestational age groups (Table 1). The median LH-ratio increased from 0.44 at 10-14 weeks to 0.85 at 15-20 weeks of gestation, but this difference did not reach statistical significance (Table 2). Therefore, in Figure 3 the mean power spectral density distribution for the entire group of 10-20 weeks is demonstrated.

Maternal circulation (uterine artery)

The median maternal heart rate of 75 bpm (QR 70-82) at 10-14 weeks did not differ significantly from the median maternal heart rate of 77 bpm (QR 74-87) at 15-20 weeks of gestation. No statistically significant difference existed between the two gestational age groups for both the median coefficient of variation (Table 1) and median LH-ratio for maternal heart rate variability (Table 2).

Figure 4 depicts the mean power spectral density distribution for maternal heart rate variability for the total group of 40 fetuses at 10 to 20 weeks of gestation.

Table 1. *Coefficients of variation for heart rate variability and blood flow velocity variability in the umbilical artery and maternal uterine artery for the two gestational age groups: 10-14 weeks (n=25) and 15-20 weeks (n=15).*

Coefficients of variation (%)

	Heart rate variability			*Blood flow velocity variability*		
	Gestation (wks)		p value	Gestation (wks)		p value
	10-14	15-20	M-W test	10-14	15-20	M-W test
Umbilical artery	0.74 (0.65-0.91)	1.09 (0.53-1.47)	0.332	3.27 (2.53-4.50)	3.25 (1.84-4.85)	0.783
Uterine artery	4.23 (3.15-4.86)	4.48 (3.17-6.08)	0.472	4.76 (3.43-6.16)	3.35 (2.77-4.25)	0.015
p value (Wilcoxon test)	< 0.001	0.001		0.013	0.955	

Table 2. *Low frequency band (0.05 – 0.2 Hz) to high frequency band (> 0.2 Hz) ratio for heart rate variability and blood flow velocity variability in the umbilical artery and maternal uterine artery for the two gestational age groups: 10-14 weeks (n=25) and 15-20 weeks (n=15).*

Low frequency band / high frequency band ratio

	Heart rate variability			*Blood flow velocity variability*		
	Gestation (wks)		p value	Gestation (wks)		p value
	10-14	15-20	M-W test	10-14	15-20	M-W test
Umbilical artery	0.05 (0.03-0.09)	0.17 (0.09-0.45)	< 0.001	0.44 (0.31-0.96)	0.85 (0.45-1.44)	0.078
Uterine artery	0.95 (0.45-2.83)	1.33 (0.69-2.09)	0.740	4.11 (2.52-6.42)	1.31 (0.46-2.51)	0.001
p value (Wilcoxon test)	< 0.001	0.001		< 0.001	0.496	

A high intensity peak in the low frequency band with a second peak representing respiration frequency at 0.3 - 0.4 Hz, describes the frequency distribution of maternal heart rate variability. A statistically significant decrease ($p = 0.015$) was established for the median coefficient of variation regarding the time averaged flow velocity variability in the maternal uterine artery from 10 - 14 to 15 - 20 weeks of gestation (Table 1). Similarly, a statistically significant decrease ($p = 0.001$) was found for the median LH-ratio during this gestational age period. (Table 2).

The graphic presentation of the mean power spectral density distribution in Figure 5 shows a highly concentrated peak in the low frequency band at 10-14 weeks, whereas at 15-20 weeks the low frequency peak is reduced by more than half with a second peak appearing in the high frequency band around 0.35 Hz.

Comparison between umbilical artery and maternal uterine artery flow velocity derived parameters.

Comparison of umbilical artery and maternal uterine artery flow velocity waveforms showed highly significant differences for the heart rate derived parameters at both 10-14 and 15-20 weeks of gestation. Regarding the median LH-ratio for heart rate variability, there was a significant increase from fetus to mother at both 10-14 weeks and 15-20 weeks of gestation (Table 2). The median coefficient of variation and median LH-ratio for time-averaged flow velocity variability were statistically significantly different between the umbilical artery and maternal uterine artery flow velocity waveforms at 10-14 weeks but not at 15-20 weeks of gestation.

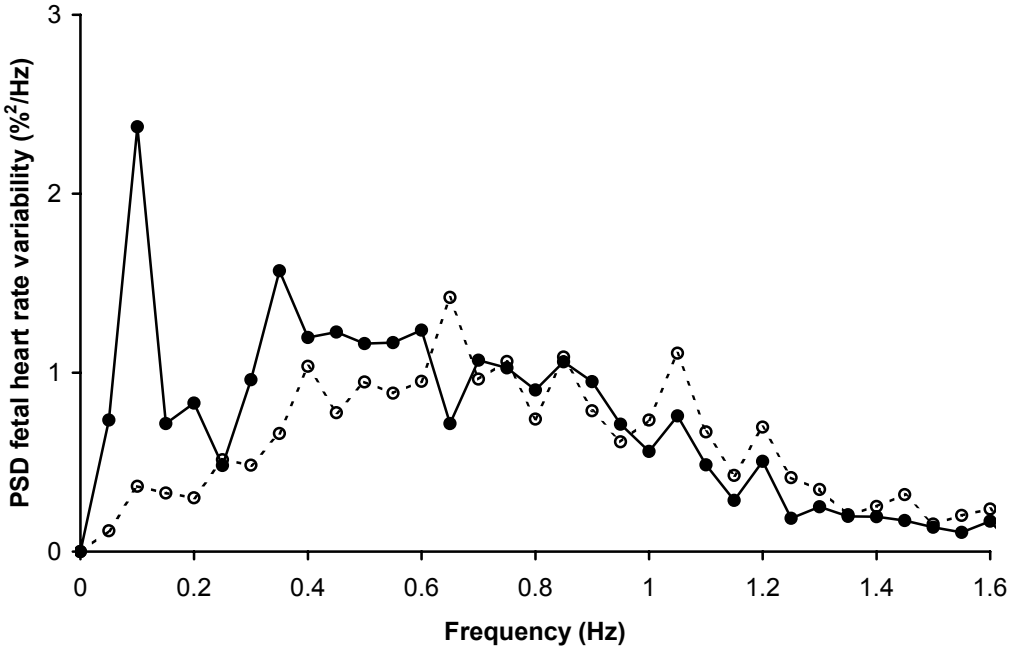

Figure 2. *Mean power spectral distribution for the fetal heart rate variability; open circles* (○) *and dashed line* (---) *represent the 10-14 wks gestational age group (N = 25) and filled circles* (●) *and solid line* (—) *represent the 15-20 wks group (N=15).*

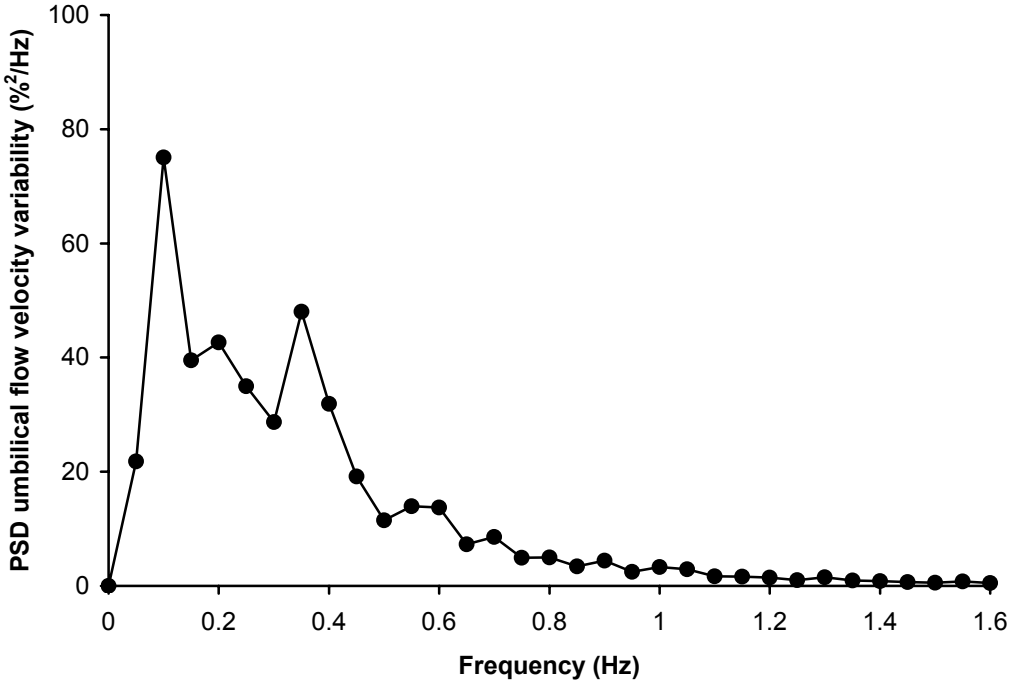

Figure 3. *Mean power spectral distribution (PSD) for the umbilical blood flow velocity variability; filled circles (•) and solid line* (—) *represent the total group (N = 40).*

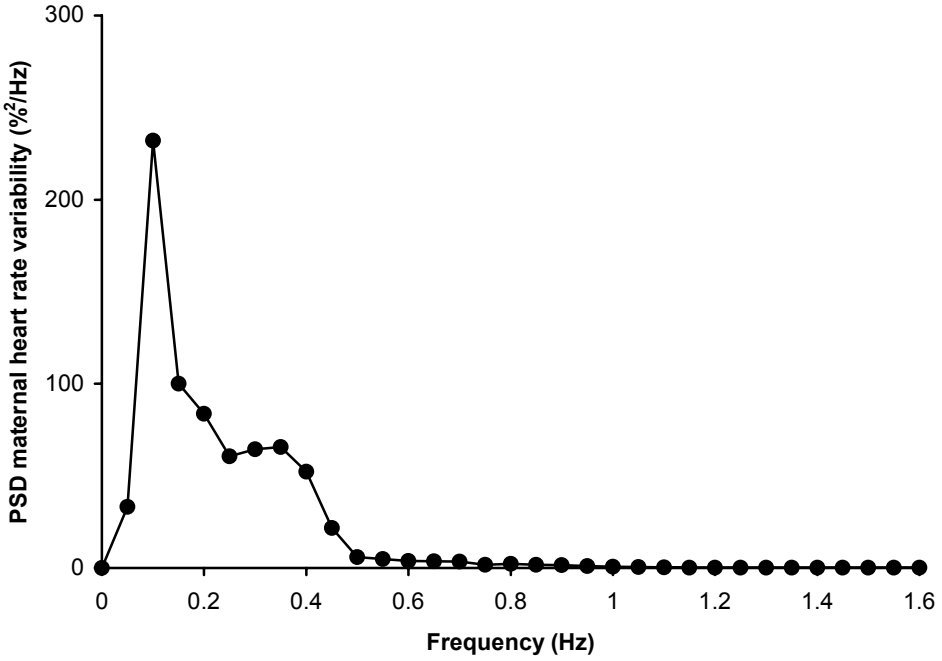

Figure 4. *Mean power spectral distribution (PSD) for the maternal heart rate variability; filled circles* (•) *and solid line* (—) *represent the total 10-20 wks gestational age group (N = 40).*

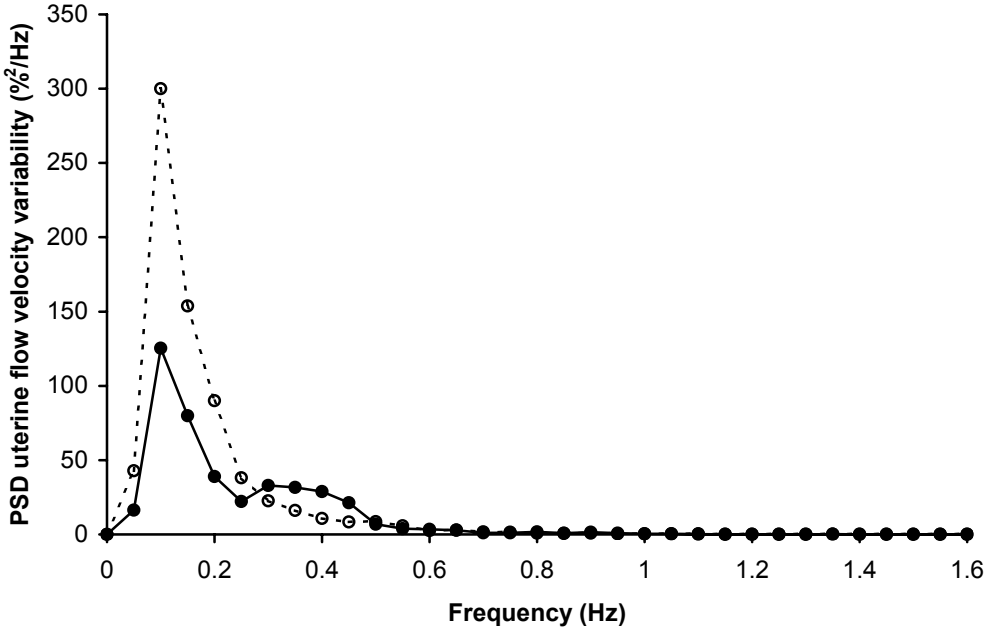

Figure 5*. Mean power spectral distribution (PSD) for the uterine blood flow velocity variability, open circles* (○) *and dashed line (---) represent the 10-14 wks gestational age group (N=25) and filled circles* (•) *and solid line* (—) *represent the 15-20 wks gestational age group (N=15).*

DISCUSSION.

This study demonstrates that in the early developing fetus prior to 15 weeks of gestation, the low frequency components of heart rate variability distribution are almost absent. From animal experiments and adult human studies it is known that the low frequency band is influenced by combined sympathetic and parasympathetic control, whereas the high frequency band primarily reflects parasympathetic control. Their ratio is thus a reflection of the sympatho-vagal balance [4-8]. The very small low-frequency components together with a very low LH-ratio strongly suggest almost complete absence of combined sympathetic and parasympathetic control under 15 weeks of gestation. From 15 - 20 weeks of gestation, a significant increase in LH-ratio associated with an increase in the mean integrated power of low frequency components of the heart rate variability frequency distribution can be seen. Fetal heart rate variability is contributed only a quarter of the heart rate variability of the mother. Nevertheless we hypothesize that the increase in LH-ratio indicates the functional development of the fetal autonomic nervous system during this gestational age period. Parasympathetic innervation may precede the sympathetic system, since various vagal agonists and antagonists have caused the expected pharmacological effects as early as the 8th gestational week [13]. It is unlikely though that all the basic requirements for an effective autonomic control system like the presence of nerves in the heart and great vessels, the ability of the nerve terminals to produce active neurotransmitters, the presence of an effector organ and the existence of functioning receptors in the effector organ are present in the 15 – 20- week-old fetus [13].

The frequency distribution of maternal heart rate variability is similar to previous reports on the adult circulation [12], including a respiration peak associated with cyclic variation of intrathoracic pressure, which mechanically perturbs venous return, pulmonary vascular and aortic pressures, and a cyclic variation in heart rate through centrally mediated mechanisms. Furthermore, cyclic variations in arterial blood pressure influence heart rate through the autonomically mediated baroreceptor reflex [12]. In a recent sheep study it was shown that there is attenuation of baroreceptor mediated sympathetic effects on the maternal heart during pregnancy [16]. No differences in maternal heart rate variability could

be found between the two gestational age periods suggesting that the growing fetus between 10 and 20 weeks of gestation does not influence maternal autonomic state.

Blood flow velocity variability in the umbilical artery is directly influenced by changes in placental perfusion, while variations in uterine arterial blood flow reflects changes in both uterine and placental perfusion. In the placenta, the situation is even more complex since one has to consider both the hemodynamics of the mother as well as the fetus, and possibly an interaction between the two. These fluctuations in peripheral resistance in turn can perturb both fetal and maternal central blood pressure and through the baroreceptor reflex, may lead to compensatory variations in heart rate.

In contrast to the fetal heart rate variability distribution, where the low frequency component is absent in the early gestational age period, the umbilical blood flow velocity variability distribution shows a low frequency component throughout the gestational age period of 10 – 20 weeks. We hypothesize that the fluctuations in the umbilical blood flow velocity are mainly determined by the mother due to the observation that neither the coefficient of variation nor the LH-ratio are significantly different in the two gestational age periods. On the maternal side of the utero-placental circulation, a strong low frequency component is present in the uterine blood flow velocity variability distribution during early gestation. In the gestational age period from 15 – 20 weeks, when trophoblast invasion reduces the resistance of the utero placental system, the uterine flow velocity variability distribution changes significantly and blood flow velocity distributions are statistically similar on both sides of the placenta. Alternatively, the presence of the syncytiotrophoblast and smaller surface area of the immature villous vascular tree may provide an effective barrier attenuating maternal hemodynamic influences.

Although not currently technically feasible, it would be of considerable interest to record both uterine and umbilical blood flow velocities simultaneously. In that case accurate analysis methods can be applied to determine possible cross-correlation and interactions between maternal and fetal hemodynamics. From our data we conclude that the umbilical blood flow velocity variability may be secondary to maternal uterine arterial flow variability rather than due to primary changes in fetal cardiovascular function.

REFERENCES

1. Van Splunder IP, Stijnen T, Wladimiroff JW. Fetal atrioventricular flow-velocity waveforms and their relation to arterial and venous flow-velocity waveforms at 8-20 weeks of gestation. Circulation 1996;94:1372-1378.
2. Wladimiroff JW, Huisman TW, Steward PA. Fetal and umbilical flow velocity waveforms between 10-16 weeks gestation: a preliminary study. Obstet Gynecol 1991;78:812-814
3. Ursem NTC, Brinkman HJF, Struijk PC, Hop WCJ, Kempsky MH, Clark EB, Keller BB, Wladimiroff JW. Umbilical waveform analysis based on maximum, mean and mode velocity in early human pregnancy. Ultrasound Med Biol 1998;24:1-7.
4. Ursem NTC, Struijk PC, Hop WCJ, Clark EB, Keller BB, Wladimiroff JW. Heart rate and flow velocity variability as determined from umbilical Doppler velocimetry at 10 – 20 weeks of gestation. Clin Science 1998;95:539-545.
5. Akselrod S, Gordon D, Uble FA, Shannon DC, Barger RJ. Power spectrum analysis of heart rate fluctuation: A quantitative probe of beat-to-beat cardiovascular control. Science 1981;213:220- 222
6. Hyndman BW, Kitney RI, Sayers BM. Spontaneous rhythms in physiological control systems. Nature 1971;233(5318):339-341.
7. Finley JP, Nugent ST. Periodicities in respiration and heart rate in newborns. Can J Physiol Pharmacol 1983;61(4):329-335.
8. Pomeranz B, Macaulay JB, Caudill MA, Kutz I, Adam D, Gordon D, Kilborn KM, Barger AC, Shannon DC, Cohen TJ, et al. Assessment of autonomic function in humans by heart rate spectral analysis.. Am J Physiol 1985;248(17):H151-153.
9. Malliani A, Pagani M, Lombardi F, Cerutti S. Cardiovascular neural regulation explored in the frequency domain. Circulation 1991;84(2):482-92
10. Wladimiroff JW, Seelen JC. Fetal heart action in early pregnancy. Development of fetal vagal function. Europ J Obstet Gynecol 1972;2:55-63.

11. Breborowicz G, Moczko J, Dzinowski J. Quantification of the fetal heart rate variability by spectral analysis in growth-retarded fetuses. Gynecol Obstet Invest 1988;26:188-195.
12. Akselrod S, Gordon D, Madwed JB, Snidman NC, Shannon DC, Cohen RJ. Hemodynamic regulation: investigation by spectral analysis. Am J Physiol 1985;249(18):H867-75.
13. Hirch M, Karin J, Akselrod S. Heart rate variability in the fetus. In Heart Rate Variability, (eds) Malik M and Camm JA. Futura publishing company, Armonk, NY 1995,517-532
14. Ursem NTC, Kempsky MH, De Ridder MAJ, Clark EB, Keller BB, Wladimiroff JW. An estimate of fetal autonomic state by spectral analysis of human umbilical artery blood flow velocity. Cardiovasc Res 1998;37:601-605.
15. Kloosterman G. On intrauterine growth. Int J Obstet Gynaecol 1970;8:895-912.
16. Lumbers ER, Yu ZY. A method for determining baroreflex mediated sympathetic and parasympathetic control of the heart in pregnant and non-pregnant sheep. J Physiol (Lond) 1999; 515:555-566.

CHAPTER 3

Fetal heart rate and umbilical artery flow velocity variability in intrauterine growth restriction

A.S.M. Vinkesteijn, P.C. Struijk, N.T.C. Ursem, W.C.J. Hop *, J.W. Wladimiroff

*Department of Obstetrics and Gynaecology, University Hospital Rotterdam-Dijkzigt, The Netherlands; *Department of Epidemiology and Biostatistics, Erasmus University Rotterdam, The Netherlands.*

Ultrasound Obstet Gynecol 2004; 23:461-5

ABSTRACT

Objectives

To study heart rate and umbilical artery blood flow velocity variability in growth-restricted fetuses and investigate the influence of the autonomic nervous system on these parameters.

Methods

Doppler velocity waveforms were collected from long-lasting umbilical artery recordings in 15 fetuses with growth restriction and 15 normal age-matched controls at 23–35 weeks of gestation. Absolute heart rate and umbilical artery blood flow velocity as well as the coefficient of variation were determined. Using power spectral analysis the low- and high-frequency bands of heart rate variability and blood flow velocity variability were calculated. The low-to-high (LH) ratio of heart rate variability and blood flow velocity variability were examined as a measure of sympathovagal balance.

Results

In growth-restricted fetuses umbilical artery velocities were significantly reduced. Heart rate variability was significantly reduced in the presence of growth restriction, but no significant difference was demonstrated for blood flow velocity variability. The LH ratio for heart rate variability was significantly decreased in growth restriction, but no difference in LH ratio was demonstrated for blood flow velocity variability.

Conclusion

Flow velocity variability in growth restriction seems not to be predominantly influenced by the autonomic nervous system, whereas the decreased heart rate variability seems to be influenced by altered sympathetic–parasympathetic balance.

INTRODUCTION

An estimated 3–10% of pregnancies are complicated by fetal growth restriction [1], and it remains the second leading known cause of fetal death [2]. Clinical monitoring of the fetal heart rate (FHR) pattern is widely used to determine fetal well-being in the presence of intrauterine growth restriction. Characteristic changes in FHR patterns associated with growth restriction include a reduction in FHR variability, number and amplitude of FHR accelerations and fetal movements [3–5]. Several methods have been developed for computerized analysis of FHR with the aim of accurately and reproducibly measuring FHR variability [6,7].

Doppler flow velocity waveform studies in the growth-restricted fetus have shown characteristic changes in the umbilical artery reflecting raised downstream impedance and, therefore, raised placental resistance [8,9]. In earlier studies we introduced the reconstruction of maximum flow velocity waveforms (envelope) from the umbilical artery from continuous Doppler audio data using computer algorithms [10]. This approach allowed us to establish flow velocity variability and heart rate variability patterns from umbilical artery waveform recordings lasting at least 18 s, reflecting hemodynamic regulation in the developing fetus. In pregnancies complicated by pregnancy-induced hypertension or insulin-dependent diabetes mellitus, significant changes in umbilical artery flow velocity variability and heart rate variability were found [11,12]. Heart rate variability is influenced by the autonomic nervous system and increases with advancing gestational age as the parasympathetic system matures [13]. Using power spectral derived variability parameters, sympathovagal balance can be examined. Previous studies have demonstrated that in animals and in the adult human, the low-frequency component of heart rate variability is influenced by combined sympathetic and parasympathetic control, whereas the high-frequency band is mainly a reflection of parasympathetic control. Their ratio is thus a reflection of sympathovagal balance [14,15].

No information is available on umbilical artery flow velocity variability as determined from long-lasting continuous Doppler flow recordings in fetal growth restriction. We hypothesize that in the presence of fetal growth restriction changes in hemodynamic

regulation occur which are reflected by umbilical artery flow velocity waveform patterns, heart rate variability and changes in sympathovagal balance. Heart rate variability and blood flow velocity variability were therefore determined from long-lasting Doppler velocity waveform recordings in the umbilical artery. Power spectral derived variability parameters were used to investigate parasympathetic and sympathetic functional development in the presence of fetal growth restriction.

METHODS

Subjects

During the period of December 1998 to August 1999, 30 pregnant women with a singleton pregnancy were selected from our out-patient clinic and consented to participate in a prospective, cross-sectional and age-matched control study at 23–35 weeks of gestation. Gestational age was calculated from the last menstrual period and confirmed by ultrasound measurements of fetal crown–rump length or fetal biparietal diameter. The hospital ethics review board approved the study.

Fifteen of the women had presented with fetal growth restriction. These pregnancies were selected according to the following criteria: (i) reliable menstrual dates; (ii) abdominal circumference below the 5th centile of the reference chart according to Snijders and Nicolaides [16]; (iii) fetal birth weight below the 5th centile according to the Kloosterman tables corrected for maternal parity and fetal sex [17]; (iv) no fetal congenital abnormalities. Two women developed pregnancy-induced hypertension, defined as a blood pressure of 140/90 mmHg or higher during the second half of pregnancy in a previously normotensive woman. One woman developed preeclampsia, defined as pregnancy-induced hypertension in combination with proteinuria of at least 300 mg/L.

The remaining 15 women served as normal controls matched for gestational age. All pregnancies progressed uneventfully and resulted in the term delivery of a healthy infant with a birth weight between the 10th and 90th percentiles corrected for maternal parity and fetal sex according to the Kloosterman tables [17]. Patient characteristics are given in Table 1.

***Table 1**. Patient characteristics for pregnancies with fetal growth restriction (FGR) and normal controls*

Characteristic	*FGR* (n =*15)*	*Controls* (n =*15)*
Maternal age (years, median (range))	30 (23–42)	29 (20–37)
Gestational age at examination (weeks, median (range))	29 (23–35)	29 (23–35)
Parity (*n*)		
Nulliparous	7	4
Parous	8	11
Fetal abdominal circumference (*n*)		
< p2.3	11	—
p2.3–p5	4	—
> p10	—	15
Gestational age at delivery (weeks, median (range))	30 (24–37)	39 (37–41)
Intrauterine death (*n*)	4	—
Cesarean section (*n*)		
Fetal distress	9	—
Other	1	4
Vaginal delivery (*n*)	5 (IUFD *n*=4)	11
Birth weight (*n*)		
< p2.3	11	—
p2.3–p5	4	—
> p10	—	15

Fetal abdominal circumference according to Snijders and Nicolaides [16], birth weight according to the Kloosterman [17] tables corrected for maternal parity and fetal sex. p, percentile; IUFD, intrauterine fetal death.

The median time interval between the ultrasound examination and delivery was 10 (range, 1–29) days in the growth-restricted subset and 10 (range, 4–18) weeks in the normal subset.

Fetal distress as an indication for Cesarean section was defined as an abnormal cardiotocogram pattern with decreased variability and/or decelerations.

The perinatal mortality rate was 25% in the growth-restricted fetuses (four cases of intrauterine death) as opposed to nil in the normal subset.

Doppler recordings

Doppler recordings were performed using a Toshiba SSH 140A (Toshiba Corp., Medical systems Division, Tokyo, Japan) ultrasound machine equipped with a 5-MHz transabdominal transducer. The system operates at power outputs of below 100 mW/cm^2 spatial peak temporal average in both imaging and Doppler modes according to the manufacturer's specifications. All Doppler studies were carried out with the woman in a semi-recumbent position and during fetal apnea. Flow velocity waveforms from the umbilical artery were obtained from a free-floating loop of the umbilical cord. The angle of insonation was always less than 15°.

Data processing

Umbilical artery Doppler recordings were stored on sVHS videotape in PAL format using a Panasonic model AG7350 (Matsushita Electric Ind Co, Takutsuki, Osaka, Japan) machine. The forward and backward audio signals were digitized at a sampling frequency of 12 kHz using an AD data acquisition board (LabPC + and BNC-2081 boards, National Instruments, Austin, TX, USA). A digital maximum velocity reconstruction method was used to estimate the maximum velocity envelope.

Time-averaged velocity was calculated from the long lasting recordings and used as a threshold to determine the instantaneous heart rate as expressed by the reciprocal of the time interval between successive interpolated threshold crossings. This was followed by calculation of the time-averaged velocity per heart beat. The mean and SD for all heart beats occurring during the 18–49-s recordings were calculated and the coefficient of

variation (SD/mean) was taken as a measure of heart rate variability or time-averaged flow velocity variability.

The beat-to-beat data points from all flow velocity waveforms were converted into time series using linear interpolation. After quadratic de-trending, these time series of 18–49 s were divided into 64 time intervals from which the mean values were taken as data points for spectral analysis, resulting in a frequency range of 0.05–1.6 Hz. To normalize the y-axis of the velocity waveforms, the data points were expressed as percentages of the mean prior to Fourier transformation. Two frequency bands were defined: (i) a low-frequency band (0.05–0.20 Hz) and (ii) a high-frequency band (0.25–1.60 Hz). The ratio between the integrated power of the low-frequency band (L) and that of the high frequency band (H) was used for further analysis (LH ratio).

The pulsatility index was calculated by dividing the difference between the maximum and minimum flow velocities by the time-averaged velocity. The mean data for the growth restricted and control groups, as presented in the figures, were calculated by averaging the squared values of the Fourier transform for each frequency bin from 0.05–1.6 Hz.

Statistical analysis

Hemodynamic parameters were compared between cases with intrauterine growth restriction and normal controls using a paired Wilcoxon's test. A p-value of <0.05 was considered to be statistically significant.

RESULTS

The mean duration of a technically acceptable umbilical artery waveform recording was 22 (range, 18–49) s. Table 2 demonstrates the median and interquartile ranges of the hemodynamic parameters in both growth-restricted fetuses and normal controls.

Table2 *Median and quartile range for hemodynamic parameters in the umbilical artery from pregnancies complicated by fetal growth restriction (FGR) and normal controls and the p-values of the paired differences (Wilcoxon's ranked test)*

Parameter	*FGR (*n *=15)*	*Controls (*n *=15)*	p
Heart rate (bpm)	142 (137–150)	141 (137–147)	0.7
Pulsatility index	2.20 (1.67–2.69)	0.94 (0.84–1.18)	0.001
Peak systolic velocity (mm/s)	264 (247–309)	396 (344–463)	0.001
Time-averaged velocity (mm/s)	116 (98–161)	259 (224–325)	0.001
End-diastolic velocity (mm/s)	−1(−27–44)	144 (104–184)	0.001
SD heart rate (bpm)	2.16 (1.30–2.86)	3.26 (2.11–4.72)	0.02
SD time-averaged velocity (mm/s)	5.38 (3.78–7.44)	7.99 (5.99–12.08)	0.003
CV heart rate (%)	1.4 (1.0–2.0)	2.3 (1.3–3.2)	0.03
CV time-averaged velocity (%)	3.9 (3.1–5.4)	3.4 (2.6–4.3)	0.2
LH ratio heart rate	1.14 (0.54–1.41)	3.03 (0.65–3.90)	0.03
LH ratio time-averaged velocity	0.44 (0.21–0.66)	1.12 (0.42–2.53)	0.07

CV, coefficient of variation; LH ratio, ratio between the integrated power of the low-frequency band (L) and that of the high-frequency band (H).

In the presence of fetal growth restriction, umbilical artery peak systolic velocity, time-averaged velocity and end-diastolic velocity were significantly reduced, and nine growth-restricted fetuses showed reversed end-diastolic flow. The same parameters increased significantly with advancing gestational age in both subsets. The PI was significantly raised in growth-restricted fetuses compared with the normal controls.

In the growth-restricted group, the SDs for FHR and time-averaged velocity were significantly decreased.

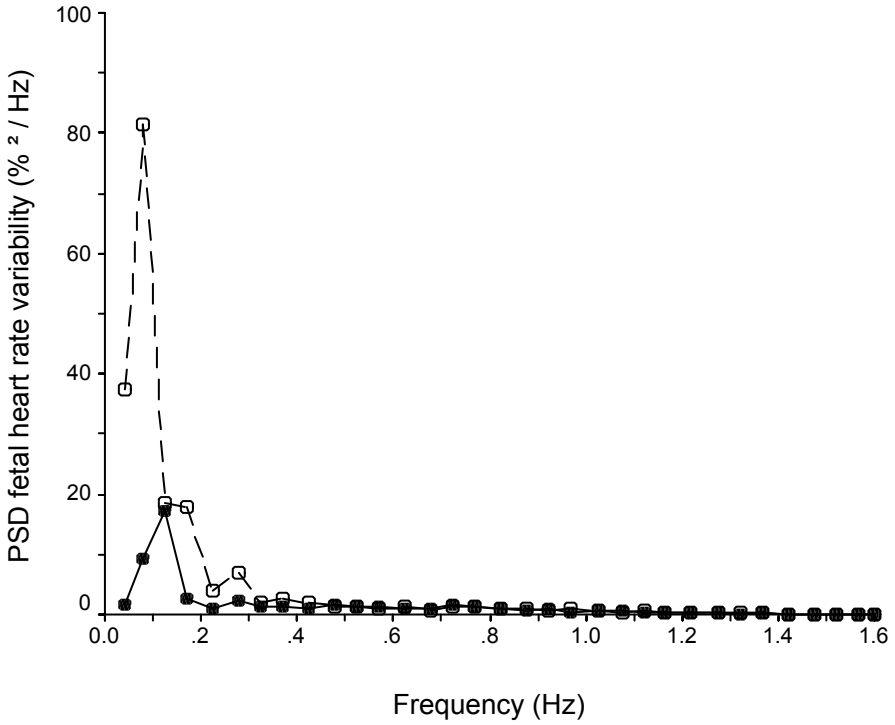

Figure 1. *Mean power spectral distribution (PSD) for fetal heart rate variability in growth-restricted fetuses (●) and in normal controls (○).*

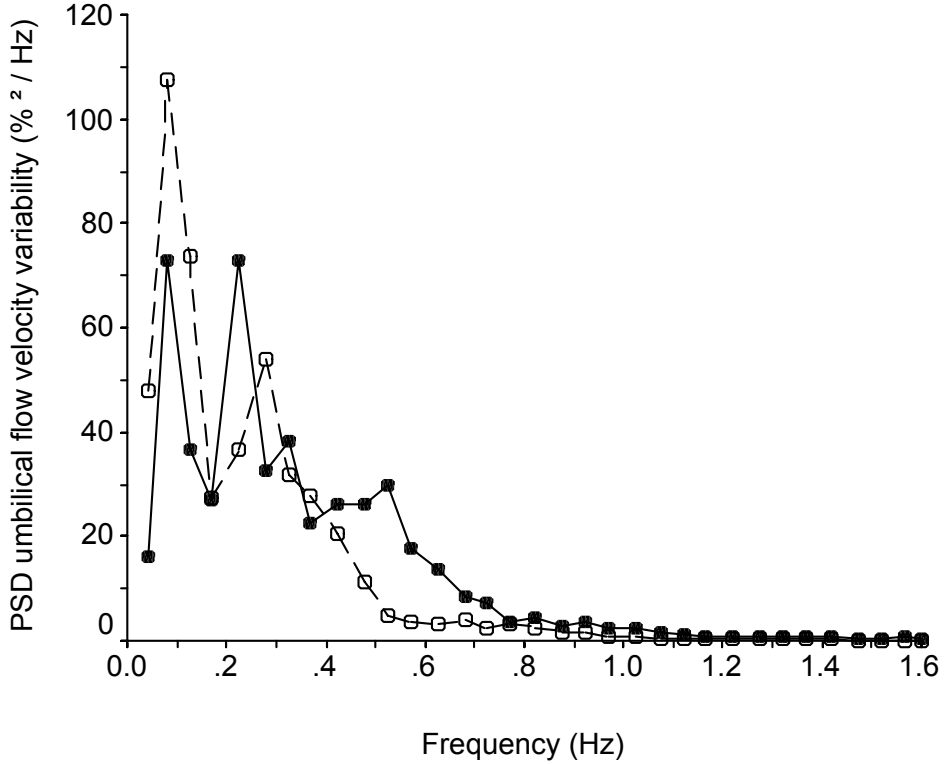

Figure 2. *Mean power spectral distribution (PSD) for umbilical artery time-averaged flow velocity variability in growth-restricted fetuses (●) and in normal controls (○).*

The coefficient of variation for heart rate variability was significantly decreased; no statistically significant difference could be demonstrated for the coefficient of variation of the umbilical time-averaged velocity between the normal and growth-restricted groups. Figures 1 and 2 display mean power spectral distribution for FHR variability and time-averaged velocity variability for both subsets. The LH ratio for heart rate variability was significantly decreased in growth-restricted cases; no difference was found for the LH ratio for time-averaged velocity variability.

DISCUSSION

In the presence of fetal growth restriction, umbilical artery peak systolic, time-averaged and end-diastolic velocities are significantly reduced. Since volume flow is equal to time-averaged velocity multiplied by vessel area, it has been postulated that volume flow correlates to some extent with time-averaged velocity. A decrease in umbilical artery peak systolic and time-averaged velocities could be secondary to a decrease in volume flow. Since volume flow is related to fetal weight, a reduction in volume flow is likely on the basis of the reduced fetal birth weight in the growth-restricted group as shown in Table 1.

A change in peak systolic velocity could be the result of altered cardiac contractile function. Changes in contractile function of the ventricle could also result in altered volume flow. In pregnancies complicated by fetal growth restriction with absent umbilical artery end-diastolic flow, alterations in left ventricular function and even a fall in cardiac output have been demonstrated [18]. Finally, the afterload that is determined by blood pressure and resistance may play a role. The raised PI in the umbilical artery suggests an increase in downstream impedance.

Time-averaged velocity variability as expressed by the coefficient of variation was not significantly different between the two groups. Power spectral analysis of time averaged blood flow velocity demonstrated a clear peak around the maternal respiratory frequency. Previously, we demonstrated the same peak in fetuses at 10–20 weeks of gestation. When comparing the gestational age periods of 10–14 weeks and 15–20 weeks, no difference in LH ratio was found, suggesting that maturation of the autonomic nervous system does not affect flow velocity variability [19]. It was therefore suggested that the fluctuations in the umbilical blood flow velocity are determined mainly by maternal hemodynamics, including maternal intervillous pressure changes associated with maternal heart rate [19,20]. The present study demonstrated no difference in LH ratio for time-averaged velocity between the two groups. This could mean that the influence of the autonomic nervous system on flow velocity variability was the same for the two groups, or that flow velocity variability was not predominantly influenced by the autonomic nervous system.

In growth-restricted fetuses, heart rate variability was significantly reduced. Several previous studies have demonstrated that in fetal growth restriction heart rate variability is reduced as determined from FHR recordings [3,4,21]. We used long-lasting Doppler waveform recordings from the umbilical artery to determine heart rate variability and the sympathovagal balance by using power spectral analysis.

Umbilical cord blood obtained by cordocentesis or at elective Cesarean section demonstrated that reduced FHR variability and the occurrence of decelerations coincide with fetal hypoxemia [22,23]. Since our growth-restricted subset showed reduced heart rate variability, some degree of hypoxemia could be assumed. Alternatively, fetal lamb studies provided strong evidence of increased sympathetic influence on the fetal heart during acute hypoxemia, which is predominantly the result of increased adrenomedullary secretion of catecholamines [24]. This would result in an increased LH ratio. This discrepancy could be the result of the fact that in the sheep studies acute hypoxemia was provoked whereas in fetal growth restriction hypoxemia is more likely to be chronic.

The decreased LH ratio for heart rate variability could be a sign of abnormal maturation of the autonomic nervous system. Parasympathetic innervation of the mammalian fetus precedes development of the sympathetic system [25]. The LH ratio for heart rate variability increases with advancing gestational age. A previous study in our center demonstrated that this is the case in normal pregnancies from 10 to 14 and from 15 to 20 weeks of gestation [19]. The decreased LH ratio in fetal growth restriction could reflect delayed maturation of the autonomic nervous system.

Alternatively, the decreased LH ratio for heart rate variability could be a sign of normal development and function of the fetal autonomic nervous system. In fetal growth restriction, the fetal circulation demonstrates redistribution of blood flow in favor of the brain [26,27]. There are reduced fetal movements and heart rate variability is decreased. This could be the result of increased parasympathetic influence as an adjustment to the pathological situation of growth restriction.

In conclusion, we postulate that flow velocity variability in growth restriction seems not to be predominantly influenced by the autonomic nervous system, whereas the decreased heart rate variability seems to be influenced by altered sympathetic–parasympathetic balance.

REFERENCES

1. Divon MY, Hsu HW. Maternal and fetal blood flow velocity waveforms in intra-uterine growth retardation. Clin Obstet Gynecol 1992; 35: 156–71.
2. Witter FR. Perinatal mortality and intra-uterine growth retardation. Curr Opin Obstet Gynaecol 1993; 5: 56–9.
3. Kariniemi V, Ammala P. Short-term variability of fetal heart rate during pregnancies with normal and insufficient placental function. Am J Obstet Gynecol 1981; 139: 33–7.
4. Henson G, Dawes GS, Redman WG. Characterisation of the reduced heart rate variation in growth-retarded fetuses. Br J Obstet Gynaecol 1984; 91: 751–755.
5. Gagnon R, Hunse C, Bocking AD. Fetal heart rate patterns in the small-for gestational-age human fetus. Am J Obstet Gynecol 1989; 161: 779–84.
6. Fisher WM, Stude I, Brandt H. A suggestion for the evaluation of the antepartal cardiotocogram. Z Geburtshilfe Perinatol 1976; 180: 117–23.
7. Dawes GS, Moulden M, Redman CW. System 8000: computerized antenatal FHR analysis. J Perinat Med 1991; 19: 47–51.
8. Trudinger BJ, Warwick BG, Cook CM, Bombardieri J, Collins L. Fetal umbilical artery flow velocity waveforms and placental resistance: clinical significance. Br J Obstet Gynaecol 1985; 92: 23–30.
9. Groenenberg IA, Wladimiroff JW, Hop WC. Fetal cardiac and peripheral arterial flow velocity waveforms in intrauterine growth retardation. Circulation 1989; 80: 1711–17.
10. Ursem NTC, Brinkman HJF, Struijk PC, Hop WCJ, Kempski MH, Keller BB, Wladimiroff JW. Umbilical artery waveform analysis based on maximum, mean and mode velocity in early pregnancy. Ultrasound Med Biol 1998; 24: 1–7.
11. Ursem NT, Clark EB, Keller BB, Hop WC, Wladimiroff JW. Do heart rate and velocity variability derived from umbilical artery velocity waveforms

change prior to clinical pregnancy induced hypertension? Ultrasound Obstet Gynecol 1999; 14: 244–9.

12. Ursem NT, Clark EB, Keller BB, Wladimiroff JW. Fetal heart rate and umbilical artery velocity variability in pregnancies complicated by insulin-dependent diabetes mellitus. Ultrasound Obstet Gynecol 1999; 13: 312–6.
13. Gagnon R, Campbell K, Hunse C. Patterns of human fetal heart rate accelerations from 26 weeks to term. Am J Obstet Gynecol 1987; 157: 743–8.
14. Akselrod S, Gordon D, Uble FA, Shannon DC, Barger RJ. Power spectrum analysis of heart rate fluctuations: a quantitative probe of beat-to-beat cardiovascular control. Science 1981; 213: 220–2.
15. Malliani A, Pagani M, Lombardi F, Cerutti S. Cardiovascular neural regulation explored in the frequency domain. Circulation 1991; 84: 482–92.
16. Snijders RJM, Nicolaides KH. Fetal biometry at 14–40 weeks' gestation. Ultrasound Obstet Gynecol 1994; 4: 34–48.
17. Kloosterman G. On intrauterine growth. Int J Obstet Gynecol 1970; 8: 895–912.
18. Rizzo G, Arduini D. Fetal cardiac function in intra-uterine growth retardation. Am JObstet Gynecol 1991; 165: 876–82.
19. Struijk PC, Ursem NTC, Mathews J, Clark EB, Keller BB, Wladimiroff JW. Power spectrum analysis of heart rate and blood flow variability measured in the umbilical and uterine arteries in early pregnancy: a comparative study. Ultrasound Obstet Gynecol 2001; 17: 316–21.
20. Power G, Longo LD. Sluice flow in placenta: maternal vascular pressure effects on fetal circulation. Am J Physiol 1973; 225: 1490–96.
21. Snijders RJM, Ribbert LSM, Visser GHA, Mulder EJH. Numeric analysis of heart rate variation in intra-uterine growthretarded fetuses: A longitudinal study. Am J Obstet Gynecol 1992; 166: 22–7.
22. Smith JH, Anand KJS, Cotes PM. Antenatal fetal heart rate variation in relation to the respiratory and metabolic status of the compromised human fetus. Br J Obstet Gynaecol 1988; 95: 980–9.

23. Visser GHA, Sadovsky G, Nicolaides KH. Antepartum heart rate patterns in small-for-gestational age third trimester fetuses: correlations with blood gas values obtained at cordocentesis. Am J Obstet Gynecol 1990; 162: 698–703.
24. Yu ZY, Lumbers ER, Gibson KJ, Stevens AD. Effects of hypoxemia on foetal heart rate variability and cardiac rhythm. Clin Exp Pharmacol Physiol 1998; 25: 577–84.
25. Hirsch M, Karin J, Akselrod S. Heart rate variability in the fetus. In Heart Rate Variability, Malik M, Camm AJ, eds. Futura Publishing Company, Inc.: Armonk, NY, 1995.
26. Wladimiroff JW, Tonge HM, Stewart PA. Doppler assessment of cerebral blood flow in the human fetus. Br J Obstet Gynaecol 1986; 93: 471–75.
27. Campbell S, Vyas S, Nicolaides KH. Doppler investigation of the fetal circulation. J Perinat Med 1991; 19: 21–6.

CHAPTER 4

The magnitude-squared coherence function between the uterine and umbilical flow velocity waveforms as an additional predictor of placental dysfunction

P. C. Struijk, K. L. Fernando [*], V.J. Mathews [*], E.A.P. Steegers, J.W. Wladimiroff, E.B. Clark**, M.W. Varner[***].

*Department of Obstetrics & Gynecology, Erasmus MC, Division Obstetrics and prenatal medicine, Rotterdam, The Netherlands, *Department of Electrical and Computer Engineering, The University of Utah, Salt Lake City, ** Department of Pediatrics, The University of Utah, Salt Lake City, *** Departments of Obstetrics & Gynecology, The University of Utah, Salt Lake City and Mc-Kay-Dee Hospital Center, Ogden, Utah.*

Submitted for publication

ABSTRACT

Objectives.

To examine whether the magnitude-squared coherence between uterine and umbilical blood flow velocity waveforms can in conjunction with estimated fetal weight, uterine and umbilical pulsatility indices, fetal and maternal heart rates, diastolic notching and the amniotic fluid index, create a sensitive and specific model for the prediction of placental dysfunction.

Study design.

Binary logistic prediction models are created for preeclampsia, pregnancy induced hypertension and fetal growth restriction in a study group of 284 unselected mid trimester pregnancies. In each pathological subset the median value of derived parameters were compared with the uncomplicated pregnancy control group.

Results.

For preeclampsia the mid trimester magnitude coherence and uterine artery diastolic notching were found statistically significant predictors. The magnitude coherence did not improve prediction of intrauterine growth restriction or pregnancy induced hypertension.

Conclusions.

The inclusion of magnitude-squared coherence may improve the identification of pregnancies subsequently complicated by preeclampsia.

INTRODUCTION

Preeclampsia (PE), pregnancy induced hypertension (PIH) and fetal growth restriction (FGR) are common pregnancy complications that are associated with placental dysfunction and increased perinatal morbidity and mortality [1]. Evidence exists linking these conditions to sub-optimum placental development early in pregnancy, long before the pregnancy complications are clinically manifest [2]. As a result, it should be possible to detect altered placental function prior to the onset of symptoms. This capability would allow for appropriate antenatal management of at-risk pregnancies as well as identification of pregnancies at low risk for complications. Over the last decade a number of studies have demonstrated that pregnancies with abnormal uterine [2-5] or umbilical [2, 6, 7] artery Doppler velocimetry are at higher risk for adverse fetal outcome. Despite the advancement in ultrasound technology there is not a test available that is highly sensitive and specific to predict adverse fetal outcome in pregnancy.

Doppler flow studies have demonstrated that umbilical artery blood flow velocity waveforms interact with environmental pressure changes. When women move from either the standing or the lateral position to the supine position the umbilical pulsatility index rapidly increases which indicates rise in vascular resistance [8, 9]. This phenomenon could be explained by compression of the very thin and elastic vasculo-syncytial membranes of the terminal villi [10].

In a previous study we showed that prior to 15 weeks gestation despite almost absence of fetal beat-to-beat heart rate variability power spectral analysis showed similarity between umbilical and uterine flow velocity variability including a peak at the maternal respiration frequency in both spectra [11]. From this study it is suggested that intervillous pressure fluctuations might induce umbilical flow velocity variability. The dynamic placenta model described by Talbert and Sebire supports this theory [12, 13]. The barrier between maternal and fetal blood, the so-called vasculo-syncytial membranes of the human placental terminal villi, is very permeable to water [14]. The high permeability of this membrane to water implies that the time average pressure on each side of the membrane should be in equilibrium to prevent excessive water transport from the fetus to the mother or, with a reverse pressure gradient, water entry from the mother to the fetus [13]. This so

called transmural pressure is dynamic and there is continual fluctuation because of pulsatility in the fetal and maternal circulations [15]. The membrane of the terminal villi will move inwards with compression and move outwards with relaxation increasing and decreasing the intra-villous volume and resistance to flow in a complex rhythm determined by both the fetal and maternal heart beat frequency. As a consequence, a frequency component at the maternal heart rate should be present in the umbilical blood flow velocity waveform. Similarly, a frequency component at the fetal heart rate should be present in the uterine velocity waveform.

In summary, there is a critical balance between intra and intervillous pressure. We hypothesize that any disturbance of this balance might be reflected by altered uterine and umbilical flow velocity interaction and indicate placental dysfunction.

The magnitude-squared coherence function [16] is a measure of the correlation between two signals in the frequency domain. In this paper, we evaluate the magnitude-squared coherence between blood flow velocity waveforms in the uterine and umbilical arteries at the maternal and the fetal heart rate to describe the interaction between maternal and fetal blood flow velocity waveforms. The objective of the study is to examine whether the magnitude-squared coherence function at the fetal and maternal heart rate could, in conjunction with estimated fetal weight, uterine and umbilical pulsatility indices, fetal and maternal heart rates, diastolic notching and the amniotic fluid index, create a sensitive and specific model for the prediction of placental dysfunction.

MATERIAL AND METHODS

Subjects

Between October 2003 and September 2004 pregnant women visiting the Maternal-Fetal Medicine Outpatient Clinic of the McKay-Dee Hospital in Ogden (Utah) for a mid trimester ultrasound examination were asked to participate in this study. The hospital Ethics Committee approved the study and written informed consent was obtained from each of the 299 women agreeing to participate in the study. Nine women were lost to follow up and six women were excluded because of incomplete data sets.

A woman was classified as belonging to a control subset if her pregnancy was uncomplicated and she delivered a healthy child at more than 36 weeks of gestation whose birth weight was between the 5th and 95th percentile reference lines of the Hadlock weight standard [17]. A patient with diastolic blood pressures greater than 90 mmHg on two different occasions during pregnancy, but with no proteinuria, was diagnosed as belonging to the pregnancy induced hypertension (PIH) group. If hypertension occurred with an episode of significant proteinuria, defined as more than 300 mg protein in a 24-hour urine collection or at least 2+ protein by dipstick, PE was diagnosed. Finally, the FGR group composed of pregnancies, not belonging to the PIH or PE groups, resulting in children whose birth weight was below the 5th percentile.

Ultrasound recordings

Ultrasound examination was performed with an Acuson Sequoia 512 ultrasound device (Acuson, Inc. Mountain View, CA), using a 6.0 MHz transabdominal transducer. Morphometric measurements on all fetuses included biparietal diameter, head and abdominal circumferences and femur length. The fetal weight was estimated using the Hadlock formula [18]. The estimated fetal weight and birth weight are expressed as z-scores using the Hadlock weight standard [17]. The four-quadrant amniotic fluid index was measured using the technique of Phelan and associates [19].

Doppler flow velocity waveforms from the umbilical artery were obtained from a free-floating loop of the umbilical cord, typically near the placental insertion to minimize movement artifacts. For the uterine artery velocity waveforms, the transducer was placed

in the lower lateral quadrant of the uterus on the placental side and angled medially until the cross-over of the main uterine artery and the external iliac artery and vein could be identified. This cross-over was used as a reference point to identify the main uterine artery. In two-dimensional color Doppler mode, the sample volume was placed on the spot where the highest color Doppler velocity was seen for both the umbilical and uterine artery to ensure that the insonation angle was as close as possible to zero degrees. The forward and backward Doppler audio signals, digitized at 12 kHz, were transferred to an external computer for offline analysis. Umbilical and uterine artery flow velocity recordings of approximately 30-second duration were obtained in sequence with a time-interval between the Doppler recordings of the two vessels of less than five minutes.

Offline analysis

The bloodflow velocity waveform was reconstructed from the audio signals using the modified geometric method for maximum frequency estimation [20]. The pulsatility index was defined as the maximum velocity minus the end diastolic velocity divided by the time averaged velocity. The mean value of all heartbeats during the registration period was calculated and used for further analysis. The maternal and fetal heart rates were derived from the first peak of the autocorrelation function of the velocity waveforms. The coherence function measures the similarity between two signals in the frequency domain. If the sequences $x(n)$ *and* $y(n)$ represent the uterine and umbilical artery flow velocity waveform then the magnitude-squared coherence between the two signals is

$$C_{xy}(f) = \frac{\left|S_{xy}(f)\right|^2}{S_{xx}(f)S_{yy}(f)}$$

where S_{xy} is the cross spectral density of the two waveforms, S_{xx} and S_{yy} are the power spectral densities of the individual waveforms and f is the frequency variable. The magnitude-squared coherence, which takes values between zero and one, is calculated at the maternal and the fetal heart rates [21]. The magnitude-squared coherence analysis is independent of phase differences and delays between two signals. Consequently, this function will remain the same for sequentially and simultaneously collected maternal and fetal blood flow velocity waveforms as long as the relationships among the signals do not change during the data collection interval. Signal stability is assumed during the time-

interval of less than five minutes between the Doppler recordings. We use sequentially collected data because simultaneous collection resulted in data with significant signal interference. MATLAB software version 6.5 release 13 (The Mathworks Inc.; Natick, MA, USA) for Windows 2000 professional was used to perform all the calculations on a Pentium *4* computer.

Statistical analysis

The variables used in the analysis are summarized by the median and interquartile range (IQR) and comparisons between groups were made using the Mann-Whitney U test. Statistical significance was defined as a p value < 0.05. In the study group of 284 pregnant women the risk of FGR as reflected by small for gestational age delivery, PIH and PE was modeled using binary logistic regression. Statistically significant effects and interactions were identified by backward stepwise elimination using the likelihood ratio test. The probability criterion for stepwise entry was set to 0.05 and for removal from the equation to 0.1. All statistical analysis was performed using the SPSS statistical package (SPSS Inc Chicago, IL) version 11.1.

RESULTS

The characteristics of the 284 subjects of this study and their pregnancy outcomes are summarized in Table I. The median values and the inter-quartile range of the body mass index of the mothers when presented for delivery were available from 49,480 Utah birth records in the year 2003. Comparison of the values associated with our study, with data from this large sample indicates that the body mass indexes of the study group are representative for Utah residents.

A total of 18 children was born small for gestational age, two in the PE group and two in the PIH group. The remaining 14 children with a birth weight < 5th percentile were born in the FGR group. The *z*-score for birth weight in the FGR group (N=14) ranged from -2.96 to -1.65.

Two hundred and sixteen women serving as the control group gave birth to a healthy child with birth weight between the 5th and 95th percentile at >= 37 weeks of gestation. The median value of the birth weight expressed as its *z*-score is -0.2 (IQR = -0.7, 0.4) in the control group. The z-score for birth weight in the PIH group (N=9), –0.68 (IQR = –1.6, -0.08) is statistically not different from that of the control group. In the preeclamptic group (N=8) the median *z*-score is -1.1 (IRQ = -2.2, 0.1).

The median and the IQR as well as the frequency of nulliparity and uterine artery diastolic notching in the pathological subsets are compared with those of the control group in Table II. On ultrasound examination the median z-score of the estimated fetal weight was significantly lower in the FGR group compared with the control group. In the PIH group the amniotic fluid index was statistically significantly lower while the maternal heart rate was significantly higher than that of the control group. The amniotic fluid index and the coherence at the maternal heart rate were both significantly lower in the preeclamptic group.

The prediction results and variables selected in the binary logistic models are summarized in Table III. In the group of 284 subjects the fetal heart rate, uterine and umbilical artery pulsatility indices and coherence at the fetal heart rate did not reach statistical significance in the binary logistic prediction models for FGR, PIH and PE.

Table I. *Patient characteristics and fetal outcome.*

Age at birth (years)	Median (IQR)	27 (24,31)
Height (cm)	Median (IQR)	165 (160,170)
BMI at birth	Median (IQR)	29 (26, 33)
Gestational age at exam (wks)	Median (IQR)	19.7 (18.9, 20.4)
Notching	N (%)	
Diastolic notch		37 (13)
No notch		247 (87)
Parity	N (%)	
Nulliparous		101 (35.6)
Multiparous		183 (64.4)
Pregnancy complications	N (%)	
Preeclampsia		8 (2.8)
Pregnancy induced hypertension		9 (3.2)
Type I diabetes mellitus		1 (0.4)
Gestational diabetes		6 (2.1)
Proteinuria		4 (1.4)
Chronic hypertension		3 (1.1)
Rh-D isoimmunization		1 (0.4)
Beta-Haemolytic streptococcus		4 (1.4)
Chlamydia		1 (0.4)
Intra uterine fetal death		2 (0.7)
Pregnancy outcome		
Gest. age at delivery (wks)	Median (IQR)	39.0 (38.1, 39.4)
Gest. age < 37 wks	N(%)	15 (5.3)
Birth weight (grams)	Median (IQR)	3312 (3014, 3573)
Birth weight < P_5	N (%)	18 (6.3)
Birth weight > P_{95}	N (%)	8 (3.2)

The z-score for estimated fetal weight and the amniotic fluid index at mid pregnancy are predictive factors for FGR. As could be expected, pregnancies with low z-scores for estimated weight at mid pregnancy are at a higher risk to give birth to a small for gestational age child. The risk is even higher if the amniotic fluid index is high at mid gestation.

Table II. *Characteristics of the control group and pathological subsets.*

	Control group	FGR	PIH	PE
GA at examination (wks)	19.7	20.1	18.9	19.0
Median (IQR)	(18.9, 20.4)	(19.0, 21.0)	(18, 19.7)	(17.9, 19,9)
GA at birth (wks)	39.0	39.2	39	37.7
Median (IQR)	(38.4, 39.6)	(38.3, 39.4)	(37.6, 39.4)	(36.2, 39.3)
Maternal age (years)	27	26	23	27
Median (IQR)	(24, 31)	(22, 30)	(21, 33)	(23, 34)
Nulliparous – N (%)	78 (36)	6 (43)	4 (44)	4 (50)
Diastolic Notching - N (%)	22 (10)	4 (29)	3 (33)	3 (38)
Z-score est. weight at exam	0.20	-0.51*	0.40	-0.12
Median (IQR)	(-0.34, 0.69)	(-1.64, 0.44)	(-0.35, 1.15)	(-0.99, 0.85)
Amniotic fluid index (cm)	13.7	14.9	12.8*	11,7*
Median (IQR)	(12.3, 15.2)	(12.8, 17.0)	(10.8, 13.4)	(10.7, 13.0)
Fetal HR (bpm)	148	149	150	145
Median (IQR)	(143, 153)	(145, 155)	(145, 152)	(141, 154)
PI umbilical art.	1.30	1. 10	1.43	1.42
Median (IQR)	(1.18, 1.42)	(0.99, 1.21)	(1.20, 1.55)	(1.01, 1.64)
Maternal HR (bpm)	80	83	91*	81
Median (IQR)	(75, 89)	(77, 85)	(84, 99)	(74, 94)
PI uterine artery	0.80	0.68	0.82	0.85
Median (IQR)	(0.64, 1.08)	(0.48, 0.93)	(0.68, 1.21)	(0.62, 1.31)
Coherence at MHR (%)	33	22	38	19*
Median (IQR)	(21, 48)	(16, 33)	(21, 68)	(10, 27)
Coherence at FHR (%)	27	17	21	24
Median (IQR)	(14, 49)	(11, 46)	(7, 29)	(14, 33)

* *$p < 0.05$ according to the Mann Whitney U test. FGR (Fetal Growth Restriction), PIH (pregnancy induced hypertension) and PE (preeclampsia) groups are compared with the control group.*

Increased maternal heart rate and the existence of diastolic notching in the uterine artery waveform are risk factors for PIH. In spite of the statistically significantly lower median value for amniotic fluid index in PIH women compared with normal controls this variable

could not contribute to a better prediction in the presence of maternal heart rate and diastolic notching in the binary logistic model. The odds ratio for maternal heart rate seems to be small but it should be considered that heart rate is expressed in beats per minute. To calculate the odds ratio for a pregnant woman whose heart rate is 10 beats per minute above average the odds ratio of 1.071 should be raised to the power of 10, which is about 2.

The risk factors found for PE are the magnitude-squared coherence at the maternal heart rate and diastolic notching. As with the prediction of PIH the relative low amniotic fluid index could not contribute to a better risk prediction for PE. On a zero to one scale for the magnitude squared coherence the odds ratio is smaller than 0.001. To avoid these small numbers we have chosen a zero to hundred-percentage scale for the magnitude squared coherence values.

The odds ratio is an estimate for relative risk. To calculate the relative risk to develop PE for a woman whose magnitude squared coherence at the maternal heart rate is 10% below average, the odds ratio of 0.921 should be raised to the power of –10, which is 2.278. If in this example diastiolic notching is present in the uterine artery blood flow velocity waveform, the relative risk to develop PIH equals approximately 12 which is the product of the odds ratio for the coherence value (2.278) and the odds ratio for the presence of notching (5.291).

Table III. *Binary logistic regression results.*

	Variables selected□	Threshold (%)•	Sensitivity (%)	Specificity (%)	Odds ratio	95% confidence interval	
FGR	Z-score est. weight	6.5	71	78	0.423	0.229	0.780
	Amniotic Fluid				1.232	1.011	1.502
PIH	Maternal HR	3.5	78	73	1.071	1.008	1.137
	Diastolic notch				3.654	0.847	15.77
PE	Coherence MHR	5	75	72	0.921	0.861	0.986
	Diastolic notch				5.219	1.107	24.61

□ *Variables selected in the binary logistic model.* • *Women were considered screened positive if the probability was above this predicted risk level. FGR; fetal growth restriction, PIH; pregnancy induced hypertension, PE; preeclampsia.*

DISCUSSION

In the PIH and the PE groups the median amniotic fluid indices are statistically significantly lower compared with the control group although all values were found within the 5th and 95th reference range [22]. In contrast the amniotic fluid index was relatively higher in the FGR group. In this series a fetus at 20 weeks of gestation with a high amniotic fluid index is more at risk for idiopathic FGR. Since the latter finding may appear counter intuitive, it must be emphasized that FGR assorted with known causes (PE 2; PIH 2) is not included in the FGR group. Furthermore, since the amniotic fluid index in these FGR pregnancies was measured at mid pregnancy it is not known if olygohydramnios developed later in pregnancy.

Sebire and Talbert have presented an interesting hypothetical model of fetal mechanisms with emphasis on the importance of the fluid balance between mother and fetus [13, 15]. A cotyledon consists of a number of fetal villous trees with tips anchored in the basal plate surrounding a spiral artery outlet. Blood from the spiral artery will stretch the fetal villous trees outwards forming a hollow globular shape as a result of the transcotyledonery flow resistance [12]. A failure of the spiral arteries to transform from high resistance arteries to low resistance pathways during pregnancy might result in low intervillous pressure. The pressure on the other side of the membrane of the terminal villi, the so-called intravillous pressure would drive water from the fetal circulation to the mother and this may lead to oligohydramnios [15]. It is likely that the fetus attempts to control its fluid volume with a corresponding increase in vasoconstrictive hormone production, which could cross into the maternal circulation. Inadequate remodeling of the spiral arteries and consequently poor perfusion of the intervillous space is widely accepted as the primary pathophysiology of PE and to a certain extent for PIH [1]. The reduced amniotic fluid index in these groups likely indicates the inability of the fetus to fully compensate for poor utero-placental perfusion. Based on a large antenatal care trial it was recently stated that preeclampsia and unexplained fetal growth restriction, often assumed to be related to placental insufficiency, seem to be independent biologic entities [1]. Our finding that increased instead of decreased amniotic fluid index is predictive for unexplained FGR seems to underline this statement.

In this series women destined to develop PIH or PE were more likely to have diastolic notching of the uterine artery Doppler waveform. Increased maternal heart rate is observed in the PIH group. Moreover, the logistic regression analysis demonstrates that maternal heart rate contributes significantly to the prediction of hypertension.

Since the magnitude-squared coherence function is a measure of the correlation between two signals in the frequency domain, the mean magnitude coherence value at the maternal heart rate of 19% (0.19) in the PE group can be considered as a lack of coherence. Using a mathematical model of the uteroplacental circulation, Talbert demonstrated that increased flow resistance of the spiral arteries does not introduce notching in the uterine flow velocity waveform, but reduces centre cotyledon pressure while the pulsatile part of the pressure waveform is almost absent due to filtering [12]. This is consistent with the lack of coherence found in the PE group. After all, if maternal pressure pulsations are absent coherence at the maternal heart rate with the fetal circulation is impossible. In Talbert's mathematical model it is also demonstrated that notching in the uterine artery flow velocity waveform is associated with increased uterine and arcuate artery compliances and not with increased flow resistance. According to this model notching reflects uterine and arcuate compliances while a lack of coherence might reflect high spiral artery resistance. Our finding that both notching and coherence contribute to the prediction of PE is consistent with this theory.

The mean magnitude squared coherence value at the maternal heart rate of 33% (0.33) between uterine and umbilical flow velocity waveforms found in uncomplicated mid pregnancies can be interpreted as a moderate correlation. The pressure waveforms in the centres of human cotyledons are unknown. The moderate coherence in uncomplicated pregnancies and the significant lack of coherence at the maternal heart rate in PE pregnancies along with its predictive value produce evidence for the existence of pulsatile pressure in centre-cotyledons in human uncomplicated pregnancies. This study provides no evidence for the existence of pulsatile pressure in the capillary villi, indicating that there are limited pulsations or that they are absent.

In a recent large English study consisting of more than 32000 pregnant women it was demonstrated that the presence of a diastolic notch and the pulsatility index of the uterine artery blood flow velocity waveform were predictive factors for preeclampsia [4]. We

speculate that the sensitivity and specificity of this observation can be further improved if the coherence at the maternal heart rate is included in future studies that target women with risk factors such as a family history of preeclampsia [24, 25], nulliparity, obesity, or underlying micro vascular diseases [4].

Although these preliminary results are encouraging, larger studies will be necessary to validate these prediction formulas. Large multicenter studies, like the English study introduced above [4] are needed to develop prediction formulas that can be applied for screening purposes. However, it can be concluded from this study that the inclusion coherence at the maternal heart beat frequency may significantly improve the prediction of PE.

Nevertheless, it must also be emphasized that a single prediction model is unlikely to identify all pregnancy-related diseases. Refinement of this technique for identification of women at low risk for placental dysfunction also deserves further study. The combination of these inexpensive bedside ultrasound measures with more sophisticated – and currently much more expensive – genomics, proteomics and metabolomics analysis, also holds great potential, perhaps akin to the integrated maternal serum and ultrasound screens now being utilized for Down Syndrome screening [26]. The objective of further study should be to optimally discriminate those pregnancies destined to develop complications from those that will remain uncomplicated.

REFERENCES

1. Villar J, Carroli G, Wojdyla D, et al. Preeclampsia, gestational hypertension and intrauterine growth restriction, related or independent conditions? Am J Obstet Gynecol 2006;194:921-31.
2. Baschat AA, Hecher K. Fetal growth restriction due to placental disease. Semin Perinatol 2004;28:67-80.
3. Papageorghiou AT, Yu CK, Nicolaides KH. The role of uterine artery Doppler in predicting adverse pregnancy outcome. Best Pract Res Clin Obstet Gynaecol 2004;18:383-96.
4. Yu CK, Smith GC, Papageorghiou AT, Cacho AM, Nicolaides KH. An integrated model for the prediction of preeclampsia using maternal factors and uterine artery Doppler velocimetry in unselected low-risk women. Am J Obstet Gynecol 2005;193:429-36.
5. Campbell S, Diaz-Recasens J, Griffin DR, et al. New doppler technique for assessing uteroplacental blood flow. Lancet 1983;1:675-7.
6. Fong KW, Ohlsson A, Hannah ME, et al. Prediction of perinatal outcome in fetuses suspected to have intrauterine growth restriction: Doppler US study of fetal cerebral, renal, and umbilical arteries. Radiology 1999;213:681-9.
7. Spinillo A, Bergante C, Gardella B, Mainini R, Montanari L. Interaction between risk factors for fetal growth retardation associated with abnormal umbilical artery Doppler studies. Acta Obstet Gynecol Scand 2004;83:431-5.
8. Marx GF, Patel S, Berman JA, Farmakides G, Schulman H. Umbilical blood flow velocity waveforms in different maternal positions and with epidural analgesia. Obstet Gynecol 1986;68:61-4.
9. van Katwijk C, Wladimiroff JW. Effect of maternal posture on the umbilical artery flow velocity waveform. Ultrasound Med Biol 1991;17:683-5.
10. Karimu AL, Burton GJ. The effects of maternal vascular pressure on the dimensions of the placental capillaries. Br J Obstet Gynaecol 1994;101:57-63.
11. Struijk PC, Ursem NT, Mathews J, Clark EB, Keller BB, Wladimiroff JW. Power spectrum analysis of heart rate and blood flow velocity variability measured in the

umbilical and uterine arteries in early pregnancy: a comparative study. Ultrasound Obstet Gynecol 2001;17:316-21.

12. Talbert DG. Uterine flow velocity waveform shape as an indicator of maternal and placental development failure mechanisms: a model-based synthesizing approach. Ultrasound Obstet Gynecol 1995;6:261-71.
13. Talbert D, Sebire NJ. The dynamic placenta: I. Hypothetical model of a placental mechanism matching local fetal blood flow to local intervillus oxygen delivery. Med Hypotheses 2004;62:511-9.
14. Sibley CP, Boyd DH. Mechanisms of transfer across the human placenta. Philadelhia: Saunders, 1992.
15. Sebire NJ, Talbert D. The dynamic placenta: II. Hypothetical model of a fetus driven transplacental water balance mechanism producing low apparent permeability in a highly permeable placenta. Med Hypotheses 2004;62:520-8.
16. Kay SM. Modern Spectral Estimation. In: Prentice Hall, ed. New Jersey: Englewood Cliffs, 1988.
17. Hadlock FP, Harrist RB, Martinez-Poyer J. In utero analysis of fetal growth: a sonographic weight standard. Radiology 1991;181:129-33.
18. Hadlock FP, Harrist RB, Sharman RS, Deter RL, Park SK. Estimation of fetal weight with the use of head, body, and femur measurements--a prospective study. Am J Obstet Gynecol 1985;151:333-7.
19. Phelan JP, Ahn MO, Smith CV, Rutherford SE, Anderson E. Amniotic fluid index measurements during pregnancy. J Reprod Med 1987;32:601-4.
20. Fernando KL, Mathews VJ, Clark EB. A mathematical basis for the application of the modified geometric method to maximum frequency estimation. IEEE Trans Biomed Eng 2004;51:2085-8.
21. Fernando KL, Mathews VJ, Varner MW, Clark EB. Prediction of Pregnancy-Induced Hypertension using Coherence Analysis. Proceedings of IEEE International Conference on Acoustics, Speech and Signal Processing, Montreal, Canada, 2004.
22. Moore TR, Cayle JE. The amniotic fluid index in normal human pregnancy. Am J Obstet Gynecol 1990;162:1168-73.

23. Yu CK, Lakasing L, Papageorghiou AT, Spencer K, Nicolaides KH. Uterine artery Doppler and mid-trimester maternal plasma homocysteine in subsequent pre-eclampsia. J Matern Fetal Neonatal Med 2004;16:134-9.
24. Esplin MS, Fausett MB, Fraser A, et al. Paternal and maternal components of the predisposition to preeclampsia. N Engl J Med 2001;344:867-72.
25. van Dijk M, Mulders J, Poutsma A, et al. Maternal segregation of the Dutch preeclampsia locus at 10q22 with a new member of the winged helix gene family. Nat Genet 2005;37:514-9.
26. Malone FD, Canick JA, Ball RH, et al. First-trimester or second-trimester screening, or both, for Down's syndrome. N Engl J Med 2005;353:2001-11.

CHAPTER 5

Wall shear stress and related hemodynamic parameters in the fetal descending aorta derived from color Doppler velocity profiles

P. C. Struijk, P.A. Stewart, K. L. Fernando [*], V.J. Mathews [*], T.Loupas [**], E.A.P. Steegers, J.W. Wladimiroff

*Department of Obstetrics & Gynaecology, Erasmus MC, Rotterdam, The Netherlands, *Department of Electrical and Computer Engineering, The University of Utah, Salt Lake City, **National Technical University of Athens, Greece.*

Ultrasound Med Biol. 2005; 31:1441-50.

ABSTRACT

Introduction

This paper presents a methodology for estimating the wall shear stress in the fetal descending aorta from color Doppler velocity profiles obtained during the second half of pregnancy.

Methods

The Womersley model was applied to determine the wall shear stress and related hemodynamic parameters.

Results

Our analysis indicates that the aortic diameter can be modeled as a function of the gestational age in weeks as: Diameter (mm) = $0.17 \cdot ga + 0.15$ ($R^2 = 0.64$, $p < 0.001$). The aortic volume flow showed a log linear gestational age related increase that fit the model: F (ml/min) = $e^{0.08 \cdot ga + 3.49}$ ($R^2 = 0.61$, $p < 0.001$). The Womersley number increased linearly with gestational age from 3.3 to 6.2 ($p < 0.001$) while the pressure gradient decreased linearly from 2.68 to 1.16 mPa/mm ($p = 0.003$) during the second half of pregnancy, the mean wall shear stress for the study group was 2.2 Pa (SD = 0.59) and independent of gestational age.

Conclusion

This study suggests that the size of the fetal aorta adapts to flow demands and maintains constant mean wall shear stress.

INTRODUCTION

Over the last several decades it has been demonstrated that hemodynamic parameters derived from fetal circulation are important determinants of fetal well being. Moreover, there is a growing awareness that adult diseases like hypertension and coronary heart disease might find their origins in impaired fetal development [1-5]. Therefore, it is important to determine fetal hemodynamic parameters, since they may serve as predictors of fetal diseases and determinants in future epidemiological studies.

This paper presents a method for estimating wall shear stress and related hemodynamic parameters from color Doppler velocity profiles obtained from the fetal descending aorta during the second half of human pregnancy. It has long been acknowledged that absolute blood flow changes can indicate organ function disorders and that wall shear stress is an important determinant of the biological activity of endothelial cells [6-10]. Arteries will typically adapt to maintain wall shear stress constant [11].

With color-Doppler imaging, it is possible to capture two-dimensional color-Doppler data in digital form for quantification and analysis. In particular, broadband beam-forming technology has considerably improved the axial resolution [12]. Today's technology allows color Doppler imaging at high frame rates implying better temporal resolution than previously possible. In contrast to spectral Doppler, color-Doppler yields detailed spatial information of distinct velocity components. Consequently, complex information such as velocity profiles along all color-Doppler lines within the color box are now available from digitally stored color-Doppler data.

Womersley (1955) derived a mathematical relationship between pressure gradient and velocity profiles associated with blood flow. He also demonstrated that volume flow and wall shear stress can be determined from flow velocity profiles. In this work, the Womersley model is applied to the velocity profiles to determine the wall shear stress and related parameters.

The objectives of this study are:

(i) to determine the abdominal fetal aortic diameter from the velocity profiles and to estimate the fetal aortic blood flow waveform using spatio-temporal integration of the velocity profiles;

(ii) to describe the ratio between inertial forces and viscous forces in the fetal descending aorta by means of the so-called Womersley number;

(iii) to apply Womersley's mathematical model to establish the pressure gradient;

(iv) to calculate the shear stress in the fetal descending aorta.

MATERIAL AND METHODS

Subjects

A total of 23 women participated in the study during uncomplicated singleton pregnancy between 19 and 38 weeks of gestation. Each woman was included in the study only once. The Ethics Committee of the Erasmus Medical Center Rotterdam, approved the study and the women were enrolled following informed consent. The gestational age was estimated from the last menstrual period. All pregnancies resulted in a term delivery of a normal infant with a birth weight between the 10th and the 90th centiles corrected for maternal parity and fetal sex [13].

Color-Doppler recordings

Ultrasound color-Doppler cineloops of the fetal descending aorta were obtained with a Philips ATL HDI 5000 (Bothell, WA, USA) ultrasound system, using a C5-2 curved array transducer. This type of transducer uses broadband beam forming technology, which means that the elements are stimulated with short pulses resulting in improved axial resolution color Doppler imaging [12]. The center frequency used was 5 MHz for 2D imaging and 2.5 MHz for color-Doppler imaging. The high pass color Doppler filter was set to "low". Within the pulse repetition frequency range used in the study this implies that the cut off frequency was always set below 100 Hz. To achieve high frame rates for color Doppler imaging, the scanning mode with minimal line density was chosen. The scan depth was set just below the visualization of the fetal descending aorta and the sector width was set to approximately 3 cm at this depth. Color Doppler scans clearly showing the longitudinal axis of the fetal descending aorta were made with an interrogation angle of approximately 60 degrees at the center of the scanned segment. The color Doppler scale was adjusted to just below the Nyquist limit and the color gain was manually selected to be just below the value where color noise appeared. Once a high quality recording was registered for several seconds, the freeze button was pushed, thus automatically storing the cineloop. The parts of the cineloop that do not exhibit significant moving artifacts were selected for further analysis. The product option "Research Link" was applied to export the digital Doppler velocity data to an external

computer for off-line analysis. The data was captured in polar coordinates with the sector angle and the distance from the transducer element as the measurements associated with each data sample. In addition to the digital Doppler velocity information, these data files included the system parameters necessary for scaling the velocity and to perform the scan conversion to Cartesian coordinates with proper scaling. MATLAB software version 6.5 release 13 (The Mathworks Inc.) for Windows 2000 professional was used to perform all the calculations on a Pentium *4* computer.

Offline analysis

Figure 1 shows a typical frame in the cineloop, the cineloop is played back offline, using MATLAB. The first and last color Doppler lines, between which the fetal aorta is clearly presented throughout the cineloop, are manually selected. Inspecting the cineloop identifies a region around the fetal descending aorta that does not contain velocities from other blood vessels. One line just above the anterior wall and another line just below the posterior wall are manually selected as well. To avoid interference with other fetal vessels, only velocity data within the region of interest are analyzed.

Determination of the interrogation angle

To estimate the interrogation angle between the ultrasound Doppler beam and the direction of blood flow, the centerline of the lumen of the vessel is first estimated in the following manner.

The cumulative sum of the unscaled velocity data within the selected region of interest is evaluated for each color Doppler line. The interpolated distance at which the cumulative sum function reached values of 1% and 99% of its maximum value were defined as the positions of the anterior (dst_a) and posterior (dst_p) fetal aortic wall, respectively. An example of computing dst_a and dst_p is displayed in Fig. 2. For every color Doppler line ($n = 1, \ldots, N$) , the midpoint between the posterior and anterior wall (dst_c) is determined. In this study the number of color Doppler lines within the region of interest ranged between 20 and 30. Subsequently, a second-degree polynomial line is fitted through the 20 to 30 midpoints between the posterior and anterior wall. This regression line is defined as the centerline of the lumen of the vessel.

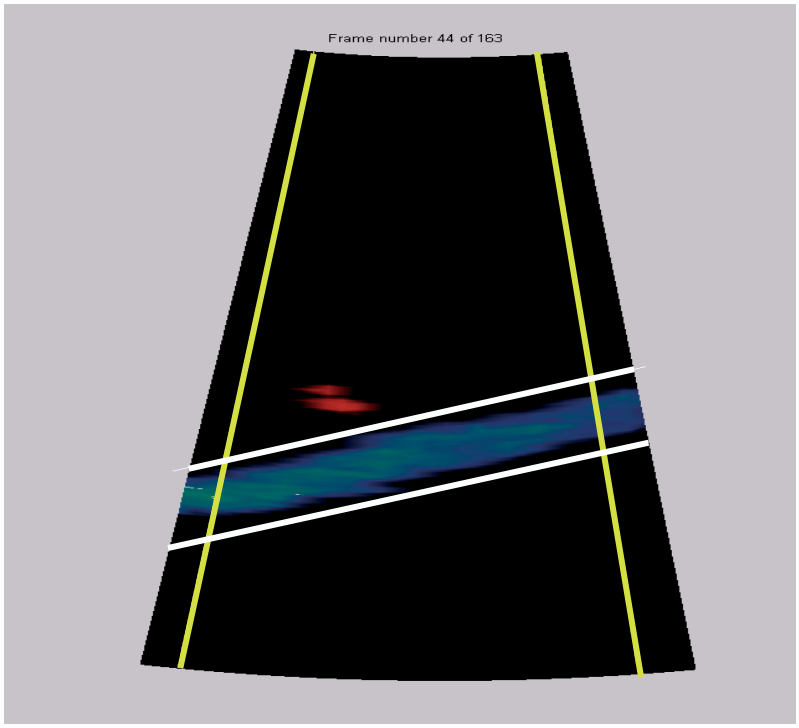

Figure 1. *The first and last color Doppler lines (yellow lines), between which the fetal aorta is clearly presented throughout the cineloop, are manually selected. One line just above the anterior wall and another line just below to posterior wall, are manually selected as well (white lines).*

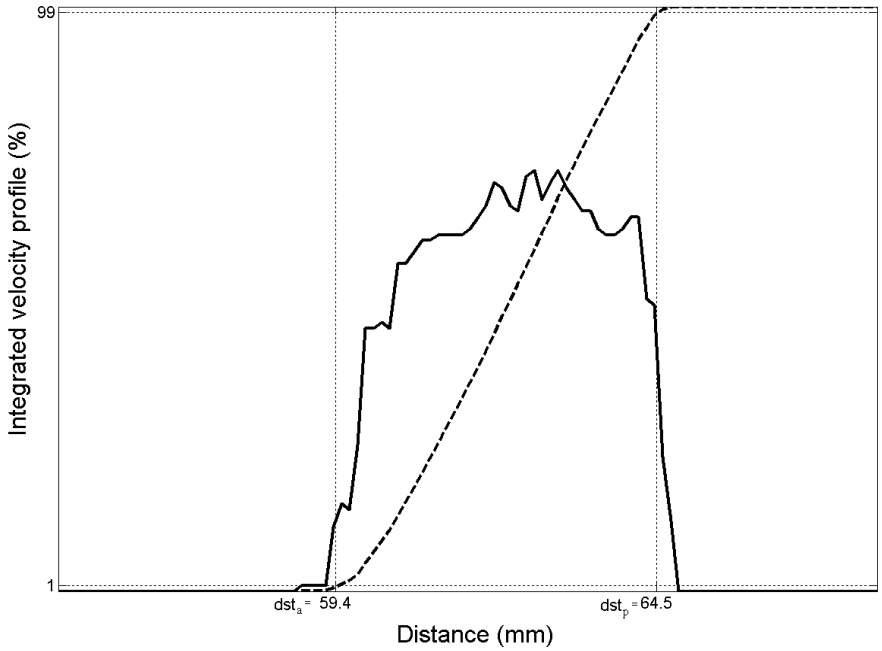

Figure 2. *Illustration of the fetal aortic wall detection, showing the velocity profile (solid line) and the integrated velocity profile (dashed line). The anterior wall (dst_a) is defined at the level of 1% velocity integration and the posterior wall (dst_p) at te level of 99% velocity integration.*

A quadratic fit was chosen since the fetal descending aorta is not perfectly straight when the fetus is in a typical "fetus position". The quadratic fit allows for a slightly curved aorta. The tangent to the regression line where it crosses the color Doppler line (n) is defined as the direction of blood flow at that particular point. As shown in Fig. 3, the angle ($\gamma_c(n)$) between these two crossing lines is

$$\gamma_c(n) = \varphi(n) - \beta(n)\,, \tag{1}$$

where $\varphi(n)$ is the angle of the color Doppler line (n) and $\beta(n)$ is the angle of the center line of the fetal descending aorta at the crossing point with the color Doppler line (n).

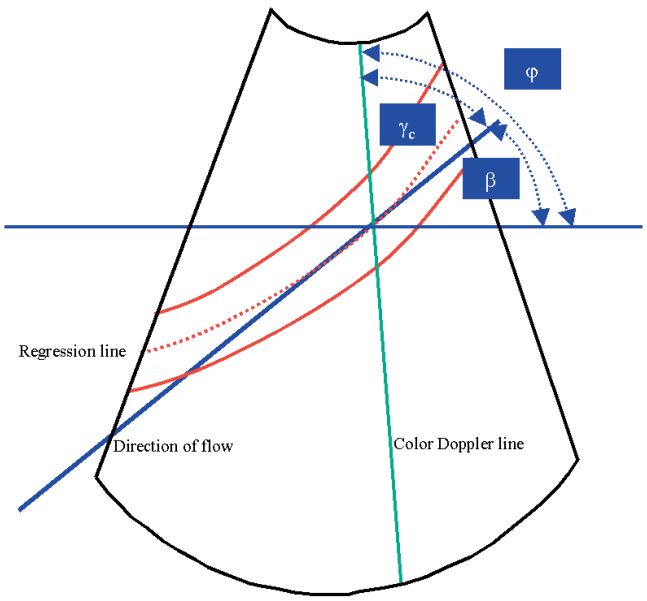

Figure 3. *Illustration of the procedure for estimating the interrogation angle (γ_c). The tangent to the regression line where it crosses the color Doppler line is defined as the direction of blood flow (β). The difference between the angle of the color Doppler line (φ) and the angle of the direction of flow determines the interrogation angle.*

The interrogation angle ($\gamma_c(n)$) is estimated for every color Doppler line and the associated calculations are performed for every frame to compensate for slight movements during the examination time. With 2-D scanning it is impossible to fully compensate for moving artifacts since the movements take place along all three directions. Furthermore, the velocity of the movement itself will generate artifacts. Therefore, measurements were taken during apnea and with the fetus at rest. The detected

Doppler frequency shift for every sample can be transformed to a velocity (v_c) using the Doppler formula.

$$v_c = \frac{F_d \cdot c}{2 \cdot F_e \cos(\gamma_c)}, \tag{2}$$

where F_d is the Doppler frequency shift, c is velocity of sound in tissue set to 1540 m/s in our analysis and F_e is the emitted frequency. The distance of the velocity sample to the centerline (r_c) is determined by

$$r_c = \left| dst_s - dst_c \right| \cdot \sin(\gamma_c), \tag{3}$$

where dst_s is the distances along the color Doppler line to the velocity sample.

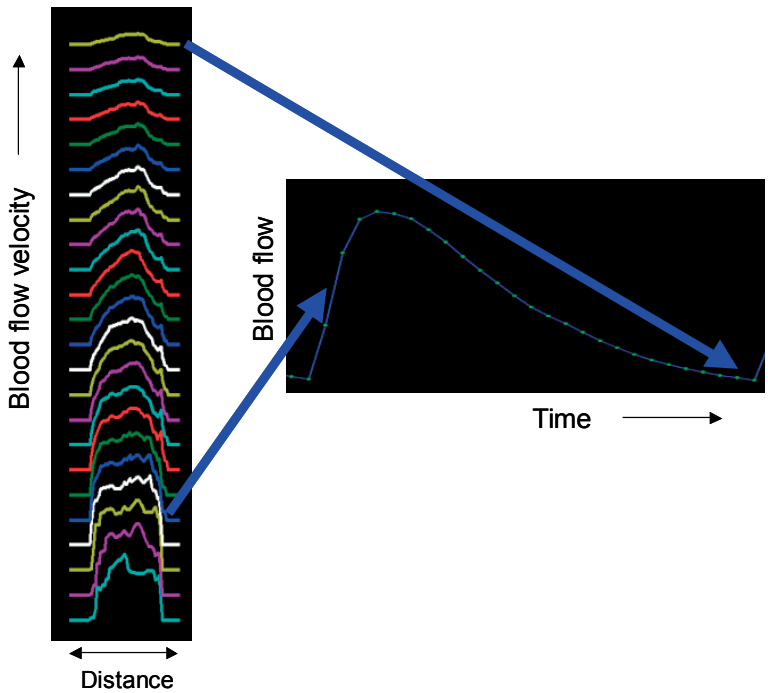

Figure 4. *An example of the blood velocity profiles during one cardiac cycle (left panel) relative to the fetal aortic blood flow waveform (right panel). The velocity profiles are relatively flat with steep edges during the acceleration phase, while they show a more rounded shape in the diastolic phase. Notice that the peak velocity is not necessarily at the center of the profile.*

Estimation of blood flow from velocity profiles

Figure 4 shows a typical example of the blood velocity profiles, during one cardiac cycle. The velocity profiles are relatively flat with steep edges during the acceleration phase, while they show a more rounded shape in the diastolic phase.

This behavior is different from the parabolic shape that fully developed steady flows exhibit at all times [7, 14]. Assuming a circular cross sectional shape of the fetal aorta, the instantaneous blood flow ($q(t)$), can be calculated by integration over the diameter. Let $v(r,t)$ denote the velocity of the blood flow where r is the distance from the center of the vessel and t is the time variable. Then the instantaneous flow is given by,

$$q(t) = \pi \int_{-R}^{R} r \cdot v(r,t) dr \,. \tag{4}$$

In the above equation, R is the radius of the vessel. The velocity profile is not necessarily symmetric with respect to the center. For this reason, the integral is taken from $-R$ to $+R$. In practice, dr can be considered as the axial velocity data spacing. The integral in (4) can therefore be approximated by a summation of the form

$$q(t) = \frac{\pi}{N} \sum_{n=1}^{N} \sum_{p=1}^{P} r_c(n,p,t) \cdot v_c(n,p,t) \cdot \Delta_p \cdot \sin(\gamma_c(n,t)), \;\; -R > r_c > R; \; v_p = 0 \,, \tag{5}$$

where N is the number of color Doppler lines, P is the number of samples along these lines, $r_c(n,p,t)$ is the distance from the center of the vessel, $v_c(n,p,t)$ is the velocity value of the sample p on line n at time t and Δ_p is the distance between two velocity samples along the color Doppler lines. The arithmetic mean of all color Doppler lines (N) is taken to represent the estimated flow waveform. Doing so will mitigate some of the estimation errors that can be expected if flow were calculated from measurements along a single line.

Estimation of the heart rate

The fetal heart rate is estimated as the frequency at which $Q(f)$, the discrete-time Fourier transform of $q(t)$, given by

$$Q(f) = \sum_{t=0}^{T-1} q(t) e^{-i2\pi ft} \,, \tag{6}$$

has the largest magnitude. In practice $Q(f)$ is evaluated at T discrete values of frequencies using the discrete Fourier transform of $q(t)$ given by

$$Q\left(\frac{k}{T}\right) = \sum_{t=0}^{T-1} q(t) e^{-\frac{i2\pi kt}{T}} \,, \tag{7}$$

We note that $Q(k/T)$ is the sampled value of $Q(f)$ at $f = k/T$ cycles/frame, which corresponds to $k \cdot F_r/T$ cycles/second, where F_r denotes the number of frames per second in the cineloop.

Estimation of the pressure gradient

For steady flow of liquids in cylindrical tubes, the Poiseuille law is valid [15]. The Poiseuille law states that the steady volume flow (q_s) is directly proportional to the pressure drop ($p1 - p2$) between two points in a cylindrical tube separated by the distance L and the fourth power of the inner radius (R) of the tube. In addition, the volume flow is inversely proportional to the viscosity (μ) of the liquid and the distance (L), giving an overall relationship of the form,

$$q_S = \frac{(p1 - p2)\pi R^4}{8\mu L}. \tag{8}$$

Since the flow in human arteries is not steady, one of the basic assumptions of deriving the Poiseuille equation is violated. The derivation of the relationship between the pulsatile pressure gradient and flow is much more complicated. In addition to the viscous resistance $8\mu L/\pi R^4$, the inertia of the fluid has to be considered because of the repeated accelerations and decelerations in pulsatile flow. Womersley (1955) developed a mathematical model for non-steady blood flow using the Navier-Stokes equations, the theoretical equations of motion for viscous fluids derived by Navier (1822) and Stokes (1845). The Womersley model predicts the velocity profile from the pressure difference along the length (ΔL) of a stiff tube. The Navier-Stokes equation relates the pressure gradients dp/dx to the velocity profile as:

$$-\frac{dp}{dx} = \rho\left[\frac{dv}{dt} + u\frac{dv}{dr} + w\frac{dv}{dx}\right] - \mu\left[\frac{d^2v}{dr^2} + \frac{1}{r}\frac{dv}{dr} + \frac{d^2v}{dx^2}\right], \tag{9}$$

where t represents the time variable, v is the velocity, and r and x are the radial and longitudinal coordinates in a cylindrical coordinate system. The parameters ρ and μ represent the density and viscosity of the liquid, respectively. The first three terms on the right hand side (multiplied by ρ) represent the inertial forces, and the last three terms

(multiplied by μ) represent the viscous losses. The equation thus states that the decrease in pressure per unit length equals the difference between the sum of the inertial forces and the sum of the viscous forces. The analysis of the unsteady flow using the Navier-Stokes equation leads to a non-dimensional number commonly referred to as the Womersley parameter, defined as

$$\alpha = R\sqrt{\frac{\rho\omega}{\mu}}, \tag{10}$$

where ω is the angular frequency $2\pi f$. The Womersley parameter can be interpreted as the ratio of the unsteady forces to the viscous forces. Womersley's model is referred to as "linearized" because the derivations do not include nonlinear terms. It has been shown that the nonlinearities are relatively small for blood flows in arteries [14]. For a blood flow waveform that is a pure (complex) sinusoid of the form $q(t) = e^{i2\pi ft}$, one can derive an expression for the pressure gradient $P_G(f)$ as [16]

$$\left.\frac{dp}{dx}\right|_f = P_G(f) = \frac{i\rho 2\pi f Q(f)}{\pi R^2\left(1-2B(\alpha)\right)} \qquad \left(-1/2F_r > f > 1/2F_r\right). \tag{11}$$

In the above equation, B is a complex function of the Womersley number α and is given by

$$B(\alpha) = \frac{J_1\left(\frac{i-1}{\sqrt{2}}\cdot\alpha\right)}{\left(\frac{i-1}{\sqrt{2}}\cdot\alpha\right)J_0\left(\frac{i-1}{\sqrt{2}}\cdot\alpha\right)}, \tag{12}$$

where J_0 and J_1 are standard solutions of differential equations known as Bessel functions[17] of order zero and one, respectively. Equation (11) relates the pressure gradient and the flow in the frequency domain. A detailed derivation of (11) and (12) can be found in the book by Zamir [16]. The inverse discrete Fourier transform of $P_G(f)$ represents the pressure gradient waveform $p_g(t)$. This waveform is estimated as

$$p_g(t) = \frac{1}{T}\sum_{k=0}^{T-1} P_G\left(\frac{k}{T}\right)e^{i2\pi\left(\frac{k}{T}\right)t}. \tag{13}$$

The above expression for the pressure gradient waveform is calculated by assuming that the flow is oscillatory. To complete the derivation, we should add the constant shear

stress produced by the steady component of pulsatile flow to (13). The steady pressure gradient component is calculated from the mean flow (q_s) using Poiseuilles law as described in (8). Thus, the expression for the pressure gradient per unit length is given by

$$p_g(t) = \frac{1}{T}\sum_{k=0}^{T-1} P_G\left(\frac{k}{T}\right) e^{i2\pi\left(\frac{k}{T}\right)t} + q_s\left(\frac{8\mu}{\pi R^4}\right). \tag{14}$$

Estimation of the Shear Stress

The shear stress at the wall (τ_w) is proportional to the velocity gradient (dv/dr) at the wall and the viscosity of blood (μ) and is given by

$$\tau_w = -\mu \frac{dv}{dr}\Big|_{r=R} \quad . \tag{15}$$

This relation was first found by Newton and in principle the shear stress can be derived directly from the velocity profile using (15). However, the problem of finding the velocity differential very close to the vessel wall is challenging for several reasons: First, wall movements interfere with the flow velocity near the arterial wall. Second, differentiation of the velocity profile amplifies random noise components. Consequently, we use the Womersley solution to generate more accurate approximations for the wall shear stress than the direct approach.

Similar to the derivation of the pressure gradient, starting with (11) for the pressure gradient $P_G(f)$ corresponding to a pure sinusoidal blood flow waveform, one can derive an expression in the wall shear stress in the frequency domain. The wall shear stress $\Gamma_w(f)$ satisfies the relationship

$$\mu \frac{dv}{dr}\Big|_f = \Gamma_w(f) = P_G(f)\cdot R \cdot B(\alpha); \quad \left(-1/2F_r > f > 1/2F_r\right). \tag{16}$$

A detailed derivation of (16) can be found in Zamir's book (2000). The inverse discrete Fourier transform of $\Gamma_w(f)$ represents the wall shear stress waveform $\tau_w(t)$.

$$\tau_w(t) = \frac{1}{T}\sum_{k=0}^{T-1} \Gamma_w\left(\frac{k}{T}\right) e^{i2\pi\left(\frac{k}{T}\right)t} \quad . \tag{17}$$

As was the case for the pressure gradient, the above result was derived assuming oscillatory flow. A complete representation of the shear stress is obtained by adding the contribution from the steady flow to (17). The steady wall shear stress (τ_s) is calculated from the mean flow using Poiseuilles law as

$$\tau_s = \frac{4\mu q_s}{\pi R^3}. \tag{18}$$

Combining (17) and (18), we get

$$\tau_w(t) = \frac{1}{T}\sum_{k=0}^{T-1} \Gamma_w\left(\frac{k}{T}\right) e^{i2\pi\left(\frac{k}{T}\right)t} + \frac{4\mu q_s}{\pi R^3} \ . \tag{19}$$

Fetal blood is not available from uncomplicated pregnancies to determine its density and viscosity. Instead we have taken values from the literature [18, 19]. Gijsen et al (1998) [28] have argued that whole blood viscosity rather than plasma viscosity is the appropriate choice for shear stress estimation. The fetal blood viscosity was set to 4.5 mPa.s and the density of fetal blood was set to 1.05 g/cm^3 in all the calculations described in this paper.

Statistics

Regression analysis was applied to relate the heart rate, blood flow, aortic diameter, Womersley number, pressure gradient and aortic wall shear stress to gestational age. The level of statistical significance was set at 0.05. No significant relation with gestational age could be demonstrated for some parameters. The mean and standard deviation of such variables will be presented in the discussion that follows.

RESULTS

Depending on the machine settings of the color Doppler system, the sample length ranged between 0.1 and 0.2 mm during data collection. The frame rates ranged between 30 and 68 Hz. The duration of the cineloops after the high quality part was selected for analysis ranged from 3 to 6 seconds. A typical example of the pressure gradient, the shear stress and the flow waveform in the fetal descending aorta at 24 weeks of gestation is given in Fig. 5.

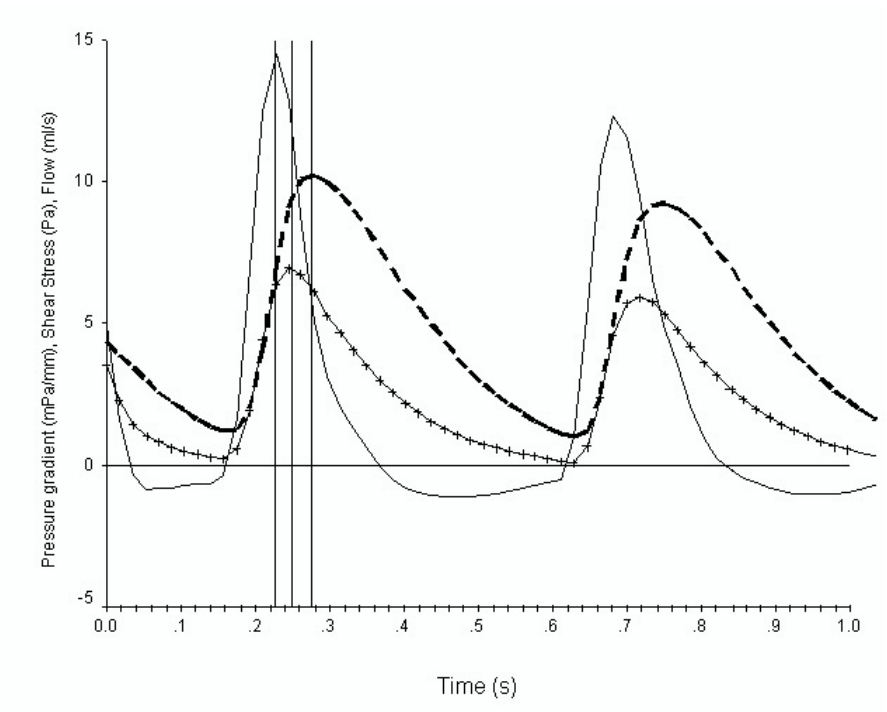

Figure 5*: Pressure gradient (solid line), Wall Shear Stress (solid line with crosses) and Aortic Blood Flow (dashed line) at 24 weeks of gestation. The peak of the pressure gradient and the wall shear stress waveforms precede the peak of the blood flow by approximately 50 and 25 ms respectively as shown by the vertical lines.*

The pressure reaches its peak value approximately 50 ms before the peak of the flow waveform is reached, while the peak of the shear stress waveform precedes the peak of the flow waveform by approximately 25 ms, indicating that substantial inertia forces are present in the fetal aorta to generate aortic blood flow.

The results of regression analyses that attempted to relate several variables associated with the blood vessel and blood flow as linear or exponential (linear in the log domain) functions of the gestational age are shown in Table 1. The mean aortic diameter regression line increased linearly from 3.4 mm at 19 weeks of gestation to 6.8 mm at 38 weeks of gestation. The mean blood flow in the fetal descending aorta increased exponentially from 150 ml/min at 19 weeks of gestation to 685 ml/min at 38 weeks of gestation.

Table 1. *Relationship of the hemodynamic parameters derived during the second half of pregnancy, to gestational age.*

Parameter	**Mathematical description**	**Significance (p)**	**R square (R^2)**
HR (beats/min)	− 0.67 • GA (wks) + 162	0.088	0.132
Log(Flow (ml/min))	0.08 • GA (wks) + 3.49	0.000 *	0.607
Diameter (mm)	0.17 • GA (wks) + 0.15	0.000 *	0.641
Womersley no	0.15 • GA (wks) + 0.48	0.000 *	0.608
PG (mPa/mm)	− 0.08 • GA (wks) + 4.20	0.003 *	0.353
Peak PG (mPa/mm)	0.20 • GA (wks) + 12.8	0.411	0.032
WSS (Pa)	− 0.03 • GA (wks) + 3.02	0.190	0.080
Peak WSS (Pa)	0.13 • GA (wks) + 3.12	0.071	0.147

** Significantly related with gestational age if $p < 0.05$.*
HR=Heart rate, PG = Pressure Gradient, WSS = Wall Shear Stress, wks = weeks.

The relationship between flow and gestational age, described by log-linear least-square regression is: Flow (ml/min) = $e^{0.08 \cdot ga + 3.49}$. As can be interpreted from the *R*-square value, 60.7 % of the flow variance between fetuses can be explained by gestational age. The mean (± SD) heart rate is 124 (± 10) beats/min and does not significantly change with gestational age. The non-dimensional Womersley number increased linearly from 3.3 to 6.2 while the pressure gradient decreased linearly from 2.68 to 1.16 (mPa/mm) during the same gestational time period. The variances that can be explained by the gestational age (64.1 % and 60.8 % for the diameter and the Womersley number,

respectively) are about the same as that found for the flow (60.7 %). However, the variance of the pressure gradient that can be explained by gestational age is less pronounced and only 35.3 %. Scatter diagrams and regression lines of blood flow, aortic diameter, the Womersley number and mean pressure gradient relative to gestational age are shown in Fig. 6 through 9. The mean peak pressure gradient of 18.5 (± 6.2) mPa/mm, the mean wall shear stress 2.16 (± 0.59) Pa and the mean peak wall shear stress 6.80 (± 1.9) Pa are not significantly related to the gestational age.

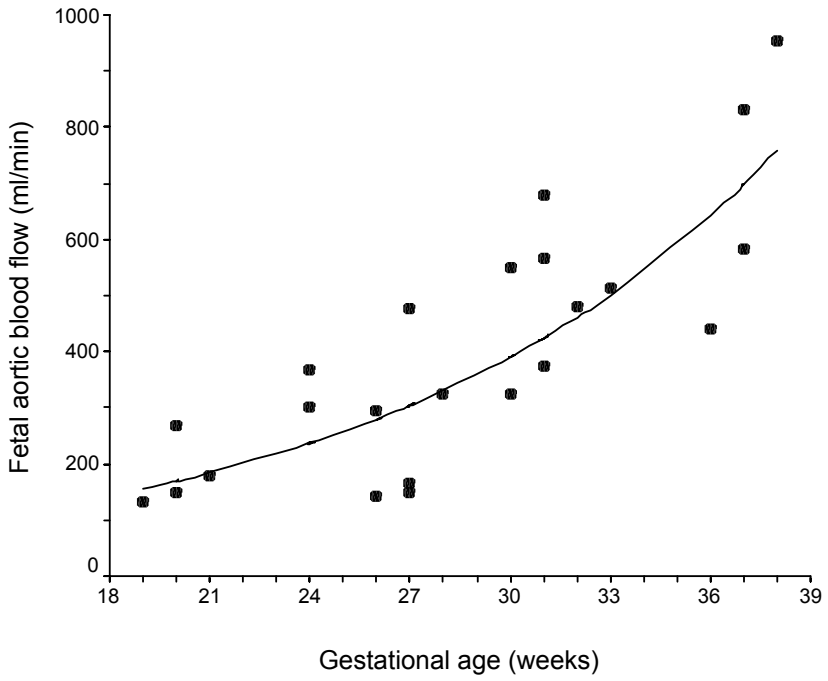

***Figure 6**: A log-linear gestational age-related increase exists for the aortic volume flow: Flow (ml/min) = $e^{0.08 \cdot ga\ (wks) + 3.49}$ (R^2 = 0.61).*

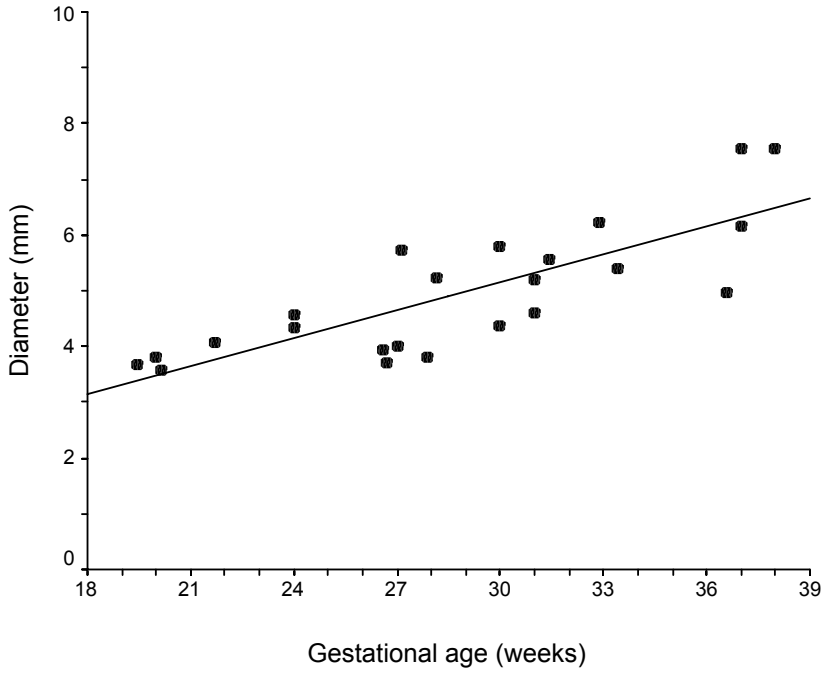

Figure 7: *The aortic diameter exhibits a gestational age dependent linear increase that can be modeled as: Diameter (mm) = 0.17 · ga (wks) + 0.15 (R^2 = 0.64).*

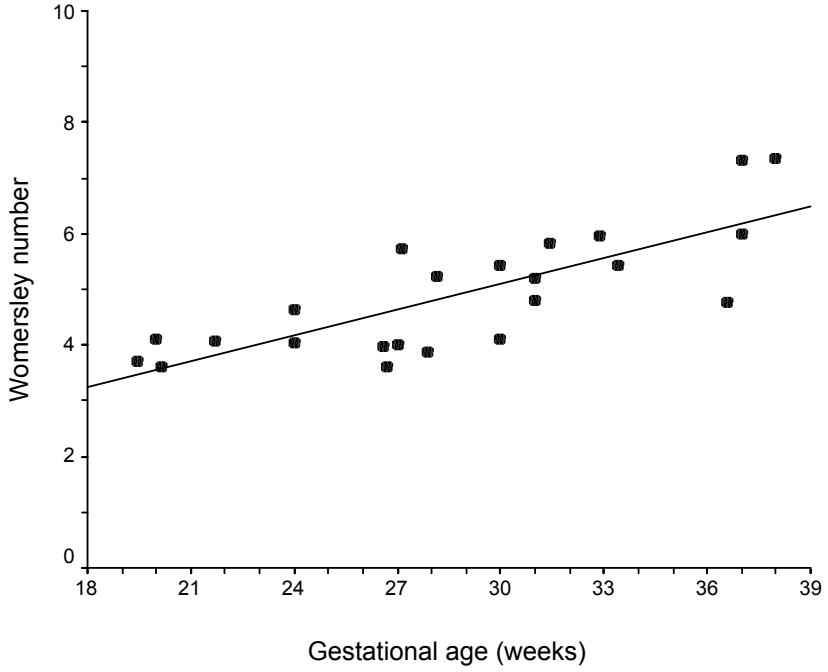

Figure 8*: The non-dimensional Womersley number is linearly related to the gestational age as: Womersley number = 0.15 · ga (wks) + 0.48 (R^2 = 0.61).*

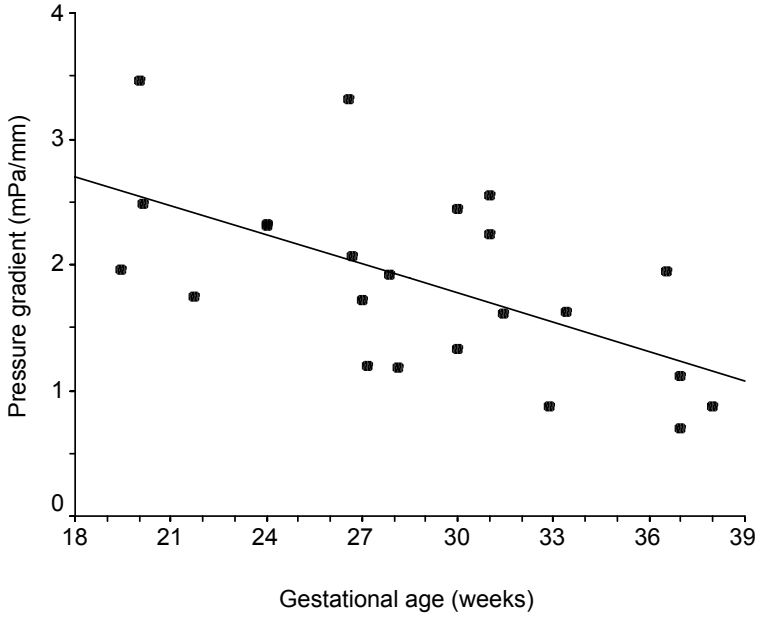

Figure 9: *The pressure gradient is linearly related to the gestational age as: Pressure gradient (mPa/mm) = -0.08 · ga (wks) + 4.20 (R^2 = 0.35).*

DISCUSSION

This study shows the application of the Womersley mathematical model to data obtained from color Doppler velocity profiles of the human fetal circulation. Womersley (1955) introduced an expression that relates the pressure gradient, the wall shear stress and the volume flow to each other in pulsatile flows. Fetal blood flow was measured in this study by spatio-temporal integration of color Doppler data. The pressure gradient and the wall shear stress were subsequently calculated using the Womersley model.

Determination of volumetric blood flow using Doppler ultra-sonography requires knowledge of the cross sectional area of the vessel and the angle corrected spatial mean velocity. Because arterial bloodflow is pulsatile, instantaneous values should be estimated. Struijk et al (1985) [32] demonstrated substantial errors when the pulsatile character of the vessel area is ignored. Independently Gill (1985) [29] reviewed actual and potential errors of blood flow measurement related to the uniform insonification method and concluded that considerable random errors occur with the method. With the introduction of duplex scanners, bloodflow can be determined from the spectral Doppler frequency shift in a small sample volume placed in the center of the lumen vessel and the cross sectional area estimate from the B-mode scan. The volumetric blood flow estimation can be completed using the Doppler formula and some assumption about the blood flow velocity distribution.

One of the complications of measuring fetal aortic bloodflow accurately using this modality is the ability of the fetus to move freely in his or her environment. When the fetus moves to another position between the times of the velocity measurement to the time of the area measurement, the exact same position within the fetal aorta of these two measurements cannot be reliably estimated. Even when the fetus does not move, it is difficult to reproduce the exact position since the optimal velocity measurement is achieved when the interrogation angle approaches zero while the vessel walls are best visualized in B-mode with perpendicular interrogation. Consequently, the probe is typically repositioned between the two measurements, making it difficult to make the measurement from exactly the same position of the aorta. The M-mode modality, color velocity imaging quantification abbreviated to CVI-Q™ (Philips) does not suffer from the

aforementioned problems associated with two-step flow measurements. The method is basically the same as the approach described in this paper except that blood flow is determined from a single M-mode line. Deane and Markus (1997) [27] evaluated the method in a flow phantom and reported errors within 10% for pulsatile flow. The CVI-Q and the methodology presented in this paper have the advantage that blood flow is estimated from velocity profiles instead of a small sample volume within the blood vessel, as done with spectral Doppler. Therefore, no assumptions about the velocity distribution are needed to estimate the blood flow. Furthermore, changes of the velocity profile during the cardiac cycle and the pulsatile nature of the fetal aortic diameter are taken into account in the calculations. Since two dimensional velocity recordings were digitally available in this study we were able to develop an algorithm to determine the angle of interrogation automatically for every frame. This removes one aspect of operator-induced variability. The cineloops were recorded with a frame rate between 30 and 68 Hz. Consequently, small fetal position changes can be corrected almost instantaneously in our approach. Finally, another advantage of two-dimensional color Doppler over one-dimensional color Doppler is that the flow is calculated from several (20 to 30) velocity profiles. This should cancel out some of the random variations in the estimated flow.

Color Doppler imaging during the second half of pregnancy needs penetration depth. Therefore, only relatively low center frequencies can be used and this limits the axial resolution of the scans. This will result in an overestimation of the diameter size. Without appropriate correction near the vessel wall, the full length of the spatial samples are used in the estimate even when the samples are only partly filled with moving erythrocytes. To compensate for overestimation, we detect the vessel wall at 1% and 99% of each integrated velocity profile, as shown in Fig. 2.

Recently Harrington [9] measured fetal aortic bloodflow using CVI-Q in fetuses with suspected fetal anemia based on blood cell antibody titers. They compared these results with CVI-Q derived measurements from uncomplicated pregnancies [20]. Bloodflow in the group suffering from anemia was significantly increased relative to the non-anemic group and relative to the uncomplicated pregnancies. The authors suggest that aortic volumetric blood flow outcome can be used to predict fetal anemia.

The Womersley number describes the ratio between the inertial and viscous forces that generate oscillatory flow. For extremely slow oscillations, the Womersley number approaches zero. As is the case for stationary flow, only viscous losses have to be compensated with viscous forces to generate the flow. In such cases there would be no phase lag between blood flow, shear stress and pressure gradient. The fact that the peak of the pressure gradient in the fetal aorta precede both the peak of the shear stress and the peak of the blood flow demonstrates that substantial inertial forces are present in the fetal aorta to generate the blood flow. As is shown in Fig. 5, the pressure gradient has to become negative before the blood flow slows down to its end diastolic value. An extensive explanation for this phenomenon that is a result of momentum forces can be found in the books by McDonald (1974) and Milner (1984). The peak pressure gradient remains constant during the second half of pregnancy in contrast to the mean pressure gradient that showed a significant decrease. This can be explained by the strong reduction of the viscous resistance caused by the linear increase of the fetal diameter. Recall that the viscous resistance is inversely proportional to the fourth power of the vessel diameter. As a result of the constant fetal heart rate and the significant increase of the aortic diameter during the second half of pregnancy, a statistically significant increase of the Womersley number could be demonstrated during the second half of pregnancy indicating that the increase of the inertial forces are more pronounced relative to the viscous losses with advancing gestational age.

The wall shear stress was estimated in this study using the Womersley mathematical model to mitigate the previously discussed limitations associated with fetal velocimetry. Brands et al (1994) [26] described an approach to estimate the wall shear stress directly from the velocity profiles. Since the authors had access to 50 Mhz sampled echo data derived from a 6.1 MHz ultrasound transducer they were able to apply an adaptive filter to reduce the interference problem associated with wall motion. Data for this study was gathered from a commercially available machine that gave access to pre-processed ultrasound color Doppler data and it was not possible to apply the adaptive technique described by Brands to our data. However, the application of the Womersley model to the estimation problem allows us to reliably estimate the wall shear stress from the pre-processed data for velocity profiles typically available from the fetal descending aorta.

We believe that by applying modern data processing techniques on high frequency sampled raw data the accuracy of wall shear stress estimation in fetal blood vessels can be improved whether or not the estimation is based on mathematical modeling. With still declining costs of high-speed computers with large storage capacities we expect that our approach will become feasible for daily practice in the near future.

Our analysis showed that both the peak and the mean wall shear stress remain constant during the second half of pregnancy in uncomplicated pregnancies. This observation could have been anticipated based on Murray's law [21], which proposes a constant wall shear stress irrespective of diameter size. The theoretically predicted value, 1.5 Pa [22, 23] is substantially lower than the mean wall shear stress of 2.16 Pa found in our study but still in the upper range of 0.75 to 2.25 found by these investigators.

For specific arteries in the human adult circulation some authors have demonstrated significant deviation from Murray's (1926) theoretically predicted value of wall shear stress. For example, healthy volunteers at rest were found to have mean wall shear stress values below 0.75 in the brachial artery [24] and also in the common and superficial femoral arteries [25]. The low shear stress in the femoral artery could mostly be explained by reflections that are also known to be present in growth-restricted fetuses [8]. Therefore, we may hypothesize that growth restricted fetuses have low shear stress in the descending aorta because of reflections resulting from high placental impedance.

Le Noble (2005) [30] concluded in his review that the basic layout of major vessels might be regulated by a deterministic patterning mechanism in the chick embryo during the very early phases of development, prior to the onset of perfusion. After perfusion, the flow related shear stresses are specifically involved in controlling vessel size and the number and position of the arterial side branches. It might well be that the same mechanisms are active in early human development and placentation. Therefore, low shear stress might also be an indicator of insufficient placentation that results in growth restriction.

This paper demonstrated that fluid mechanical forces acting on endothelial cells could be estimated in the human fetus. Studying the fluid mechanical forces in a growth-restricted group relative to a normal population might contribute to a better understanding of the mechanisms involved in fetal growth restriction.

REFERENCES

1. Barker DJ, Osmond C. Infant mortality, childhood nutrition, and ischaemic heart disease in England and Wales. Lancet 1986;1:1077-81.
2. Barker DJ. Fetal origins of coronary heart disease. Bmj 1995;311:171-4.
3. Leon DA. Twins and fetal programming of blood pressure. Questioning the role of genes and maternal nutrition. Bmj 1999;319:1313-4.
4. Robinson R. The fetal origins of adult disease. Bmj 2001;322:375-6.
5. Forsen T, Osmond C, Eriksson JG, Barker DJ. Growth of girls who later develop coronary heart disease. Heart 2004;90:20-4.
6. Holland CK, Taylor KJ. Blood flow quantitation: waveform analysis, volume measurement, tumor flow, and the role of color imaging. Clin Diagn Ultrasound 1993;28:125-39.
7. McDonald DA. Blood flow in arteries, 1974.
8. Maulik D. Hemodynamic interpretation of the arterial Doppler waveform. Ultrasound Obstet Gynecol 1993;3:219-27.
9. Harrington K, Fayyad A, Nicolaides KH. Predicting the severity of fetal anemia using time-domain measurement of volume flow in the fetal aorta. Ultrasound Obstet Gynecol 2004;23:437-41.
10. Malek AM, Izumo S. Molecular aspects of signal transduction of shear stress in the endothelial cell. J Hypertens 1994;12:989-99.
11. Ku DN. Blood flow in arteries. 1997;29:399-434.
12. Bonnefous O, Pesque P. Time domain formulation of pulse-Doppler ultrasound and blood velocity estimation by cross correlation. Ultrason Imaging 1986;8:73-85.
13. Kloosterman G. On intrauterine growth. Int J Obstet Gynaecol 1970;8:895-912.
14. Womersley JR. Oscillatory motion of a viscous liquid in a thin walled elastic tube: The Linear approximation for long waves. Philosophical magazine 1955;46:199-221.
15. Tokaty GA. A history and philosophy of fluid mechanics.: Foulis, Henley-on-Thames, Oxfordshire, 1971.

16. Zamir Z. The physics of pulsatile flow. New York: Springer-Verlag, 2000.
17. McLachlan NW. Bessel functions for engineers. Oxford: Claredon Press, 1955.
18. Steel SA, Pearce JM, Nash G, Christopher B, Dormandy J, Bland JM. Correlation between Doppler flow velocity waveforms and cord blood viscosity. Br J Obstet Gynaecol 1989;96:1168-72.
19. Jouppila P, Kirkinen P, Puukka R. Correlation between umbilical vein blood flow and umbilical blood viscosity in normal and complicated pregnancies. Arch Gynecol 1986;237:191-7.
20. Thompson O, Gunnarson G, Vines K, Fayyad A, Wathen N, Harrington K. Time domain measurement of blood flow in the human fetal aorta during normal pregnancy. Ultrasound Obstet Gynecol 2004;23:257-61.
21. Murray CD. The physiological principle of minimum work. I. The vascular system and the cost of blood volume. Proc Natl Acad Sci USA 1926;12:207-214.
22. LaBarbera M. Principles of design of fluid transport systems in zoology. Science 1990;249:992-1000.
23. Kamiya A, Togawa T. Adaptive regulation of wall shear stress to flow change in the canine carotid artery. Am J Physiol 1980;239:H14-21.
24. Dammers R, Stifft F, Tordoir JH, Hameleers JM, Hoeks AP, Kitslaar PJ. Shear stress depends on vascular territory: comparison between common carotid and brachial artery. J Appl Physiol 2003;94:485-9.
25. Kornet L, Hoeks AP, Lambregts J, Reneman RS. Mean wall shear stress in the femoral arterial bifurcation is low and independent of age at rest. J Vasc Res 2000;37:112-22.
26. Brands PJ, Hoeks AP, Hofstra L et al. A noninvasive method to estimate wall shear rate using ultrasound. Ultrasound Med Biol 1995; 21:171-85.
27. Deane CR, Markus HS. Colour velocity flow measurement: in vitro validation and application to human carotid arteries. Ultrasound Med Biol 1997; 23:447-52.
28. Gijsen FJ, van de Vosse FN, Janssen JD. Wall shear stress in backward-facing step flow of a red blood cell suspension. Biorheology 1998; 35:263-79.
29. Gill RW. Measurement of blood flow by ultrasound: accuracy and sources of error. Ultrasound Med Biol 1985;11(4):625– 641. Review.

30. le Noble F, Fleury V, Pries A et al. Control of arterial branching morphogenesis in embryogenesis: go with the flow. Cardiovasc Res 2005; 65:619-28.
31. Milnor WR. Hemodynamics. Baltimore, MD: Williams and Wilkins.1984.
32. Struyk PC, Pijpers L, Wladimiroff JW et al. The time-distance recorder as a means of improving the accuracy of fetal blood flow measurements. Ultrasound Med Biol 1985; 11:71-7.

CHAPTER 6

BLOOD PRESSURE ESTIMATION IN THE HUMAN FETAL DESCENDING AORTA.

P. C. Struijk, V.J. Mathews [*], T.Loupas [**], P.A. Stewart, E.B. Clark***, E.A.P. Steegers, J.W. Wladimiroff.

*Department of Obstetrics & Gynaecology, Erasmus MC, Rotterdam, The Netherlands, *Department of Electrical and Computer Engineering, The University of Utah, Salt Lake City, **National Technical University of Athens, Greece, *** Department of Pediatrics, The University of Utah, Salt Lake City*

Submitted for publication.

ABSTRACT

Objective

The objective of this study is to estimate fetal blood pressure from 2D color Doppler derived aortic blood flow and diameter waveform by applying the Womersley model in combination with the two-element Windkessel model.

Results

In 21 normal pregnancies the estimated mean aortic pressure regression line increased linearly from 28 mmHg at 20 weeks gestation to 45 mmHg at 40 weeks of gestation.
A statistically significant eightfold increase was observed for the aortic compliance. The compliance C_a exhibited a log linear relationship with the gestational age as C_a (mmHg / ml) = $e^{0.098 \cdot ga - 6.42}$ ($R^2 = 0.72$). The aortic downstream peripheral resistance decreased fourfold during the same time. R_p exhibited an exponentially decaying relationship with gestational age as R_p (mmHg . s / ml) = $e^{-0.0065 \cdot ga + 3.38}$ ($R^2 = 0.45$) .

Conclusion

The magnitude of fetal aortic blood pressure during the second half of pregnancy is comparable to the aortic blood pressure measured shortly after birth in infants born prematurely at similar gestational ages.

INTRODUCTION

The human fetal circulation has been extensively studied by Doppler ultrasound with emphasis on Doppler flow velocity waveforms and blood flow estimates [1]. Both pressure and blood flow waveforms are needed to describe a circulatory system in terms of peripheral resistance and compliance. This paper describes a method to estimate blood pressure waveforms and flow volume information in the human fetal circulation system using ultrasound techniques.

The fetal circulation differs from the adult circulation in that it has an undivided pulmonary and systemic circulation with the ductus venosus, ductus arteriosus and foramen ovale acting as shunts and the left and right heart working in parallel. A particularly striking feature of the fetal circulation is that almost half of the combined output of the two ventricles is delivered to the placenta. These and other differences make the pressure-flow relationships in the adult circulation hardly comparable to those in the fetal circulation [2].

Fetal blood pressure could be considered an important parameter to monitor in clinical settings like preeclampsia. In preeclampsia, maternal hypertension may be a response to poor placental perfusion since sufficient maternal placental circulation is needed to meet fetal demands [3]. Lowering the maternal pressure could be harmful to the fetus. Additionally, it is known that anti-hypertensive drugs pass the placenta. Consequently, the arterial blood pressure may change in response to anti hypertensive treatment of the mother. Monitoring the fetal blood pressure may be important in order to balance the benefits to the mother and risks to the fetus during anti-hypertensive treatment. The importance of pressure monitoring in fetuses is also anticipated in pathophysiology associated with intra-uterine growth retardation and prematurity.

Direct arterial pressure measurements are not feasible due to the inaccessibility of the fetus. Information on fetal arterial pressure is hardly available in the literature. In prior work our group estimated the human fetal arterial pulse pressure by applying a derivation of the Moens-Korteweg equation on pulsatile aortic diameter recordings obtained at two different locations of the fetal descending aorta [4]. A lack of information on simultaneously derived blood flow did not allow the estimation of mean blood pressure at

that time. A method to estimate the systolic and diastolic pressures based on a mathematical model was reported by Capper et al for a 28-week-old fetus [5]. To the best of the authors' knowledge, no additional information on human fetal pressure has been published since then.

Digital recording of color Doppler cineloops of the fetal aorta allows the calculation of both aortic blood flow and diameter waveforms [6]. The objective of this study was to estimate fetal blood pressure from simultaneously derived blood flow and diameter waveform recordings by applying the Womersley model [7, 8] in combination with the two-element windkessel model [9].

MATERIAL AND METHODS

Subjects

A total of 21 women with uncomplicated singleton pregnancies between 19 and 41 weeks of gestation consented to participate in the study, which was approved by the Ethics Committee of the Erasmus Medical Center, Rotterdam. The gestational age was estimated from the last menstrual period and confirmed by fetal crown rump or biparietal diameter measurements. Each woman was included in the study once, all pregnancies resulted in a term delivery of a normal infant with a birth weight between the 10th and the 90th centiles corrected for maternal parity and fetal sex [10].

Color-Doppler recordings

Ultrasound color-Doppler cineloops of the fetal descending aorta were obtained with a Philips ATL HDI 5000 (Bothell, WA, USA) ultrasound system, using a C5-2 curved array transducer. The center frequency used was 5 MHz for 2D imaging and 2.5 MHz for color-Doppler imaging. To achieve the highest possible frame rates for color Doppler imaging, the minimal line density was chosen. The scan depth was set just below the visualization of the fetal descending aorta and the sector width was set to approximately 3 cm at this depth. Color Doppler scans clearly showing the longitudinal axis of the fetal descending aorta with an interrogation angle of approximately 60 degrees at the center of the scanned segment were accepted. The color Doppler scale was adjusted to just below the Nyquist limit and the color gain was optimized to just below the value where color noise appeared. Once a recording was registered for several seconds, the freeze button was pushed which automatically stores the cineloop for further analysis. The product option "Research Link" in the color Doppler system was applied to export the digital data to an external computer for off-line analysis. In addition to the digital Doppler velocity information, these data files include the system parameters necessary to perform quantitative spatio-temporal analysis of scan-converted color velocity frames. MATLAB software version 6.5 release 13 (The Mathworks Inc.) for Windows 2000 professional was used to perform all the calculations on a Pentium *4* computer.

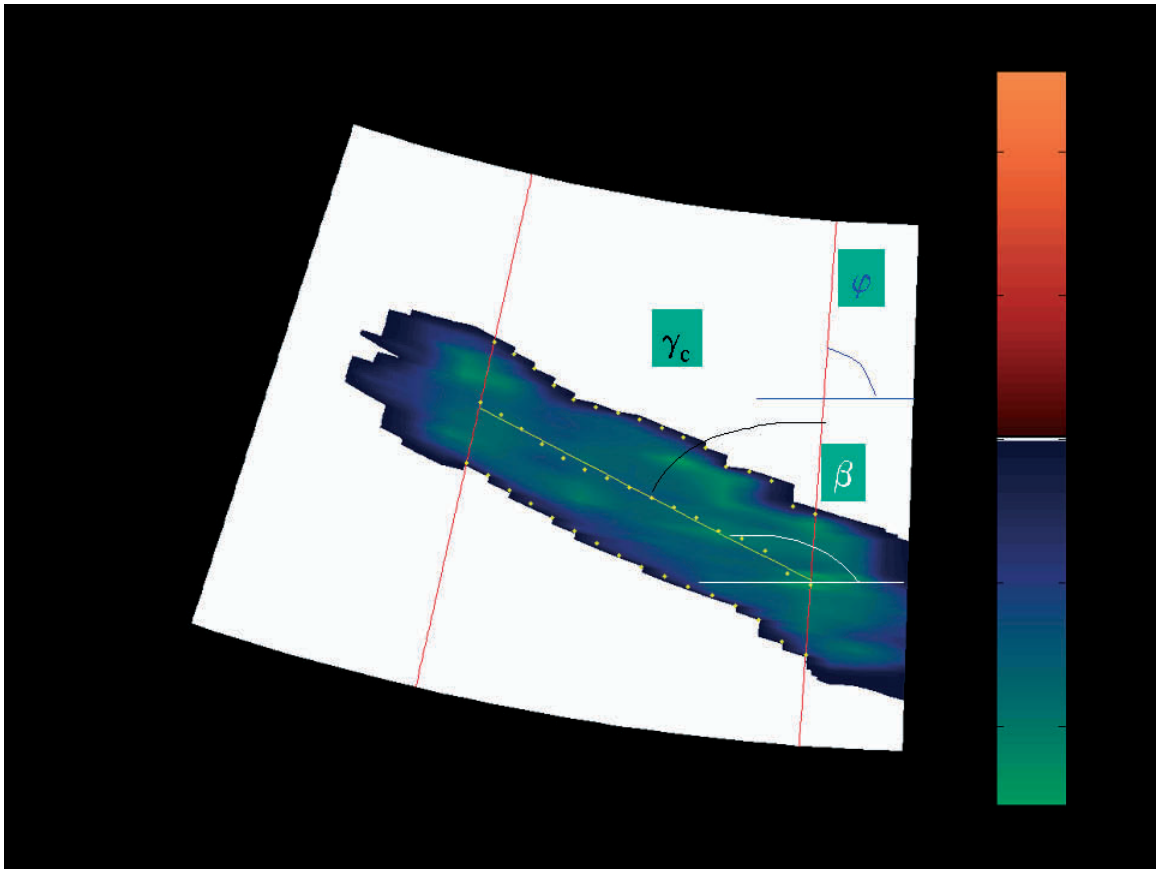

Figure 1. *Color Doppler presentation of the descending aorta in a 34 weeks old fetus. The red lines show the first and last color Doppler line selected. Outer yellow dots represent the wall detection points for all selected color Doppler lines. The dots in the middle represent the mean of the outer and inner wall detection points. The yellow solid in the middle of the aortic representation is the least square regression line for the centerline of the aorta. The interrogation angle (γ_c) is determined by the difference between the angle of the color Doppler line (φ) and the angle of the direction of flow (β).*

Blood flow determination

Determination of blood flow and diameter waveforms from color Doppler cineloops is described in detail previously [6]. The numeric data of the color Doppler scan lines plotted versus the distance represents the velocity profiles. In our method, the cumulative sum of the unscaled velocity data is evaluated for each color Doppler line. The interpolated distance at which the cumulative sum function reached values of 1% and 99% of its maximum value are then estimated to be the positions of the anterior and posterior fetal

aortic vessel wall along the scan line. For every color Doppler line, the midpoint between the posterior and anterior wall was determined. Figure 1 shows a color Doppler frame with the fetal aortic wall detection points and the second-degree polynomial line fitted through the midpoints. For a color Doppler line (n) the interrogation angle ($\gamma_c(n)$) with the aorta is determined as the difference between the color Doppler line angle ($\varphi(n)$) and the regression line angle ($\beta(n)$):

$$\gamma_c(n) = \varphi(n) - \beta(n) . \tag{1}$$

The interrogation angle was estimated for every color Doppler line and the associated calculations were performed for every frame to compensate for slight movements during the examination time. The Doppler formula is applied to scale the velocity data as

$$v_c = \frac{F_d \cdot c}{2 \cdot F_e \cos(\gamma_c)}, \tag{2}$$

where v_c is the calibrated velocity, F_d is the Doppler frequency shift, c is velocity of sound in tissue set to 1540 m/s in our analysis and F_e is the emitted frequency.

Assuming a circular cross sectional shape of the fetal aorta, the instantaneous blood flow ($q(t)$) can be calculated by integration over the distance between the positions of the anterior and posterior fetal aortic vessel wall along the scan line. The radius R of the aorta is calculated as the distance of the posterior or anterior wall to the centerline. Let $v_c(r,t)$ denote the velocity of a velocity sample at a distance r from the center of the vessel and let t be the time variable. Then the instantaneous flow if given by,

$$q(t) = \pi \int_{-R}^{R} r \cdot v_c(r,t) dr . \tag{3}$$

Pressure estimation

The method of pressure estimation is partly based on the "Womersley model". The classical papers of Womersley deal with the complicated problem of pulsatile flow in an elastic tube [7, 8]. The derivation starts with the basic Navier-Stokes equations of motion for viscous fluids derived by Navier (1822) and Stokes (1845). It has been shown that the nonlinearities are relatively small for blood flows. For the linearized Navier-Stokes equations Womersley found a standard solution employing Bessel functions. Applying Fourier analysis the Womersley model can predict the velocity profile from the pressure

within an elastic tube. Despite the complexity of the theory, a simple relation between the aortic pressure and the wall extension is derived assuming two generally accepted assumptions [11]. First, we assume that the Poisson ratio of the elastic wall is 0.5, which means that the volume of the elastic wall remains constant during expansion. Second, we also assume that the elastic wall is "tethered" by an axial elastic constraint. Describing the aortic vessel radius pulsations $r_p(t)$ as the difference between the instantaneous radius $r(t)$ and the mean radius (R), the aortic pressure pulsations $p_p(t)$ as the difference between the instantaneous pressure $p(t)$ and the mean pressure P, the relation between radius and pressure pulsations is [8]:

$$r_p(t) = \frac{3R}{8\rho c_o} p_p(t) \tag{4}$$

where ρ represents the density of blood, t is the time variable and c_o represents the pulse wave velocity. The pulse wave velocity in equation (4) is set to 3.15 m/s, the mean value of the pulse wave velocity found in the fetal descending aorta during the second half of pregnancy [4].

Womersley has demonstrated that the above equation relating the harmonic components of the variations in pressure with the corresponding variations in diameter takes the same form in the presence of a reflected wave and validated the result with experimental data [8]. The aortic downstream impedance can be approximated well with the Windkessel model. In this model an electrical resistor is analogous to the peripheral resistance (R_p) and the compliance (C_a) is analogous to the electrical capacitor. As in electrical circuitry, the downstream impedance (Z) can be calculated as;

$$Z = \frac{R_p}{1 + i2\pi f C_a R_p} \tag{5}$$

where i represent the square root of –1 and f is the frequency. The pressure waveform can now be calculated in the frequency domain. The discrete-time Fourier transform of $q(t)$ is given by

$$Q(f) = \sum_{t=0}^{T-1} q(t) e^{-i2\pi ft}, \tag{6}$$

The pressure waveforms *p(t)* in the time domain can be evaluated as the inverse Fourier transform of the product of the bloodflow waveform and the down stream impedance in the frequency domain.That is,

$$p(t) = \frac{1}{S} \sum_{f=-\frac{F_r}{2}}^{f=\frac{F_r}{2}} Q(f) \frac{R_p}{1 + i2\pi f C_a R_p} e^{i2\pi f t} , \tag{7}$$

where F_r denotes the number of frames per second and S is the number of frames in the cineloop. The algorithm to estimate the aortic pressure from measured flow and radius waveforms is schematically shown in Fig. 2.

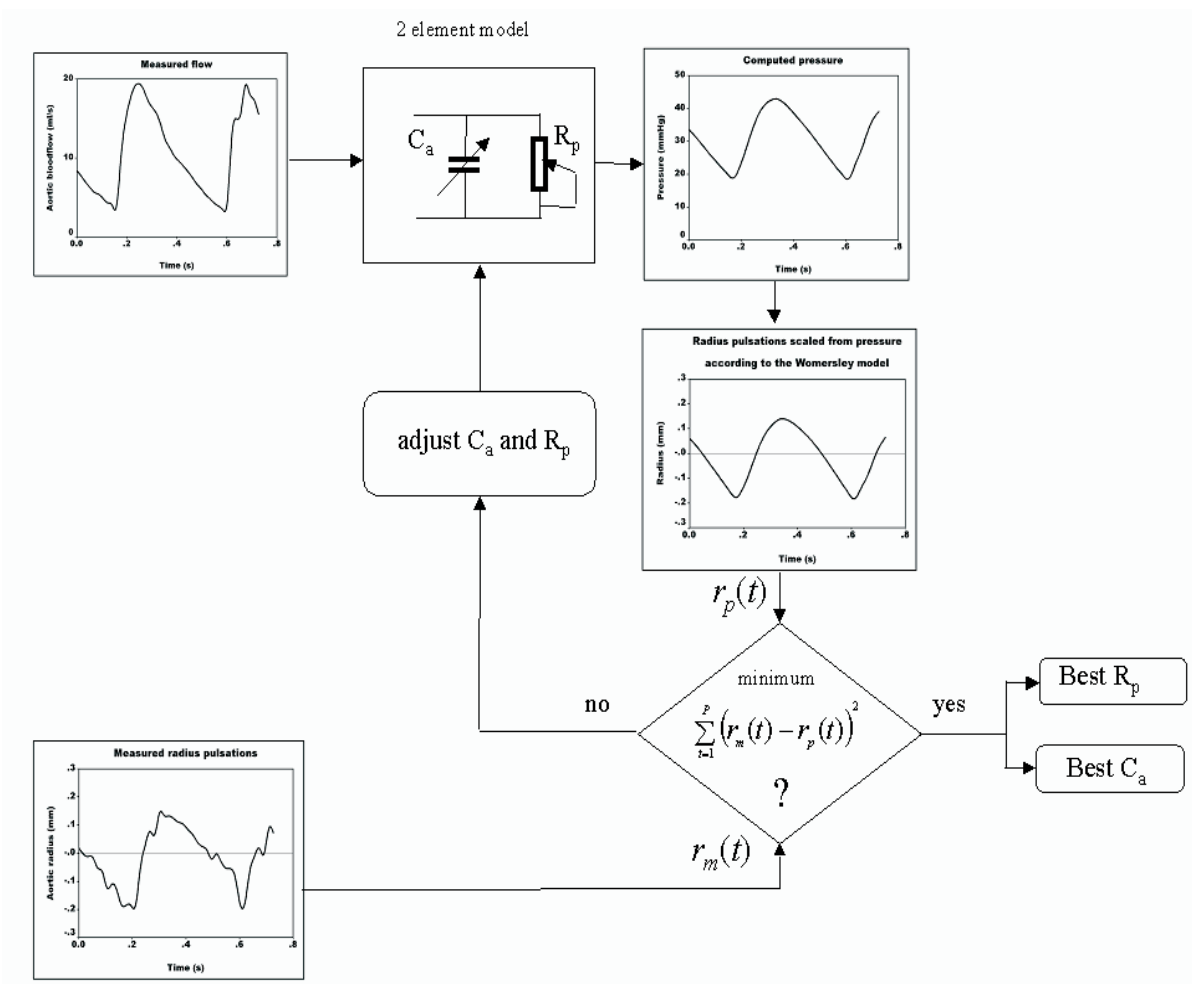

Figure 2. *Schematic showing the algorithm to determine fetal blood pressure.*

The three upper blocks represent equation 7. The best estimates for peripheral resistance R_p and compliance C_a are found when the calculated pressure scaled to radius pulsations ($r_p(t)$) best fit with the actually measured radius pulsations ($r_m(t)$). An iterative algorithm minimizes the sum of squared differences between these two waveforms from beat to beat. The function to be minimized F_{min} is

$$F_{\min} = \sum_{t=1}^{P} (r_p(t) - r_m(t))^2 \tag{8}$$

where P is the period time of a single heart beat. In this work, the "simplex search method", generally referred to as unconstrained nonlinear optimization, was applied to find this minimum [12].

To determine the initial values for R_p and C_a the pulsatile part of the radius waveform is scaled to the pulsatile pressure using equation (4). The initial value for R_p is calculated by taking the quotient of the RMS values of the pulsatile part of pressure and flow waveforms. The quotient of the stroke volume and the pulse pressure is taken as the initial value for C_a. If for a particular heartbeat the search function did not converge to a solution or the coefficient of determination is smaller than 0.7, this beat is not accepted.

The fetal heart rate and the pulsatile index defined as $PI = (V_{max} - V_{min}) / V_{mean}$, are derived from the maximum velocity tracing.

Statistics

Regression analysis was applied to relate the estimated downstream aortic compliance, peripheral resistance, aortic radius, blood flow, heart rate, systolic, diastolic and mean pressure to gestational age. The level of statistical significance was set at 0.05. The mean and standard deviation will be presented if no statistically significant relation with gestational age could be demonstrated.

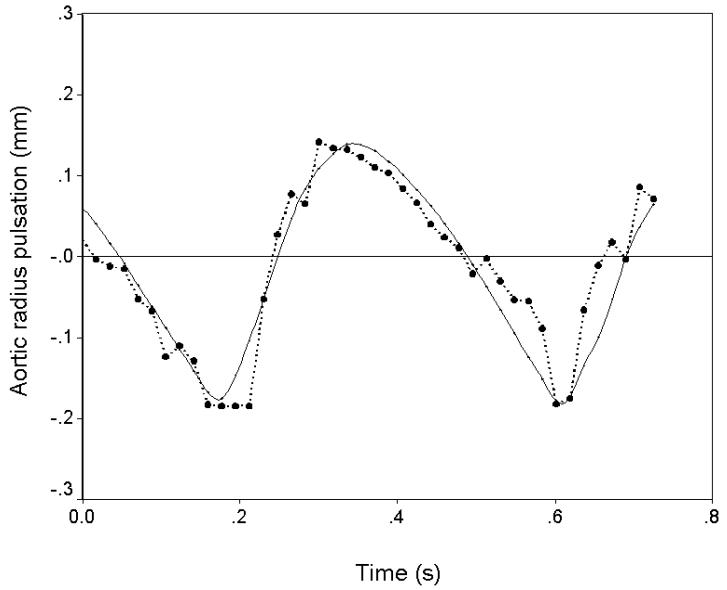

Figure 3. *The dots (·) connected by the dotted line (·····) represent the measured pulsatile radius waveform. The best fit through these data points is represented by the solid line (_____).*

Table 1: *Relation between hemodynamic parameters and gestational age during the second half of pregnancy.*

Parameter	**Mathematical description**	**Sign. (p)**	**(R^2)**
Systolic. BP (mmHg)	1.06 • GA (wks) + 15.91	0.005 *	0.342
Mean BP (mmHg)	0.87 • GA (wks) + 10.33	0.015 *	0.275
Diastolic BP (mmHg)	0.67 • GA (wks) + 2.47	0.052	0.185
Log(Compliance (ml/mmHg))	0.097 • GA (wks) - 6.42	0.000 *	0.712
Log(PR (mmHg.s/ml))	-0.065 • GA (wks) + 3.38	0.000 *	0.454
Log(Flow (ml/s))	0.089 • GA (wks) - 0.548	0.000 *	0.763
Diameter (mm)	0.19 • GA (wks) + 0.23	0.000 *	0.734
Heart rate (beats / min)	-0.268 • GA (wks) + 162	0.770	0.005
Pulsatile Index	0.008 • GA (wks) + 1.01	0.495	0.025

** Significantly related to gestational age if $p < 0.05$.*
BP = Blood Pressure, PR = Peripheral Resistance, Sign. = Statistical significance.

RESULTS

Depending on the machine settings of the color Doppler system, the pixel sizes ranged between 0.1 and 0.2 mm during data collection. The frame rates ranged between 30 and 68 Hz. The number of heartbeats selected for analysis ranged from 4 to 14. A typical example of the measured aortic radius at 34 weeks of gestation along with the best least-squares fit waveform is given in Fig. 3.

The systolic aortic pressure regression line increased linearly from 37 mmHg at 20 weeks gestation to 58 mmHg at 40 weeks of gestation. The mean aortic pressure regression line increased linearly from 28 mmHg at 20 weeks gestation to 45 mmHg at 40 weeks of gestation. The mean (± SD) diastolic pressure was 21 (±9.5) mmHg and did not significantly change with the gestational age.

The mean values of the estimated downstream peripheral resistance in the fetal descending aorta decreased exponentially from 8.0 mmHg.s/ml at 20 weeks of gestation to 2.2 mmHg.s/ml at 40 weeks of gestation. The estimated compliance increased exponentially from 0.01 ml/mmHg at 20 weeks of gestation to 0.08 ml/mmHg at 40 weeks of gestation on average. Gestational age related scatter diagrams and regression lines for these variables are shown in Fig. 4 through 6.

The results of regression analyses that attempted to relate the variables as linear or exponential (linear in the log domain) functions of the gestational age are shown in Table 1. Both the mean (± SD) heart rate 154 (± 24) beats/min and mean Pulsatile Index 1.23 (± 0.31) do not significantly change with gestational age.

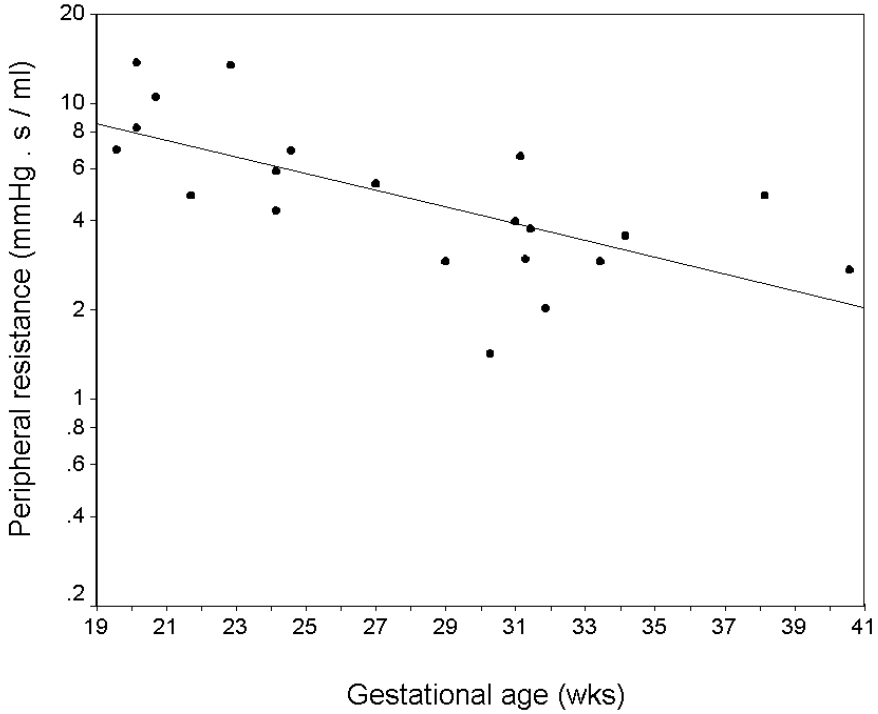

Figure 4. *A log linear gestational age-related decrease existed for estimated downstream peripheral resistance: Peripheral resistance (mmHg . s / ml) =* $e^{-0.065.GA(wks)+3.38}$.

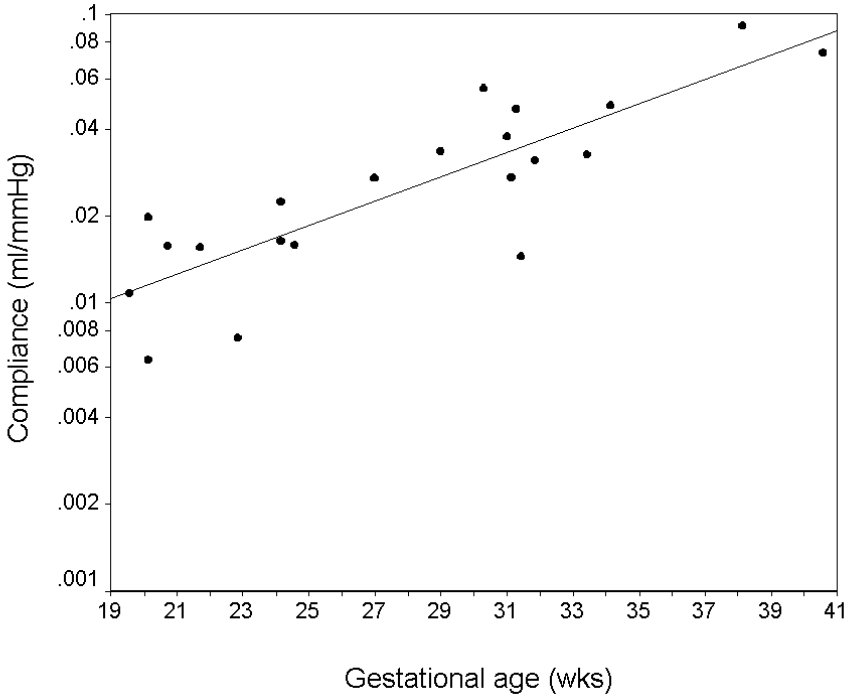

Figure 5. *A log linear gestational age-related increase existed for estimated fetal arterial compliance: Compliance (ml / mmHg) =* $e^{0.097.GA(wks)-6.42}$.

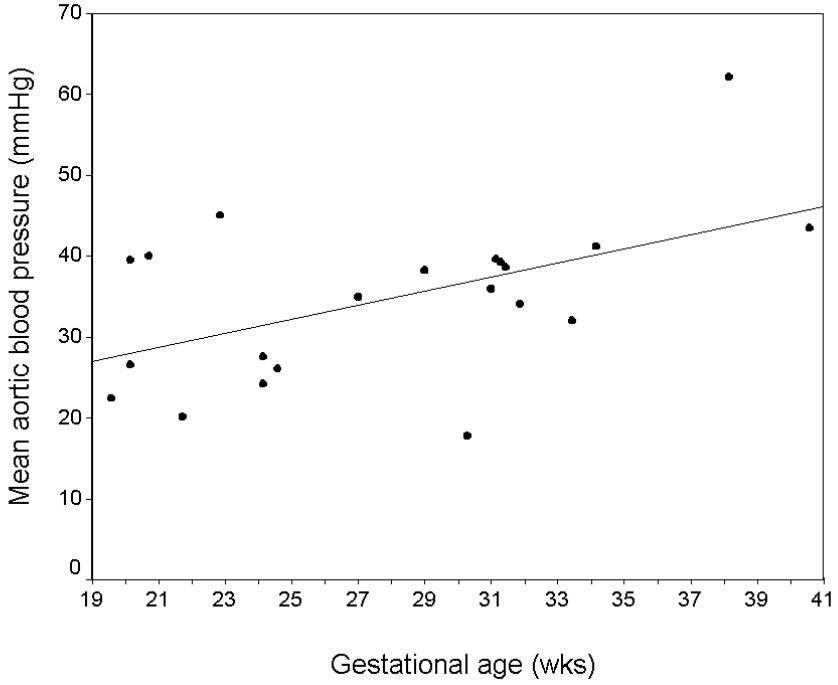

Figure 6. *The mean blood pressure is linearly related to gestational age as: Pressure (mmHg) = 0.87 · GA (wks) + 10.33.*

DISCUSSION

The Windkessel model has proven its value although it suffers from several limitations [13, 14]. A computer based parameter estimation method to obtain peripheral resistance and compliance was introduced and validated by Toorop [9]. In human adults this method has been successfully applied, mostly in adaptive form, to estimate bloodflow from pressure curves [15] and to estimate compliance in animal experiments [16, 17]. It should be noted that no direct method exists to determine arterial compliance.

In the present study fetal arterial pressure was determined from the measured aortic flow and radius waveform. Fetal aortic radius pulsations are scaled to pulse pressure by applying the scaling factor based on pulse wave velocity as suggested by Womersley. Pulse pressure and pulse blood flow gives the opportunity to estimate the downstream impedance using the Windkessel model and finally the mean pressure is determined by multiplying the mean blood flow with the resistance component of the Windkessel model.

The advantage of the two-dimensional color Doppler mode is that pulsatile blood flow velocity and diameter waveforms are simultaneously derived with no distortion of the phase relationship between them. The exact phase relation between diameter and flow or more precisely between pressure and flow is of utmost importance in the estimation of compliance.

The increasing compliance and decreasing downstream peripheral resistance with gestational age seems to be in accordance with the fetal growth process in the second half of pregnancy. The large increase in systolic and mean arterial pressures, but not diastolic pressures during the second half of pregnancy is less obvious. Since no fetal pressure data is available we compare these results with umbilical arterial catheter derived aortic pressures in preterm infants during the first 12 hours of life [18]. A statistically significant increase of 1.32, 1.01 and 0.88 mmHg per week gestation for systolic, mean and diastolic pressure respectively was found in a group of 55 infants with birth weights appropriate for gestational age. In our study, pressure estimates during intra uterine life showed a slightly less steep increase with gestational age. However, the estimated intra uterine aortic pressures obtained by applying the Hadlock formula for 24 and 40 weeks of

gestation [19] for a 670 grams and 3600 grams fetus are within the 95% confidence limits of published nomograms [18]. This might indicate baroreceptor control during perinatal life. Despite circulatory changes, such as disconnection of the placental circulation and activation of the lungs that occur soon after birth, the arterial pressure is only slightly affected when compared with intra uterine life.

Capper at al 2002 described an interesting mathematical model for the human fetal circulation in literature [20]. This model predicts the aortic and umbilical artery waveforms in the fetal circulation. However, the estimated systolic and diastolic pressures of 77 mmHg and 55 mmHg respectively for a 28-week-old human fetus are outside the range of premature newborns at the same gestational age [18, 21, 22]. The magnitudes of these pressure values are also high compared with the findings in the present study indicating that placental resistance is estimated relatively high in Capper et al 2002 [20]. When more data related to the fetal cardiovascular system becomes available, refinement of such mathematical models might improve our understanding of the complex fetal circulation.

Limitations of the study

The method for diameter determination described in this study assumes the presence of a measurable end diastolic velocity. It is not always possible to accurately measure the end diastolic velocity. Furthermore, in some cases of fetal growth restriction, the end diastolic velocity may be absent in the velocity waveform. Efforts to use gray scale information instead of the velocity profiles to determine the diameter of the blood vessels are underway at this time. The phase relation between the blood flow velocity waveform and the diameter waveform can be recovered from the scanning sequence information of the ultrasound machine. Another advantage of using gray scale or better high frequency amplitude information is the improved resolution such approaches will provide [23]. High-resolution, detailed diameter recordings are demonstrated in literature for growth restricted as well as large for gestational age fetuses using a phase locked loop echo tracking system [24].

The poor temporal resolution (typically 20 ms) in this study is not sufficient to measure pulse wave velocity accurately in individual fetuses. An echo tracking system may be used to obtain the high temporal (1-2 kHz) as well as high spatial resolution (40 - 50

microns) measurements of the pulse wave velocity in the fetal aorta [4]. When specially designed ultrasound equipment, dedicated to fetal pressure measurements becomes available, the aforementioned limitations will no longer exist.

Conclusion

During the second half of pregnancy, the feto-placental resistance seems to decrease four fold while the compliance increases eight fold. This study demonstrates the feasibility of estimating the arterial blood pressure in the human fetus. The fetal mean arterial pressures are comparable to the aortic pressures shortly after birth in neonates, born at the same gestational age.

REFERENCES

1. Baschat AA. The fetal circulation and essential organs-a new twist to an old tale. Ultrasound Obstet Gynecol 2006;27:349-54.
2. Hill AA, Surat DR, Cobbold RS, Langille BL, Mo LY, Adamson SL. A wave transmission model of the umbilicoplacental circulation based on hemodynamic measurements in sheep. Am J Physiol 1995;269:R1267-78.
3. Haig D. Genetic conflicts in human pregnancy. Q Rev Biol 1993;68:495-532.
4. Struijk PC, Wladimiroff JW, Hop WC, Simonazzi E. Pulse pressure assessment in the human fetal descending aorta. Ultrasound Med Biol 1992;18:39-43.
5. Myers LJ, Capper WL. A transmission line model of the human foetal circulatory system. Med Eng Phys 2002;24:285-94.
6. Struijk PC, Stewart PA, Fernando KL, et al. Wall shear stress and related hemodynamic parameters in the fetal descending aorta derived from color Doppler velocity profiles. Ultrasound Med Biol 2005;31:1441-50.
7. Womersley JR. Oscillatory motion of a viscous liquid in a thin walled elastic tube: The Linear approximation for long waves. Philosophical magazine 1955;46:199-221.
8. Womersley JR. Oscillatory flow in arteries: the constrained elastic tube as a model of arterial flow and pulse transmission. Phys Med Biol 1957;2:178-87.
9. Toorop GP, Westerhof N, Elzinga G. Beat-to-beat estimation of peripheral resistance and arterial compliance during pressure transients. Am J Physiol 1987;252:H1275-83.
10. Kloosterman G. On intrauterine growth. Int J Obstet Gynaecol 1970;8:895-912.
11. Pedley T. The fluid mechanics of large blood vessels: Cambridge University Press, Cambridge, 1980.
12. Lagarias JC, Reeds JA, Wright MH, Wright PE. Convergence Properties of the Nelder-Mead Simplex method in Low Dimensions. SIAM Journal of Optimization 1998;9:112-147.

13. Stergiopulos N, Westerhof BE, Westerhof N. Total arterial inertance as the fourth element of the windkessel model. Am J Physiol 1999;276:H81-8.
14. Milnor WR. Hemodynamics. Baltimore, MD: Williams and Wilkins, 1984.
15. Wesseling KH, Jansen JR, Settels JJ, Schreuder JJ. Computation of aortic flow from pressure in humans using a nonlinear, three-element model. J Appl Physiol 1993;74:2566-73.
16. Segers P, Verdonck P, Deryck Y, et al. Pulse pressure method and the area method for the estimation of total arterial compliance in dogs: sensitivity to wave reflection intensity. Ann Biomed Eng 1999;27:480-5.
17. Stergiopulos N, Segers P, Westerhof N. Use of pulse pressure method for estimating total arterial compliance in vivo. Am J Physiol 1999;276:H424-8.
18. Versmold HT, Kitterman JA, Phibbs RH, Gregory GA, Tooley WH. Aortic blood pressure during the first 12 hours of life in infants with birth weight 610 to 4,220 grams. Pediatrics 1981;67:607-13.
19. Hadlock FP, Harrist RB, Martinez-Poyer J. In utero analysis of fetal growth: a sonographic weight standard. Radiology 1991;181:129-33.
20. Capper WL, Cowper JG, Myers LJ. A transfer function-based mathematical model of the fetal-placental circulation. Ultrasound Med Biol 2002;28:1421-31.
21. Hegyi T, Anwar M, Carbone MT, et al. Blood pressure ranges in premature infants: II. The first week of life. Pediatrics 1996;97:336-42.
22. Hegyi T, Carbone MT, Anwar M, et al. Blood pressure ranges in premature infants. I. The first hours of life. J Pediatr 1994;124:627-33.
23. Brands PJ, Willigers JM, Ledoux LA, Reneman RS, Hoeks AP. A noninvasive method to estimate pulse wave velocity in arteries locally by means of ultrasound. Ultrasound Med Biol 1998;24:1325-35.
24. Mori A, Iwabuchi M, Makino T. Fetal haemodynamic changes in fetuses during fetal development evaluated by arterial pressure pulse and blood flow velocity waveforms. BJOG 2000;107:669-77.

CHAPTER 7

General discussion

The objective of this thesis was to determine novel hemodynamic parameters in the fetal and utero-placental circulation. The tools available for examining the human fetus are obviously limited when compared with the wide range of diagnostic tools available for children and adults. Ultrasound technology continuously offers new modalities, which are safe to apply in prenatal medicine. In this thesis spectral Doppler and color Doppler, two modalities of ultrasound technology, are applied to study the fetal and utero-placental circulation and their hemodynamic interaction.

SPECTRAL DOPPLER DERIVED PARAMETERS.

With range gated Doppler, also known as pulsed Doppler, a specific area or volume along the ultrasound beam is sampled. The size and position of this sample volume, which is presented in the 2D ultrasound image, can be changed. By positioning the sample volume to coincide with the 2D presentation of a pre-defined vessel of interest, Doppler audio signals of the blood flow velocity are derived. Offline analysis software is applied to reconstruct flow velocity waveforms by means of maximum frequency estimation [1, 2].

Heart rate variability

Flow velocity waveforms can be collected from the uterine and umbilical arteries using range gated spectral Doppler. The human heart does not beat in a constant rhythm, but shows fluctuations in time between consecutive heart beats. The spectral Doppler derived pulsatile flow velocity waveform allowed us to measure beat-to-beat intervals in maternal and fetal heart rate. The mean and standard deviation (SD) for all heart beats collected during the recordings were calculated and the coefficient of variation (CV = SD/mean) was taken as a measure of heart rate variability. When examining beat-to-beat fluctuations in the frequency domain in human adults, three peaks can be distinguished at frequencies near 0.04, 0.1 and 0.3 Hz [3, 4]. The first peak is of uncertain origin. The 0.1 Hz peak is mediated by the baroreflex and reflects the variable sympathetic tone of the autonomic nervous system. The peak near 0.3 Hz may reflect the parasympathetic tone linked to respiration [5]. If we consider both the integrated power of the low (L) frequency

band (< 0.2 Hz) and the integrated power of the high (H) frequency band (> 0.2 Hz), their ratio (LH-ratio) is a reflection of sympatho-vagal balance. In adults heart rate variability information is mostly derived from ECG recordings of at least several minutes duration. Artifact free umbilical flow velocity recordings can be obtained only if the fetus is at rest. The typical duration of a flow velocity recording in previous studies from our department [6, 7] was 20 seconds and limited to 50 seconds at most to ensure signal quality of the umbilical flow velocity registration. The advantage of flow velocity recording over ECG registration is that in addition to heart rate variability, flow velocity variability can be studied.

The median coefficient of variation (CV) values demonstrate that fetal heart rate variability does not differ significantly between the gestational age periods 10-14 weeks (CV=0.74%) and 15-20 weeks (CV=1.09%). However, increased integrated low frequency components and LH-ratio suggest the development of sympathetic and parasympathetic control during 15th-20th weeks of gestation. Later in pregnancy at 23-35 weeks the fetal heart rate variability was 2.3 % in uncomplicated pregnancies and significantly lower (CV=1.4%) in matched controlled growth restricted fetuses. Moreover, the LH-ratio (1.14) was also lower in comparison with the matched control group (LH-ratio=3.03) suggesting immaturity of the autonomic nervous system in the growth-restricted fetus.

Small for gestational age neonates have reduced indices of autonomic activity when compared with controls [8]. If the growth restricted fetus is unable to improve its autonomic nervous system functionality after birth, the child may suffer from inadequate blood pressure control. This might support the Barker hypothesis about the fetal origin of adult disease. Barker found that children born small for gestational age are at higher risk for hypertension and cardiovascular disease later in adult life (Barker, 1992).

Flow velocity variability

Analysis of the data from this study indicated that the beat-to-beat flow velocity variability in the umbilical artery did not change significantly during gestational age period studied. The mean coefficient of variation was 3.27 % and 3.25 % in the 10–14 and 15– 20 weeks gestation groups, respectively. Similar values were found in the age

matched control study at 23-35 weeks of gestation: 3.4% in the control group which was not statistically different from 3.9 % found in the fetal growth restricted group. Comparing heart rate and flow velocity variabilities of the fetus and the mother at 10-20 weeks gestation, a marked difference can be noted. In the mothers heart rate variability and flow velocity variability are approximately the same, varying between 3 and 4 %.
In the fetuses the heart rate variability is much lower at merely 1% while the flow velocity variability is relative high at 3% approaching the variability level in the mother.
Furthermore, the characteristic peak at 0.3 Hz found in the maternal power spectrum that is associated with maternal breathing is also found in the power spectrum of fetal flow velocity variability. The observation that in the early developing fetus prior to 15 weeks of gestation the combined sympathetic and parasympathetic control is almost absent, leads to the conclusion that umbilical blood flow variability may be influenced by the maternal uterine arterial flow variability rather than by changes in fetal cardiovascular function. This implies interaction (cross-talk) between maternal and fetal cardiovascular hemodynamics during early stages of pregnancy.

Interaction between uterine and umbilical blood flow velocity waveforms

The interaction between uterine and umbilical blood flow velocity waveforms could be demonstrated by means of the magnitude squared coherence function. The vasculo-syncytial membranes of the human placental terminal villi have elastic properties and besides are very permeable to water [9, 10]. The high permeability of this vasculo-syncytial membrane to water implies that the pressure on each side of the membrane should equalize to prevent excessive water transport. Hemochorial placentas such as those of humans and primates are essentially low-pressure placentas [11]. In the spiral artery outlet of the monkey a mean pressure of 13-18 mmHg was measured [12, 13]. It is assumed that maternal pressure pulsations are present in the human spiral artery outlet in uncomplicated human pregnancies [14]. The existence of these pressure pulsations will push back and forth on the elastic vasculo-syncytial membrane and feto-placental flow will be modulated. This explains the moderate mean magnitude coherence value of 33% found in uncomplicated pregnancies at mid gestation between uterine and umbilical flow velocity waveforms. In the preeclampsia group the coherence is only 19%, which can be

considered as a lack of coherence. The binary logistic regression model in this study showed that the lack of coherence together with diastolic notching are statistically significant predictors of preeclampsia. It is generally accepted that inadequate trophoblast invasion and therefore high spiral artery resistance is associated with preeclampsia. Using a mathematical model of the uteroplacental circulation, Talbert demonstrated that increased flow resistance of the spiral arteries does not introduce notching in the uterine flow velocity waveform, but reduces centre cotyledon pressure while the pulsatile part of the pressure waveform is almost absent due to filtering [14]. This is consistent with the lack of coherence found in the preeclampsia group. After all, if maternal pressure pulsations are almost absent in the intervillous space, coherence at the maternal heart rate with the fetal circulation is impossible. In Talbert's mathematical model it is demonstrated that notching in the uterine artery flow velocity waveform is associated with increased uterine and arcuate artery compliances and not with increased flow resistance. According to this model notching reflect uterine and arcuate compliances while a lack of coherence might reflect high spiral artery resistance. Our finding that both notching and coherence contribute to the prediction of preeclampsia is consistent with this theory.

From an ethical perspective it is impossible to manipulate uteroplacental hemodynamics in humans. Animal experiments are therefore indispensable to validate and understand the above-mentioned findings. To study the uteroplacental hemodynamics, the hemochorial placenta in the rat is likely to be the first choice for low cost research. Computer modelling studies have proven to be helpful in understanding the physiology and pathophysiology of such a complex organ as the human placenta [10, 14-20]. Future human and animal experimental data are needed to further improve our knowledge of the coupling between mother and fetus.

In summary, autonomic nervous activity causes frequency specific alterations in the heart rate power spectrum of the fetus. Therefore, power spectrum analysis of these fluctuations provides a quantitative non-invasive means of assessing the functionality of fetal cardiovascular control. This thesis provides new insights into the functional development of the autonomic nervous system in the early developing human fetus and hemodynamic interaction between mother and fetus.

COLOR DOPPLER DERIVED PARAMETERS

Color Doppler has been introduced as an imaging tool to visualize moving blood volume in 2D ultrasound images. With the advancement of image quality and improvement of temporal and spatial resolution it has become possible to use color Doppler for quantification. In this thesis methods are described to determine fetal aortic blood flow simultaneously with the aortic diameter waveform. In addition, from the derived blood flow and diameter waveforms a method is described to estimate shear stress at the aortic wall and fetal aortic blood pressure. Data collected from the human fetal descending aorta in uncomplicated pregnancies are applied to study fetal physiology.

Fetal aortic blood flow

Velocity information from spectral Doppler can be used to infer volume blood flow. The advantages of color Doppler to spectral Doppler are the following: (i) The direction of aortic flow and the Doppler angle can be calculated from the representation of a longitudinal cross sectional area of the aorta. This Doppler angle can be updated for every frame in the cineloop to compensate for slight fetal movements; (ii) no model assumptions are needed to estimate the mean of the flow velocity profile since volume flow determination is derived from all velocities across the scan line and not from the maximum velocity in the profile as is the case when using spectral Doppler; (iii) volume flow determination is achieved by integration of the velocity profile. Thus, the pulsatile nature of the fetal aortic diameter is taken into account.

In this thesis it is demonstrated that in uncomplicated pregnancies a log-linear gestational age related increase exists for the aortic volume flow while the mean aortic diameter exhibits a linear gestational age related increase. The final goal of this study was to determine wall shear stress and blood pressure in the fetal aorta.

Fetal aortic shear stress

Blood flow in arteries generates fluid mechanical forces acting on endothelial cells. This so-called wall shear stress is an important determinant of the biologic activity of endothelial cells. Flow related increased wall shear stress would stimulate vessel growth. This control mechanism in which vessels adapts to flow demand plays an important role in embryonic and fetal development [21]. This thesis describes a method of calculating the pulsatile wall shear stress from color Doppler derived cineloops. The Womersley solution is applied to generate more accurate approximations for the wall shear stress than the direct approach by means of finding the velocity differential close to the vessel wall. The study shows that in uncomplicated pregnancies the mean wall shear stress; 2.16 (SD= 0.59) Pa and the peak wall shear stress; 6.80 (SD=1.9) Pa are not significantly related to gestational age during the second half of pregnancy indicating that the aortic size adapts to blood flow.

In the growth restricted fetus the flow velocity waveform is more pulsatile than in the normally developing fetus. Therefore, the peak shear stress will be relatively high in comparison with time averaged wall shear stress. As a consequence, the temporal gradient shear, that is the slope from end diastolic to peak systolic shear will be relatively high in the growth-restricted fetus. Bao (1999) has demonstrated that pulsatile blood flow provides two distinct stimuli, -the steady shear and the temporal gradient in shear-, which play distinct roles in atherogenesis [22]. The temporal gradient in shear stress leads to enhanced expression of platelet-derived growth factor A (PDGF-A) and monocyte chemoattractant protein-1 (MCP-1), whereas the presence of steady shear stress reduces these levels. The arteries in the growth restricted fetus may therefore be maladapted as a result of flow waveform differences. It is shown in literature that newborn babies with growth restriction have significant aortic wall thickening [23]. It will be of interest to apply the shear stress method described in this thesis in a case control study to test the hypothesis that temporal gradient shear is involved in aortic wall thickening in the growth restricted fetus.

Fetal aortic pressure

Direct arterial pressure measurements are not feasible due to the inaccessibility of the human fetus. Arterial blood pressure is an important determinant because it provides the driving force for organ perfusion. As previously discussed, aortic blood flow can be measured in the fetus. However, the lack of information on fetal pressure implies that quantification of important developmental parameters such as peripheral resistance and compliance of the vascular bed cannot be performed in the human fetus. The indirect method of pressure estimation described in this thesis is based on the physical principles that in an elastic tube, the wall extension is related to pressure and that the elasticity constant of the elastic wall is related to the pulse wave velocity. Womersley described the relation between aortic pressure and wall extension assuming that the Poisson ratio of the aortic wall is 0.5 and that the aorta is longitudinally tethered by an elastic constraint [24]. These assumptions are generally accepted for the human aorta. By applying the Womersley relation, the pulsatile part of the pressure waveform can be calculated from the aortic diameter waveform. Since the pulsatile pressure and flow waveforms are derived simultaneously from the velocity profiles, their time relation is preserved. Fundamentally, the downstream aortic impedance is known from the pulsatile part of the pressure and flow waveforms. The Windkessel model is adopted to divide downstream impedance into peripheral resistance and compliance. The advantage of the simple two-element Windkessel model is that only two parameters, the compliance (C) and the resistance (R), have to be estimated. An iterative algorithm is applied to find the best C and R by least-squares fitting the observed and computed pulsatile diameter waveforms. The mean aortic blood pressure is derived as the product of the mean aortic flow and the peripheral resistance.

The results obtained from the human fetus are promising. The pressure values are in the range of umbilical arterial catheter derived aortic pressures in preterm infants, which is in line with the baroreceptor control found in perinatal life [25].

The ultimate goal of future research is to arrive at a point where the accuracy of the method of pressure estimation allows characterization of the individual fetus. To achieve this, the pulse wave velocity in the fetal aorta should be accurately determined prior to pressure estimation. The method described by Brands et al adapted to fetal ultrasound

scanning can serve this purpose [26]. The same group described methods for analyses based on digitally sampled ultrasound echo signals [27]. Improved performance can be expected if these innovative methods that were basically designed for applications in the carotid arteries are adapted to the fetal aorta. This adaptation requires ultrasound equipment specially designed for fetal pressure assessment.

Improved definition of velocity and diameter signals will not only serve the accuracy and reproducibility of pressure estimation but will also allow higher order impedance models to be tested. For the complex umbilical-placental circulation, it is likely to be more realistic to combine the two-element Windkessel model with a wave transmission model that can compute the contribution of reflected velocity and pressure waves [28-31]. To validate the method of pressure estimation under physiological and patho-physiological conditions, an animal experimental setting is needed. It is anticipated that accurate fetal arterial blood pressure determination will benefit prenatal care.

From animal studies there is evidence that it is important to monitor blood pressure under some severe fetal conditions. In sheep fetuses suffering from both severe hypotension and hypoxia after 10 minutes cord occlusion only hypotension correlated with histologic outcome of cerebral damage [32]. Ashwal showed that autoregulation of cerebral blood flow is lost when mean arterial pressure falls below 30 mmHg. This might explain the better correlation for brain damage with pressure than with hypoxia [33].

Although pregnancy induced hypertension is not completely understood, hypertension might be a response to poor utero-placental perfusion and needed to obtain sufficient maternal placental circulation to meet fetal demands [34]. Therefore, lowering the maternal blood pressure could be harmful to the fetus. Furthermore, most anti-hypertensive drugs will pass the placenta, which might lower fetal pressure and deteriorate fetal well being. Fetal blood pressure monitoring can be of importance to balance the benefits to the mother and risks to the fetus during anti-hypertensive treatment.

Timing of birth is critical in pathologic conditions such as intra uterine growth restriction and prematurity. Fetal hemodynamic information including blood pressure, peripheral resistance and arterial compliance may assist obstetricians and pediatricians in making the right clinical decisions.

REFERENCES

1. Ursem NT, Brinkman HJ, Struijk PC, et al. Umbilical artery waveform analysis based on maximum, mean and mode velocity in early human pregnancy. Ultrasound Med Biol 1998;24:1-7.
2. Fernando KL, Mathews VJ, Clark EB. A mathematical basis for the application of the modified geometric method to maximum frequency estimation. IEEE Trans Biomed Eng 2004;51:2085-8.
3. Akselrod S, Gordon D, Ubel FA, Shannon DC, Berger AC, Cohen RJ. Power spectrum analysis of heart rate fluctuation: a quantitative probe of beat-to-beat cardiovascular control. Science 1981;213:220-2.
4. Task-Force. Heart rate variability. Standards of measurement, physiological interpretation, and clinical use. Task Force of the European Society of Cardiology and the North American Society of Pacing and Electrophysiology. Eur Heart J 1996;17:354-81.
5. van Steenis HG. On time frequency analysis of heart rate variability (Ph.D. Thesis), 2002.
6. Vinkesteijn AS, Ursem NT, Struijk PC, Wladimiroff JW. Fetal heart rate and blood flow velocity variability in the presence of increased nuchal translucency: a preliminary study. Ultrasound Obstet Gynecol 2004;23:19-22.
7. Ursem NT, Struijk PC, Hop WC, Clark EB, Keller BB, Wladimiroff JW. Heart rate and flow velocity variability as determined from umbilical Doppler velocimetry at 10-20 weeks of gestation. Clin Sci (Lond) 1998;95:539-45.
8. Spassov L, Curzi-Dascalova L, Clairambault J, et al. Heart rate and heart rate variability during sleep in small-for-gestational age newborns. Pediatr Res 1994;35:500-5.
9. Sibley CP, Boyd DH. Mechanisms of transfer across the human placenta. Philadelhia: Saunders, 1992.
10. Talbert D, Sebire NJ. The dynamic placenta: I. Hypothetical model of a placental mechanism matching local fetal blood flow to local intervillus oxygen delivery. Med Hypotheses 2004;62:511-9.

11. Moll W, Kunzel W, Herberger J. Hemodynamic implications of hemochorial placentation. Eur J Obstet Gynecol Reprod Biol 1975;5:67-74.
12. Reynolds SR, Freese UE, Bieniarz J, Caldeyro-Barcia R, Mendez-Bauer C, Escarcena L. Multiple simultaneous intervillous space pressures recorded in several regions of the hemochorial placenta in relation to functional anatomy of the fetal cotyledon. Am J Obstet Gynecol 1968;102:1128-34.
13. Moll W, Wallenburg HC, Kastendieck E, Voslar M. The flow resistance of the spiral artery and the related intervillous space in the rhesus monkey placenta. Pflugers Arch 1978;377:225-8.
14. Talbert DG. Uterine flow velocity waveform shape as an indicator of maternal and placental development failure mechanisms: a model-based synthesizing approach. Ultrasound Obstet Gynecol 1995;6:261-71.
15. Denbow ML, Talbert D, Fisk NM. Determinants of flow along arterio-arterial anastomoses in monochorionic placentae by dynamic computer modelling of chorionic plate vasculature. Prenat Diagn 2006;26:433-42.
16. Sebire NJ, Jain V, Talbert DG. Spiral artery associated restricted growth (SPAARG): a computer model of pathophysiology resulting from low intervillous pressure having fetal programming implications. Pathophysiology 2004;11:87-94.
17. Sebire NJ, Talbert D. 'Cor placentale': placental intervillus/intravillus blood flow mismatch is the pathophysiological mechanism in severe intrauterine growth restriction due to uteroplacental disease. Med Hypotheses 2001;57:354-7.
18. Sebire NJ, Talbert D. The dynamic placenta: II. Hypothetical model of a fetus driven transplacental water balance mechanism producing low apparent permeability in a highly permeable placenta. Med Hypotheses 2004;62:520-8.
19. Sebire NJ, Talbert DG. The dynamic placenta: a closer look at the pathophysiology of placental hemodynamics in uteroplacental compromise. Ultrasound Obstet Gynecol 2001;18:557-61.
20. Talbert DG, Johnson P. The pulmonary vein Doppler flow velocity waveform: feature analysis by comparison of in vivo pressures and flows with those in a computerized fetal physiological model. Ultrasound Obstet Gynecol 2000;16:457-67.

21. le Noble F, Fleury V, Pries A, Corvol P, Eichmann A, Reneman RS. Control of arterial branching morphogenesis in embryogenesis: go with the flow. Cardiovasc Res 2005;65:619-28.
22. Bao X, Lu C, Frangos JA. Temporal gradient in shear but not steady shear stress induces PDGF-A and MCP-1 expression in endothelial cells: role of NO, NF kappa B, and egr-1. Arterioscler Thromb Vasc Biol 1999;19:996-1003.
23. Skilton MR, Evans N, Griffiths KA, Harmer JA, Celermajer DS. Aortic wall thickness in newborns with intrauterine growth restriction. Lancet 2005;365:1484-6.
24. Womersley JR. Oscillatory flow in arteries: the constrained elastic tube as a model of arterial flow and pulse transmission. Phys Med Biol 1957;2:178-87.
25. Segar JL. Ontogeny of the arterial and cardiopulmonary baroreflex during fetal and postnatal life. Am J Physiol 1997;273:R457-71.
26. Brands PJ, Willigers JM, Ledoux LA, Reneman RS, Hoeks AP. A noninvasive method to estimate pulse wave velocity in arteries locally by means of ultrasound. Ultrasound Med Biol 1998;24:1325-35.
27. Brands PJ, Hoeks AP, Willigers J, Willekes C, Reneman RS. An integrated system for the non-invasive assessment of vessel wall and hemodynamic properties of large arteries by means of ultrasound. Eur J Ultrasound 1999;9:257-66.
28. Capper WL, Cowper JG, Myers LJ. A transfer function-based mathematical model of the fetal-placental circulation. Ultrasound Med Biol 2002;28:1421-31.
29. Myers LJ, Capper WL. A transmission line model of the human foetal circulatory system. Med Eng Phys 2002;24:285-94.
30. Menigault E, Vieyres P, Lepoivre B, Durand A, Pourcelot L, Berson M. Fetal heart modelling based on a pressure-volume relationship. Med Biol Eng Comput 1997;35:715-21.
31. Hill AA, Surat DR, Cobbold RS, Langille BL, Mo LY, Adamson SL. A wave transmission model of the umbilicoplacental circulation based on hemodynamic measurements in sheep. Am J Physiol 1995;269:R1267-78.

32. Mallard EC, Gunn AJ, Williams CE, Johnston BM, Gluckman PD. Transient umbilical cord occlusion causes hippocampal damage in the fetal sheep. Am J Obstet Gynecol 1992;167:1423-30.
33. Ashwal S, Dale PS, Longo LD. Regional cerebral blood flow: studies in the fetal lamb during hypoxia, hypercapnia, acidosis, and hypotension. Pediatr Res 1984;18:1309-16.
34. Haig D. Genetic conflicts in human pregnancy. Q Rev Biol 1993;68:495-532.

CHAPTER 8

Summary
Samenvatting
Curriculum Vitae
Publicatie lijst
Dankwoord

SUMMARY

Chapter 1

A short history of ultrasound in obstetrics and gynecology is given. So far there is no evidence that diagnostic ultrasound is harmful to the human fetus. However, it is known that ultrasound energy is partly absorbed by tissue and bony structures. As a result, temperature warming can be expected if during a considerable time the ultrasound beam is aimed at one particular spot. Modern ultrasound scanners are equipped with temperature index monitoring upon which the user may decide to use lower machine output settings or limit examination time to minimize any possible risk. The combination of the Doppler principle and two-dimensional ultrasound imaging enables blood flow velocity measurement in fetal blood vessels. This modality of ultrasound contributed to a better understanding of the physiology and pathophysiology of the fetal cardiovascular system. The aim of this Ph.D. study was to further improve our knowledge of the fetal and utero-placental circulation. To this purpose, fetal hemodynamic parameters were assessed and tested on spectral- and color Doppler derived data.

Chapter 2

Spectral Doppler derived data from both the uterine and umbilical artery in early pregnancy are discussed in this chapter. Flow velocity waveforms were reconstructed from the Doppler frequency shift by estimating the maximum frequency shift in the frequency domain during short time intervals. Subsequently, heart rate and mean blood flow velocity per heartbeat were determined from these waveforms. It is known that in the adult circulation beat-to-beat heart rate variability originates from autonomic nervous system control. When examining beat-to-beat heart rate variability in the frequency domain, two peaks can be distinguished: the first near 0.1 Hz as a result of baro-receptor activity and the second peak near 0.3 Hz which is associated with respiration. Results from this study showed that the two characteristic peaks are also seen during pregnancy. However, in the fetal circulation the first peak in the frequency domain of the heart rate variability power spectrum was absent prior to 15 weeks of gestation and total variability was small. Only after 15 weeks of gestation the peak in the low frequency band (< 0.2

Hz) can be seen, suggesting the development of sympathetic and parasympathetic control during the 15th – 20th week of gestation. Results of the beat-to-beat flow velocity variability showed no major differences between mother and fetus. The two characteristic peaks in the frequency spectrum were found in both the maternal and fetal circulation. The fact that prior to 15 weeks gestation a first peak was seen in the velocity variability frequency spectrum but not in the heart rate variability spectrum of the fetus and that the second peak is associated with respiration, suggests that the maternal utero-placental circulation may influence fetal blood flow variability in the umbilical artery.

Chapter 3

This chapter focuses on heart rate and flow velocity variability in the umbilical artery of the growth restricted fetus. The ratio between integrated power of the low frequency band (< 0.2 Hz) and the integrated power of the high frequency band (> 0.2 Hz) reflects sympatho-vagal balance. The fact that this ratio was significantly lower in the growth-restricted fetus suggests immaturity of the autonomic nervous system in the growth-restricted fetus. The flow velocity variability in the umbilical artery was not statistically significantly different between uncomplicated and growth restricted pregnancies.

Chapter 4

The interaction between the maternal and fetal circulation was studied by evaluating the magnitude-squared coherence function between blood flow velocity waveforms of the uterine and umbilical arteries. The thickness of the elastic vasculo syncytial membranes of the human placental terminal villi is only a few microns. Large molecules can pass the placenta, which implies high permeability to water. To prevent excessive water transport the mean pressure on each side of the membrane should equalize. During the systolic phase the maternal intervillous pressure will press the membrane inwards reducing the intra villous space. During the diastolic phase of the maternal heartbeat the intravillous space will return to its original size. The magnitude-squared coherence function was applied to measure the presence of a frequency component at the maternal heart rate in the power spectrum of the umbilical blood flow velocity waveform. A total of 299 pregnant women underwent an ultrasound examination at mid gestation. The predictive

value of the magnitude-squared coherence function was evaluated for pregnancy induced hypertension, preeclampsia and intrauterine growth restriction. It was demonstrated that inclusion of the magnitude-squared coherence can significantly improve the prediction of preeclampsia.

Chapter 5

In contrast to spectral Doppler that measures the Doppler frequency at one spot within the two-dimensional image, color Doppler measures the Doppler frequency at as many spots as possible within the two dimensional image. Initially this modality was applied to visualize blood vessels in the fetal circulation. Due to improved spatial- and time resolution the utilization of color Doppler has been considerably enlarged. Two dimensional color Doppler images acquired at a high frame rate were digitally stored for offline analysis. From the color Doppler derived fetal aortic diameter and blood flow waveform the wall shear stress was calculated. Depending on wall shear stress endothelial activity will stimulate or diminish aortic growth. The study described in this chapter demonstrates that fetal aortic wall shear stress is not related to gestational age, suggesting that the size of the fetal aorta adapts to flow demands and maintains a constant wall shear stress.

Chapter 6

This chapter describes a method to apply color Doppler ultra-sonography to estimate fetal aortic blood pressure. The method relies on two physical principles as described by the mathematician and physicist Womersley in 1957. Firstly, in an elastic tube the wall extension is related to pressure and secondly, the elasticity constant of the aortic wall is related to the pulse wave velocity. By modeling the downstream impedance as the arterial compliance parallel to the peripheral resistance ("Windkessel") model, an algorithm was found to estimate aortic pressure from simultaneously derived aortic blood flow and diameter waveforms. Using these waveforms the best estimates for peripheral resistance and compliance were found. The pressure waveform in the time domain can be evaluated as the inverse Fourier transform of the product of the blood flow waveform and the downstream impedance in the frequency domain. The magnitude of the fetal aortic blood

pressure during the second half of pregnancy was comparable to the aortic blood pressure measured shortly after birth in infants born prematurely at similar gestational age. These results are promising since it is known from literature that baro-receptor control is active in perinatal life and similar pressures could be expected.

Chapter 7

In this chapter a general discussion is provided considering the results of the combined studies described in this thesis. A view on future research based on results gathered so far is described.

SAMENVATTING

Hoofdstuk 1

In een kort overzicht wordt de geschiedenis van ultrageluid in de verloskunde en gynaecologie geschetst. Er zijn tot op heden geen bewijzen dat ultrageluid schade veroorzaakt bij het ongeboren kind. Wel is bekend dat ultrageluidenergie gedeeltelijk wordt geabsorbeerd door weefsel en met name door botstructuren, waardoor de temperatuur lokaal zal toenemen wanneer de ultrageluidbundel gedurende langere tijd op één plaats is gericht. Bij moderne echo apparatuur wordt afhankelijk van de instelling de mogelijke temperatuur toename aangegeven. De gebruiker kan met deze informatie de apparatuur instelling kiezen waarbij een minimaal akoestisch vermogen wordt afgegeven en/of de scanduur aanpassen om mogelijke risico's tot een minimum te beperken. Door toepassing van het Doppler principe in combinatie met twee dimensionaal echoscopisch verkregen beelden is het mogelijk geworden de bloeddoorstroming in foetale bloedvaten te meten. Dit heeft in belangrijke mate bijgedragen tot verrijking van de kennis op het gebied van de fysiologie en pathofysiologie van het cardiovasculaire systeem in het ongeboren kind. De doelstelling van dit proefschrift is de bestaande kennis op het gebied van de utero-placentaire- en foetale circulatie te verbreden. Hiertoe zijn nieuwe analyse technieken ontwikkeld en toegepast op spectraal- en kleuren Doppler verkregen data.

Hoofdstuk 2

De onderzoeksresultaten van vroeg in de zwangerschap verkregen spectraal Doppler data van zowel de arterie uterina als de arterie umbilicalis worden in dit hoofdstuk beschreven. De golfvormen van de arteriële bloeddoorstroming zijn gereconstrueerd door de maximale frequentie verschuiving te bepalen in de Doppler spectra van kort opeenvolgende tijdintervallen. Vervolgens is de hartslag frequentie en de gemiddelde bloeddoorstroming per hartslag vastgesteld. Het is bekend dat ten gevolge van regulerende signalen van het autonome zenuwstelsel de hartslag frequentie in de volwassen circulatie van slag tot slag varieert. In de spectrale verdeling van deze variabiliteit zijn twee pieken waarneembaar, de eerste in de buurt van 0.1 Hz ten gevolge van de baro-receptor activiteit en de tweede piek in de buurt van 0.3 Hz welke wordt

geassocieerd met de ademhaling. Uit het hier beschreven onderzoek is gebleken dat deze karakteristieke pieken in het frequentie spectrum ook tijdens de zwangerschap kunnen worden waargenomen. Echter in de foetale circulatie is voor de 15 weken zwangerschap de eerste piek in het frequentie spectrum vrijwel geheel afwezig en wordt slechts een geringe variabiliteit in de hartslag frequentie waargenomen. Pas na 15 weken zwangerschap wordt een piek waargenomen in de lage frequentie band (< 0.2 Hz) van het frequentie spectrum. Op grond hiervan is geconcludeerd dat in de humane foetus het foetale autonome zenuwstelsel pas na 15 weken zwangerschap actief wordt. De frequentie verdelingen van de slag tot slag bloeddoorstroming blijken tussen moeder en kind slechts weinig te verschillen. Zowel bij moeder als kind worden de twee karakteristieke pieken in het frequentie spectrum waargenomen. Daar de tweede piek is geassocieerd met ademhaling, kan gesteld worden dat de variabiliteit in de foetale placentaire doorstroming in belangrijke mate wordt bepaald door interactie met de maternale circulatie.

Hoofdstuk 3

Dit onderzoek concentreert zich op de variabiliteit van de foetale hartfrequentie en de placentaire bloeddoorstroming tijdens foetale groeivertraging. De verhouding tussen de geïntegreerde variabiliteit in het lage frequentie gebied (< 0.2 Hz) en het hoge frequentie gebied (> 0.2 Hz) is een maat voor sympathische / parasympathische regulatie. Het feit dat deze verhouding in de groeivertraagde zwangerschap is verlaagd, doet vermoeden dat het autonome zenuwstelsel in de groeivertraagde foetus minder is ontwikkeld. De variabiliteit van de bloeddoorstroming in de arterie umbilicalis is tussen de groeivertraagde zwangerschap en ongecompliceerde zwangerschap statistisch niet significant verschillend.

Hoofdstuk 4

De interactie tussen de maternale - en de foetale placentaire circulatie is nader onderzocht door de wiskundige coherentie te bepalen tussen de bloeddoorstroming in de arterie uterina en de arterie umbilicalis. Het arteriële vaatbed van de placenta eindigt in de zogenaamde villi, deze eindigen in een zeer dun membraan waar de uitwisseling van

stoffen tussen moeder en kind plaatsvindt. Omdat relatief grote moleculen uitgewisseld kunnen worden zijn de membranen in hoge mate permeabel voor watermoleculen. Tevens is bekend dat in de ongecompliceerde zwangerschap geen excessief watertransport tussen moeder en kind plaatsvindt, derhalve zal de vloeistofdruk aan beide zijden van het membraan gemiddeld gelijk moeten zijn. Het membraan is elastisch waardoor het tijdens de maternale systolische bloeddruk naar binnen wordt gedrukt. De doorstromingsruimte voor foetaal bloed in de villi zal op dat moment minimaal zijn. Tijdens de diastole fase van de maternale bloeddruk zal deze doorstromingsruimte weer toenemen. Met de coherentie functie is onderzocht of in de foetale placentaire bloeddoorstroming veranderingen optreden in het ritme van de maternale hartfrequentie.
Bij 299 vrouwen die deelnamen aan dit onderzoek is halverwege de zwangerschap echoscopisch onderzoek verricht. Er is onderzocht of de coherentie functie afwijkend is voor vrouwen die later in de zwangerschap hoge bloeddruk of preeclampsie ontwikkelden dan wel bevielen van een kind met groeiachterstand. Uit dit onderzoek is gebleken dat vrouwen die later preeclampsie hebben ontwikkeld gemiddeld een verminderde coherentie laten zien ten opzichte van een ongecompliceerde zwangerschap. Tevens bleek deze verminderde coherentie een statistisch significante bijdrage te leveren aan de voorspelling van preeclampsie.

Hoofdstuk 5

In tegenstelling tot spectraal Doppler waar op één plaats in het twee dimensionaal beeld de Doppler frequentie wordt gemeten, wordt met kleuren Doppler op zoveel mogelijk plaatsen in het twee dimensionaal beeld de Doppler frequentie vastgesteld. Aanvankelijk werd deze techniek uitsluitend toegepast om in het twee dimensionaal beeld bloedvaten te visualiseren. De resolutie van deze techniek is in de loop der tijd sterk verbeterd waardoor het toepassingsgebied veel breder is geworden. Naast een goede afstandsresolutie kan ook een hoge beeld frequentie worden bereikt. Snel opeenvolgende kleurenbeelden van de longitudinale doorsnede van de foetale aorta zijn digitaal opgeslagen en geanalyseerd. De pulserende bloeddoorstroming en de diameter van de foetale aorta kunnen simultaan uit de kleuren Doppler registratie worden verkregen. Met behulp van deze gegevens is de wrijvingskracht op de vaatwand berekend. Afhankelijk

van de wrijvingskracht welke ten gevolge van de bloeddoorstroming door de endotheel cellen wordt ervaren, zal de groei van bloedvaten worden bevorderd dan wel verminderd. In de tweede helft van de zwangerschap blijkt de wrijvingskracht uitgeoefend op de vaatwand van de foetale aorta onafhankelijk te zijn van de zwangerschapsduur. Dit resultaat bevestigt het reeds bestaande vermoeden dat de regulerende functie van de endotheel cellen ook tijdens het foetale leven actief is.

Hoofdstuk 6

In dit hoofdstuk wordt beschreven hoe door toepassing van kleuren Doppler echografie een schatting gemaakt kan worden van de bloeddruk in de foetale aorta. Hierbij wordt gebruik gemaakt van de golf theorie in een elastische buis en de relatie tussen bloeddruk en de uitzetting van de aorta zoals deze door de wis- en natuurkundige Womersley in 1957 is beschreven. De frequentie afhankelijke weerstand voor bloeddoorstroming (impedantie) kan beschreven worden door de parallel schakeling van een perifere weerstand en een compliantie ("Windkessel") model. Met compliantie wordt de elastische eigenschap van het arteriële vaatbed bedoeld waarbij het bloedvolume toeneemt naarmate de bloeddruk hoger wordt. Uit de in hoog tempo opgeslagen kleuren Doppler beelden is een simultaan registratie verkregen van zowel de golfvorm van de bloeddoorstroming als de diameter verandering van de foetale aorta. Gebruik makend van deze golfvormen is een iteratief algoritme toegepast om de beste waarde voor de perifere weerstand en de compliantie te vinden. Door vermenigvuldiging van de bloeddoor-stroming en de impedantie is een schatting gemaakt van de arteriële bloeddruk golfvorm in de foetale aorta. De foetale bloeddruk waarden, gevonden in de tweede helft van de zwangerschap, kwamen overeen met in de literatuur beschreven bloeddrukwaarden gemeten bij vroeg geboren kinderen die betreffende zwangerschapsduur vergelijkbaar waren. Dit is een bemoedigend resultaat omdat tevens in de literatuur is beschreven dat gedurende het perinatale leven, het bloeddruk regulerende baroreceptor mechanisme actief is op grond waarvan kort voor en na de geboorte vergelijkbare drukken verwacht mogen worden.

Hoofdstuk 7

In dit hoofdstuk wordt de samenhang tussen de verschillende hoofdstukken besproken en worden de resultaten van dit promotie onderzoek algemeen beschouwd. Tevens wordt een visie geschetst voor vervolgonderzoek.

CURRICULUM VITAE

6 juni 1952	Geboren te Sliedrecht.
1973	Eindexamen Middelbaar Technisch Onderwijs afdeling Elektronica.
1973 - 1974	Praktijkjaar elektronicus: Instituut voor zintuigfysiologie, Soesterberg en Academisch Dijkzigt Ziekenhuis Rotterdam (AZR).
1974 - 1975	Elektronisch ontwerper, Erasmus Universiteit Rotterdam (E.U.R), Centrale Research Werkplaatsen afdeling ontwikkeling.
1975 - 1982	Service / veiligheids elektronicus, A.Z.R.
1982 - 1989	Medisch instrumentatie technicus, afdeling Centrale Research Werkplaatsen A.Z.R.
1989 - 1994	50 % aanstelling Hoger Röntgen Technicus, A.Z.R. 50 % aanstelling Specialist software beheer, systeemondersteuning en educatie, Laboratorium Gynaecologie / Obstetrie. E.U.R.
1994 - 2001	Volledige aanstelling Erasmus Universiteit Rotterdam afdeling Verloskunde & Vrouwenziekten in de functie van: Specialist software beheer, systeemondersteuning en educatie.
2001 - heden	Wetenschappelijk onderzoeker Erasmus MC, Universitair Medisch Centrum.

Publicatie lijst

1. Wladimiroff JW, **Struijk PC**, Stewart PA, Clusters P, de Villeneuve VH. Fetal cardiovascular dynamics during cardiac dysrhythmia. Case report. Br J Obstet Gynaecol 1983 90:573-7.
2. Tonge HM, **Struijk PC**, Custers P, Wladimiroff JW.Vascular dynamics in the descending aorta of the human fetus in normal late pregnancy.Early Hum Dev 1983 9:21-6.
3. Tonge HM, **Struijk PC**, Wladimiroff JW. Blood flow measurements in the fetal descending aorta: technique and clinics. Clin Cardiol 1984 7:323-9.
4. **Struijk PC**, Pijpers L, Wladimiroff JW, Lotgering FK, Tonge M, Bom N. The time-distance recorder as a means of improving the accuracy of fetal blood flow measurements. Ultrasound Med Biol. 1985 11:71-7.
5. Noordam MJ, Wladimiroff JW, Lotgering FK, **Struijk PC**, Tonge HM. Fetal blood flow velocity waveforms in relation to changing peripheral vascular Resistance. Early Hum Dev 1987 15:119-27.
6. Tonge HM, **Struijk PC**, van Kooten C, Wladimiroff JW, Bom N. The first derivative as a means of synchronizing pulsatile flow velocity and vessel diameter waveforms in the fetal descending aorta. J Perinat Med 1988 16:299-304.
7. Lotgering FK, van Doorn MB, **Struijk PC**, Pool J, Wallenburg HC. Maximal aerobic exercise in pregnant women: heart rate, O2 consumption, CO2 production, and ventilation. J Appl Physiol 1991 70:1016-23.
8. Lotgering FK, **Struijk PC**, van Doorn MB, Wallenburg HC. Errors in predicting maximal oxygen consumption in pregnant women. J Appl Physiol. 1992 72:562-7.
9. **Struijk PC**, Wladimiroff JW, Hop WC, Simonazzi E. Pulse pressure assessment in the human fetal descending aorta. Ultrasound Med Biol 1992 18:39-43.
10. Lotgering FK, van den Berg A, **Struijk PC**, Wallenburg HC. Arterial pressure response to maximal isometric exercise in pregnant women. Am J Obstet Gynecol 1992 166:538-42.
11. van Doorn MB, Lotgering FK, **Struijk PC**, Pool J, Wallenburg HC. Maternal and fetal cardiovascular responses to strenuous bicycle exercise. Am J Obstet Gynecol 1992 166:854-9.

12. Broekhuizen ML, Mast F, **Struijk PC**, van der Bie W, Mulder PG, Gittenberger-de Groot AC, Wladimiroff JW. Hemodynamic parameters of stage 20 to stage 35 chick embryo. Pediatr Res 1993 34:44-6.
13. Lotgering FK, **Struijk PC**, van Doorn MB, Spinnewijn WE, Wallenburg HC. Anaerobic threshold and respiratory compensation in pregnant women. J Appl Physiol 1995 78:1772-7.
14. Spinnewijn WE, Wallenburg HC, **Struijk PC**, Lotgering FK. Peak ventilatory responses during cycling and swimming in pregnant and nonpregnant women. J Appl Physiol 1996 81:738-42.
15. Schneider TJ, **Struijk PC**, Lotgering FK, Wallenburg HC. Placental transfer and maternal and fetal hemodynamic effects of ketanserin in the pregnant ewe. Eur J Obstet Gynecol Reprod Biol 1996 68:179-84.
16. Spinnewijn WE, Lotgering FK, **Struijk PC**, Wallenburg HC. Fetal heart rate and uterine contractility during maternal exercise at term. Am J Obstet Gynecol 1996 174:43-8.
17. Beckmann I, Visser W, **Struijk PC**, van Dooren M, Glavimans J, Wallenburg HC. Circulating bioactive tumor necrosis factor-alpha, tumor necrosis factor-alpha receptors, fibronectin, and tumor necrosis factor-alpha inducible cell adhesion molecule VCAM-1 in uncomplicated pregnancy. Am J Obstet Gynecol 1997 177:1247-52.
18. Laudy JA, Janssen MM, **Struijk PC**, Stijnen T, Wladimiroff JW. Three-dimensional ultrasonography of normal fetal lung volume: a preliminary study. Ultrasound Obstet Gynecol 1998 11:13-6.
19. Laudy JA, Janssen MM, **Struijk PC**, Stijnen T, Wallenburg HC, Wladimiroff JW. Fetal liver volume measurement by three-dimensional ultrasonography: a preliminary study.Ultrasound Obstet Gynecol 1998 12:93-6.
20. Lotgering FK, Spinnewijn WE, **Struijk PC**, Boomsma F, Wallenburg HC. Respiratory and metabolic responses to endurance cycle exercise in pregnant and postpartum women. Int J Sports Med 1998 19:193-8.
21. Ursem NT, **Struijk PC**, Hop WC, Clark EB, Keller BB, Wladimiroff JW. Heart rate and flow velocity variability as determined from umbilical Doppler velocimetry at 10-20 weeks of gestation. Clin Sci (Lond) 1998 95:539-45.

22. Ursem NT, Brinkman HJ, **Struijk PC**, Hop WC, Kempski MH, Keller BB, Wladimiroff JW. Umbilical artery waveform analysis based on maximum, mean and mode velocity in early human pregnancy. Ultrasound Med Biol 1998 24:1-7.
23. Kaaij MW, **Struijk PC**, Lotgering FK. Accuracy of sonographic estimates of fetal weight in very small infants. Ultrasound Obstet Gynecol 1999 13:99-102.
24. Schneider TJ, **Struijk PC**, Wallenburg HC. Placental transfer of the thromboxane synthetase inhibitor ridogrel in the late-pregnant ewe. Eur J Obstet Gynecol Reprod Biol 1999 86:83-7.
25. Basdogan F, Visser W, **Struijk PC**, Jansen JR, Vletter WB, Wladimiroff JW, Lotgering FK. Automated cardiac output measurements by ultrasound are inaccurate at high cardiac outputs. Ultrasound Obstet Gynecol. 2000 15:508-12.
26. De Leeuw JW, **Struijk PC**, Vierhout ME, Wallenburg HC. Risk factors for third degree perineal ruptures during delivery. BJOG 2001 08:383-7.
27. **Struijk PC**, Ursem NT, Mathews J, Clark EB, Keller BB, Wladimiroff JW. Power spectrum analysis of heart rate and blood flow velocity variability measured in the umbilical and uterine arteries in early pregnancy: a comparative study. Ultrasound Obstet Gynecol 2001 17:316-21.
28. Ursem NT, **Struijk PC**, Poelmann RE, Gittenberger-de Groot AC, Wladimiroff JW. Dorsal aortic flow velocity in chick embryos of stage 16 to 28. Ultrasound Med Biol 2001 27:919-24.
29. De Leeuw JW, Vierhout ME, **Struijk PC**, Hop WC, Wallenburg HC. Anal sphincter damage after vaginal delivery: functional outcome and risk factors for fecal incontinence. Acta Obstet Gynecol Scand 2001 80:830-4.
30. Kappers-Klunne MC, de Haan M, **Struijk PC**, van Vliet HH. Serum thrombopoietin levels in relation to disease status in patients with immune thrombocytopenic purpura. Br J Haematol 2001 115:1004-6.
31. Boito S, **Struijk PC**, Ursem NT, Stijnen T, Wladimiroff JW. Umbilical venous volume flow in the normally developing and growth-restricted human fetus. Ultrasound Obstet Gynecol 2002 19:344-9.

32. Boito SM, Laudy JA, **Struijk PC**, Stijnen T, Wladimiroff JW. Three-dimensional US assessment of hepatic volume, head circumference, and abdominal circumference in healthy and growth-restricted fetuses. Radiology 2002 223:661-5.

33. Breeveld-Dwarkasin VN, **Struijk PC**, Eijskoot F, Lotgering FK, van Dissel-Emiliani FM, van der Weyden GC, Taverne MA. Ultrasonic cervimetry to study the dilatation of the caudal cervix of the cow at parturition. Theriogenology. 2002 57:1989-2002.

34. de Leeuw JW, Vierhout ME, **Struijk PC**, Auwerda HJ, Bac DJ, Wallenburg HC. Anal sphincter damage after vaginal delivery: relationship of anal endosonography and manometry to anorectal complaints. Dis Colon Rectum 2002 45:1004-10.

35. Breeveld-Dwarkasing VN, **Struijk PC**, Lotgering FK, Eijskoot F, Kindahl H, van der Weijden GC, Taverne MA. Cervical dilatation related to uterine electromyographic activity and endocrinological changes during prostaglandin F(2alpha)-induced parturition in cows. Biol Reprod 2003 68:536-42.

36. Boito S, **Struijk PC**, Ursem NT, Fedele L, Wladimiroff JW. Fetal brain/liver volume ratio and umbilical volume flow parameters relative to normal and abnormal human development. Ultrasound Obstet Gynecol 2003 21:256-61.

37. Lotgering FK, Bishai JM, **Struijk PC**, Blood AB, Hunter CJ, Power GG, Longo LD. Ten-minute umbilical cord occlusion markedly reduces cerebral blood flow and heat production in fetal sheep. Am J Obstet Gynecol 2003 189:233-8.

38. Boito SM, **Struijk PC**, Ursem NT, Stijnen T, Wladimiroff JW. Assessment of fetal liver volume and umbilical venous volume flow in pregnancies complicated by insulin-dependent diabetes mellitus. BJOG 2003 110:1007-13.

39. Baalbergen A, Ewing-Graham PC, Hop WC, **Struijk P**, Helmerhorst TJ. Prognostic factors in adenocarcinoma of the uterine cervix. Gynecol Oncol 2004 92:262-7.

40. Boito SM, Ursem NT, **Struijk PC**, Stijnen T, Wladimiroff JW. Umbilical venous volume flow and fetal behavioral states in the normally developing fetus.Ultrasound Obstet Gynecol 2004 23:138-42.

41. Vinkesteijn AS, Ursem NT, **Struijk PC**, Wladimiroff JW. Fetal heart rate and blood flow velocity variability in the presence of increased nuchal translucency: a preliminary study. Ultrasound Obstet Gynecol 2004 23:19-22.

42. Boito SM, **Struijk PC**, Pop GA, Visser W, Steegers EA, Wladimiroff JW. The impact of maternal plasma volume expansion and antihypertensive treatment with intravenous dihydralazine on fetal and maternal hemodynamics during pre-eclampsia: a clinical, echo-Doppler and viscometric study. Ultrasound Obstet Gynecol 2004 23:327-32.
43. Vinkesteijn AS, **Struijk PC**, Ursem NT, Hop WC, Wladimiroff JW. Fetal heart rate and umbilical artery flow velocity variability in intrauterine growth restriction: a matched controlled study.Ultrasound Obstet Gynecol. 2004 23:461-5.
44. Pop GA, de Backer TL, de Jong M, **Struijk PC**, Moraru L, Chang Z, Goovaerts HG, Slager CJ, Bogers AJ.On-line electrical impedance measurement for monitoring blood viscosity during on-pump heart surgery.Eur Surg Res. 2004 36:259-65.
45. Lotgering FK, Bishai JM, **Struijk PC**, Blood AB, Hunter CJ, Oberg KC, Power GG, Longo LD. Absence of robust ischemic preconditioning by five 1-minute total umbilical cord occlusions in fetal sheep.J Soc Gynecol Investig. 2004 11:449-56.
46. **Struijk PC**, Stewart PA, Fernando KL, Mathews VJ, Loupas T, Steegers EA, Wladimiroff JW. Wall shear stress and related hemodynamic parameters in the fetal descending aorta derived from color Doppler velocity profiles.Ultrasound Med Biol. 2005 Nov;31(11):1441-50.
47. Gerada M, **Struijk PC**, Stewart PA, Guerriero S, Melis GB, Wladimiroff JW. Comparison between color Doppler cineloop- and conventional spectral Doppler-derived maximum velocity and flow in the umbilical vein. Ultrasound Obstet Gynecol. 2006 Jul 6;

Dankwoord

De hoogleraren Henk Wallenburg, Juriy Wladimiroff en Theo Helmerhorst wil ik bedanken voor het schrijven van de aanbevelingsbrieven ter ondersteuning van mijn aanvraag toegelaten te worden tot het promotie traject.

Mijn promotoren Juriy Wladimiroff en Eric Steegers wil ik bedanken voor hun inzet.

This research project could not have been successfully completed without the collaboration between the University of Utah and Erasmus MC. Dear Professors Ed Clark, John Mathews and Mike Varner working with you on these research projects was a great pleasure and has enriched my life.

Lanka Fernando thanks for being my teacher when I started working with MATLAB. To all the people I have been working with in Salt Lake City I would like to say, you were great. Dear Susan Greaves thanks for taking care of almost everything but most of all for being such a nice person.

Astrid Vinkesteijn het was zeer leerzaam om met jou samen te werken. Jouw artikel heeft het klinisch belang van spectraal analyse in de prenatale diagnostiek aangetoond en is daarmee een verrijking van mijn proefschrift. Patricia Stewart ik heb grote bewondering voor je vakmanschap, je doorzettingsvermogen en de wijze waarop je met patiënten omgaat.

Mijn waardering is groot voor Wim Holland, Sandra de Vos, Jolanda Wentzel, Frank Gijsen, Anneke Verkleij, Mark Rutten, Nicolette Ursem, Hugo van Steenis, Cees Slager, Jerry Westerweel, Nico de Jong, Annemieke van Wamel, Rene Delfos, Annelous Beerends, Marjan Coolman en alle anderen waarmee ik over de inhoud van dit boekje van gedachten heb gewisseld.

I would like to acknowledge the co-authors for their contribution to this research.

Mijn oprechte dank gaat uit naar de vrouwen die aan dit onderzoek hebben deelgenomen.

De collega's van de 22e wil ik bedanken voor hun morele steun.

Dear Carleen Clark the hospitality Sjanie and I experienced was overwhelming, flying to Salt Lake City felt like going home.

Angelina en Paco betere paranimfen had ik mij niet kunnen wensen.

Lieve Sjanie na 30 jaar huwelijk heeft de veelzijdigheid van jouw talenten mij opnieuw doen verbazen. Naast het corrigeren van mijn Engelse teksten was je heel snel in staat zelfstandig signaal analyses uit te voeren en bovenal orde te brengen in mijn chaotische manier van werken. Ik vind het geweldig dat we het bedrijven van de wetenschap toe hebben kunnen voegen aan alle mooie dingen die we samen al doen.